NORSAR Scientific Report No. 1-2010

Semiannual Technical Summary

1 July - 31 December 2009

Frode Ringdal (ed.)

Kjeller, February 2010

REPORT DOCUMENTATION PAGE

Form Approved
OMB No. 0704-0188

1. REPORT DATE *(DD-MM-YYYY)*	2. REPORT TYPE	3. DATES COVERED *(From - To)*
15-02-2010	Semiannual Technical Summary	1 July - 31 December 2009

4. TITLE AND SUBTITLE
Semiannual Technical Summary, 1 July - 31 December 2009

5a. CONTRACT NUMBER
FA2521-06-C-8003

5b. GRANT NUMBER

5c. PROGRAM ELEMENT NUMBER
NDC Support / R&D

6. AUTHOR(S)
Frode Ringdal (Ed.)

5d. PROJECT NUMBER
T/6110

5e. TASK NUMBER
SOW Task 4.2 & 4.3

5f. WORK UNIT NUMBER
CDRL sequence nos. A001-A004

7. PERFORMING ORGANIZATION NAME(S) AND ADDRESS(ES)
Stiftelsen NORSAR
Post Box 53
NO-2027 Kjeller
Norway

8. PERFORMING ORGANIZATION REPORT NUMBER
Scientific Report No. 1-2010

9. SPONSORING/MONITORING AGENCY NAME(S) AND ADDRESS(ES)
AFTAC/TTS, 1030 South Highway A1A MS 1000, Patrick AFB, FL 32925-3002

Army Space and Missile Defense Command , 1515 Wilson Blvd., Suite 720
Arlington, VA 22209

10. SPONSOR/MONITOR'S ACRONYM(S)
AFTAC/TTS & USASMDC

11. SPONSOR/MONITOR'S REPORT NUMBER(S)

12. DISTRIBUTION/AVAILABILITY STATEMENT
Approved for public release; distribution unlimited

13. SUPPLEMENTARY NOTES

14. ABSTRACT
This report describes activities carried out at NORSAR under Contract No. FA2521-06-C-8003 (T/6110) for the period 1 July - 31 December 2009. In addition, it provides summary information on operation and maintenance (O&M) activities at the Norwegian National Data Center (NDC) during the same period. The O&M activities, including operation of transmission links within Norway and to Vienna, Austria, are being funded jointly by the CTBTO/PTS and the Norwegian Government, with the understanding that the funding of O&M activities for primary stations in the International Monitoring System (IMS) will gradually be transferred to the CTBTO/PTS. The O&M statistics presented in this report are included for the purpose of completeness, and in order to maintain consistency with earlier reporting practice. Some of the research activities described in this report are funded by the United States (cont.)

15. SUBJECT TERMS
NORSAR, Norwegian Seismic Array

16. SECURITY CLASSIFICATION OF: a. REPORT	b. ABSTRACT	c. THIS PAGE	17. LIMITATION OF ABSTRACT	18. NUMBER OF PAGES	19a. NAME OF RESPONSIBLE PERSON
U	U	U	SAR	77	Mr. Kyle S. Roberts, AFTAC/TTX
					19b. TELEPHONE NUMBER *(Include area code)* (321) 494-9471

Reset

Standard Form 298 (Rev. 8/98)
Prescribed by ANSI Std. Z39.18

Abstract (cont.)

Government, and the United States also covers the cost of transmission of selected data from the Norwegian NDC to the United States NDC.

The seismic arrays operated by NOR-NDC comprise the Norwegian Seismic Array (NOA), the Arctic Regional Seismic Array (ARCES) and the Spitsbergen Regional Array (SPITS). This report presents statistics for these three arrays as well as for additional seismic stations which through cooperative agreements with institutions in the host countries provide continuous data to NOR-NDC. These additional stations include the Finnish Regional Seismic Array (FINES) and the Hagfors array in Sweden (HFS).

The NOA Detection Processing system has been operated throughout the period with an uptime of 100%. A total of 1,903 seismic events have been reported in the NOA monthly seismic bulletin during the reporting period. On-line detection processing and data recording at the NDC of data from ARCES, FINES, SPITS and HFS data have been conducted throughout the period. Processing statistics for the arrays for the reporting period are given.

A summary of the activities at the NOR-NDC and relating to field installations during the reporting period is provided in Section 4. Norway is now contributing primary station data from two seismic arrays: NOA (PS27) and ARCES (PS28), one auxiliary seismic array SPITS (AS72), and one auxiliary three-component station JMIC (AS73). These data are being provided to the IDC via the global communications infrastructure (GCI). Continuous data from the three arrays are in addition being transmitted to the US NDC. The performance of the data transmission to the US NDC has been satisfactory during the reporting period.

So far among the Norwegian stations, the NOA and the ARCES array (PS27 and PS28 respectively), the radionuclide station at Spitsbergen (RN49) and the auxiliary seismic stations on Spitsbergen (AS72) and Jan Mayen (AS73) have been certified. Provided that adequate funding continues to be made available (from the CTBTO/PTS and the Norwegian Ministry of Foreign Affairs), we envisage continuing the provision of data from these and other Norwegian IMS-designated stations in accordance with current procedures. As part of NORSAR’s obsolescence management, a recapitalization plan for PS27 and PS28 has been submitted to CTBTO/PTS in order to prevent severe degradation of the stations due to lack of spare parts.

The IMS infrasound station originally planned to be located near Karasjok (IS37) may need to be moved to another site, since the local authorities have not granted the permissions required for the establishment of the station. Alternative locations outside Karasjok are currently being pursued. We have identified two alternative sites in northern Norway for possible installation of IS37. The CTBTO PrepCom has approved a corresponding coordinate change for the site.

Summaries of five scientific and technical contributions presented in Chapter 6 of this report are provided below:

Section 6.1 contains a study of a seismic event in the eastern Barents Sea on 11 November 2009. It is the first recorded seismic event in this region since the new high-frequency system was installed at the ARCES array on 23 March 2008. Our analysis of this event confirms the preliminary results of Ringdal et al. (2008) that there is a remarkably efficient propagation from distant events recorded at ARCES at frequencies up to 30 Hz and above. This result is similar to what has been previously observed at the Spitsbergen array for paths from Novaya Zemlya crossing the Barents Sea.

As to the source type of the 11 November 2009 event, we are not at this time in a position to give a firm conclusion. The cepstral analysis would indicate that the event is more likely an earthquake than an underwater explosion, but the reliability of the cepstral peak as a discriminant cannot be reliably assessed in this region, due to lack of a sufficient data base.

As more data is accumulated by the ARCES and Spitsbergen high-frequency systems, we may in the future be in a position to carry out a detailed study of the propagation characteristics for additional paths in the region, and make a systematic study of the benefits from combining the high-frequency observations from Spitsbergen and ARCES. This would be expected to contribute to a better understanding of various discriminants for the Barents region. The usefulness of the horizontal components for high-frequency S-phase detection, already demonstrated for the Spitsbergen array, is also an area that needs further study for ARCES.

Section 6.2 is a study of infrasound signals from two recent Russian rocket launches in the White Sea. The first event took place on 15 July 2009, when an intercontinental Bulava missile was launched from a submarine. According to the Russian Defense Ministry, the first stage of the missile malfunctioned and the weapon self-destructed. Infrasound signals associated with this missile launch were recorded at NORSAR's infrasound station at ARCES and the four stations in Sweden and Finland operated by the Swedish Institute of Space Physics. On each of these stations, we noted two clear phases separated by about two minutes. These strong signal pulses at each station most likely correspond to different stratospheric arrivals. However, both the take-off of the missile and the self-destruction may have lead to the generation of distinct signal pulses at different times, but we are unable to resolve this from our data.

The second launch took place on 9 December 2009, and caused significant attention in the media because strange and initially unexplained light phenomena were observed in northern Norway at about 6.50 UTC that day. After a while it became evident that the phenomena were caused by another failure of the Russian Bulava missile. According to the Russian Defense Ministry there was an engine failure in the third stage of the flight that caused the problem. According to recent information provided by the Norwegian Ministry of Defence, they believe that the missile exploded at an altitude between 100 and 300 km above the Novaya Zemlya region, and that the missile was launched from a submarine in the north-eastern part of the White Sea. No infrasound recordings by the Swedish array network were found for this event, but useful infrasound data was obtained from the ARCES and Apatity arrays. We were able to determine an approximate source location of these signals, and it appeared to be in the White Sea somewhat to the northeast of the previous event.

Section 6.3 is entitled "A New Source of Seismo-Acoustic Events for the Study of Infrasound Propagation over Regional Distances". As previously reported in various Semiannual Technical Summaries, industrial and military sources in northern Fennoscandia and NW Russia generate seismic and infrasound signals observed at regional distances. Similar seismic signals constrain origin times and explosion yield and, using correlation detectors at the ARCES array, have enabled us to detect and classify hundreds of events from a small number of sites which have in turn provided superb data sets for infrasound propagation studies. Thus, near-surface explosions at Hukkakero in northern Finland generate infrasound signals on the seismic sensors at ARCES, 175 km to the north, and we have made extensive studies of these events in the past.

We have recently identified a new site in northern Finland, where we first noted an event on October 2, 2009. The October 2 event occurred shortly after the end of the 2009 Hukkakero explosion sequence but, due to the event origin time and poor signal correlation with known events, was deemed unlikely to be from the same source location. Using seismic waveforms from stations of the Finnish national seismic network, in addition to ARCES, indicated an event location approximately 10 km to the west of the Hukkakero site. A consultation with colleagues at the Institute of Seismology at the University of Helsinki concluded that the source of the October 2 event was almost certainly the Kittilä Gold Mine, operated by Agnico-Eagle, at Suurikuusikko (67.90154 N, 25.39102 E).

Using an array-based waveform correlation detector with the seismic signal at ARCES from the October 2, 2009 event as a template, we obtained a total of 493 detections since July 2006. No convincing detections have been made prior to July 2006, and a consultation with the information provided by Agnico-Eagle confirms that this is consistent with the operational history of the mine.

The detection of infrasound signals at ARCES following many events in this sequence indicates that this source may be of great interest for the study of sound propagation of regional distances. The mine location is fortuitous in relation to the network of infrasound sensors in Norway, Sweden, Finland and Russia which provide an almost optimal coverage of the different directions from the source. Some of the stations are located either at the edge of or well within the so-called "Zone of Silence" within which the propagation of infrasound is currently very poorly understood. While initial indications are that the Suurikuusikko mine is a less efficient generator of infrasound than the military explosions at Hukkakero, the new data set has a great advantage in that the events occur throughout the year, and so will sample many different atmospheric profiles, and may contribute more to understanding the conditions under which infrasound is observed from explosions at a known location.

Section 6.4 summarizes our efforts to relocate the NDC Preparedness Exercise 2009 (NPE09) event with the use of near-regional data. The issued Reviewed Event Bulletin (REB) solution of the International Data Centre (IDC) for the event gives a location in Eastern Kazakhstan, close to the Kara-Zhyra open mine, which is situated in the Balapan sector of the former Soviet Semipalatinsk Test Site (STS). According to information received from the Kazakh NDC (KNDC), the event was the result of an open pit mining explosion, close to the border of the Western Kara-Zhyra mine. Complete ground truth information about the event is not available, but some characteristics of the ripple fired explosion are known and are reproduced in the paper.

A review of the REB observations showed rather large residuals for certain stations, both for arrival times and backazimuths. The worst case was KURK, which is a large, cross-shaped array situated at a distance of approximately 70 km from the event and which is deployed over variable site conditions. Due to the large array aperture, usual plane wave approximation cannot be used for events located so close. In addition, the signals of this event are quite incoherent between array sites far apart. We did attempt array processing by using only a part of the array, with reasonable results. Another problematic case was the Sn phase at ZALV, which turned out to be a clear case of phase misidentification and was consequently repicked. Minor changes were also made for other readings. The event was subsequently relocated using the (modified) REB information as well as additional regional data provided to us by KNDC and from KNET stations. Several different travel-time models were used in this connection.

The process of relocating the NPE09 event revealed several interesting aspects of possible path and structure interference in earthquake location and highlighted the importance of the availability of appropriate velocity models and SSSCs, in particular within the CTBTO monitoring framework.

Section 6.5 is a continued overview of NORSAR system responses, specifically addressing the Hagfors and FINES seismic arrays, as well as single three-component seismic stations in Åknes, western Norway, and on Hornsund, Spitsbergen. This series of contributions aims to recalculate and organize all of the system instrument responses of the seismic facilities operated or used routinely by NORSAR, from the time of the first installation to the present. All sources of information are being catalogued and archived. Furthermore, detailed documentation is being compiled, describing the methodology followed to obtain the necessary information, the calculation of the responses, as well as more practical issues, such as organizing and storing the results for future usage. Therefore, no information such as individual instrument poles and zeroes, serial numbers, sensitivity values, etc. are provided here; instead, the reader is referred to the relevant NORSAR internal documentation.

AFTAC Project Authorization	:	T/6110
Purchase Request No.	:	F3KTK85290A1
Name of Contractor	:	Stiftelsen NORSAR
Effective Date of Contract	:	1 March 2006
Contract Expiration Date	:	30 September 2011
Amount of Contract	:	$ 1,003,494.00
Project Manager	:	Frode Ringdal +47 63 80 59 00
Title of Work	:	The Norwegian Seismic Array (NORSAR) Phase 3
Period Covered by Report	:	1 July - 31 December 2009

The views and conclusions contained in this document are those of the authors and should not be interpreted as necessarily representing the official policies, either expressed or implied, of the U.S. Government.

Part of the research presented in this report was supported by the Army Space and Missile Defense Command, under contract no. W9113M-05-C-0224. Other activities were supported and monitored by AFTAC, Patrick AFB, FL32925, under contract no. FA2521-06-C-8003. Other sponsors are acknowledged where appropriate.

The operational activities of the seismic field systems and the Norwegian National Data Center (NDC) are currently jointly funded by the Norwegian Government and the CTBTO/PTS, with the understanding that the funding of appropriate IMS-related activities will gradually be transferred to the CTBTO/PTS.

Table of Contents

1 Summary

This report describes activities carried out at NORSAR under Contract No. FA2521-06-C-8003 for the period 1 July - 31 December 2009. In addition, it provides summary information on operation and maintenance (O&M) activities at the Norwegian National Data Center (NOR-NDC) during the same period. The O&M activities, including operation of transmission links within Norway and to Vienna, Austria are being funded jointly by the CTBTO/PTS and the Norwegian Government, with the understanding that the funding of O&M activities for primary stations in the International Monitoring System (IMS) will gradually be transferred to the CTBTO/PTS. The O&M statistics presented in this report are included for the purpose of completeness, and in order to maintain consistency with earlier reporting practice. Some of the research activities described in this report are funded by the United States Government, and the United States also covers the cost of transmission of selected data from the Norwegian NDC to the United States NDC.

The seismic arrays operated by NOR-NDC comprise the Norwegian Seismic Array (NOA), the Arctic Regional Seismic Array (ARCES) and the Spitsbergen Regional Array (SPITS). This report presents statistics for these three arrays as well as for additional seismic stations which through cooperative agreements with institutions in the host countries provide continuous data to NOR-NDC. These additional stations include the Finnish Regional Seismic Array (FINES) and the Hagfors array in Sweden (HFS).

The NOA Detection Processing system has been operated throughout the period with an uptime of 100%. A total of 1,903 seismic events have been reported in the NOA monthly seismic bulletin during the reporting period. On-line detection processing and data recording at the NDC of data from ARCES, FINES, SPITS and HFS data have been conducted throughout the period. Processing statistics for the arrays for the reporting period are given.

A summary of the activities at the NOR-NDC and relating to field installations during the reporting period is provided in Section 4. Norway is now contributing primary station data from two seismic arrays: NOA (PS27) and ARCES (PS28), one auxiliary seismic array SPITS (AS72), and one auxiliary three-component station JMIC (AS73). These data are being provided to the IDC via the global communications infrastructure (GCI). Continuous data from the three arrays are in addition being transmitted to the US NDC. The performance of the data transmission to the US NDC has been satisfactory during the reporting period.

So far among the Norwegian stations, the NOA and the ARCES array (PS27 and PS28 respectively), the radionuclide station at Spitsbergen (RN49) and the auxiliary seismic stations on Spitsbergen (AS72) and Jan Mayen (AS73) have been certified. Provided that adequate funding continues to be made available (from the CTBTO/PTS and the Norwegian Ministry of Foreign Affairs), we envisage continuing the provision of data from these and other Norwegian IMS-designated stations in accordance with current procedures. As part of NORSAR's obsolescence management, a recapitalization plan for PS27 and PS28 has been submitted to CTBTO/PTS in order to prevent severe degradation of the stations due to lack of spare parts.

The IMS infrasound station originally planned to be located near Karasjok (IS37) may need to be moved to another site, since the local authorities have not granted the permissions required for the establishment of the station. Alternative locations outside Karasjok are currently being pursued. We have identified two alternative sites in northern Norway for possible installation of IS37. The CTBTO PrepCom has approved a corresponding coordinate change for the site.

Summaries of five scientific and technical contributions presented in Chapter 6 of this report are provided below:

Section 6.1 contains a study of a seismic event in the eastern Barents Sea on 11 November 2009. It is the first recorded seismic event in this region since the new high-frequency system was installed at the ARCES array on 23 March 2008. Our analysis of this event confirms the preliminary results of Ringdal et al. (2008) that there is a remarkably efficient propagation from distant events recorded at ARCES at frequencies up to 30 Hz and above. This result is similar to what has been previously observed at the Spitsbergen array for paths from Novaya Zemlya crossing the Barents Sea.

As to the source type of the 11 November 2009 event, we are not at this time in a position to give a firm conclusion. The cepstral analysis would indicate that the event is more likely an earthquake than an underwater explosion, but the reliability of the cepstral peak as a discriminant cannot be reliably assessed in this region, due to lack of a sufficient data base.

As more data is accumulated by the ARCES and Spitsbergen high-frequency systems, we may in the future be in a position to carry out a detailed study of the propagation characteristics for additional paths in the region, and make a systematic study of the benefits from combining the high-frequency observations from Spitsbergen and ARCES. This would be expected to contribute to a better understanding of various discriminants for the Barents region. The usefulness of the horizontal components for high-frequency S-phase detection, already demonstrated for the Spitsbergen array, is also an area that needs further study for ARCES.

Section 6.2 is a study of infrasound signals from two recent Russian rocket launches in the White Sea. The first event took place on 15 July 2009, when an intercontinental Bulava missile was launched from a submarine. According to the Russian Defense Ministry, the first stage of the missile malfunctioned and the weapon self-destructed. Infrasound signals associated with this missile launch were recorded at NORSAR’s infrasound station at ARCES and the four stations in Sweden and Finland operated by the Swedish Institute of Space Physics. On each of these stations, we noted two clear phases separated by about two minutes. These strong signal pulses at each station most likely correspond to different stratospheric arrivals. However, both the take-off of the missile and the self-destruction may have lead to the generation of distinct signal pulses at different times, but we are unable to resolve this from our data.

The second launch took place on 9 December 2009, and caused significant attention in the media because strange and initially unexplained light phenomena were observed in northern Norway at about 6.50 UTC that day. After a while it became evident that the phenomena were caused by another failure of the Russian Bulava missile. According to the Russian Defense Ministry there was an engine failure in the third stage of the flight that caused the problem. According to recent information provided by the Norwegian Ministry of Defence, they believe that the missile exploded at an altitude between 100 and 300 km above the Novaya Zemlya region, and that the missile was launched from a submarine in the north-eastern part of the White Sea. No infrasound recordings by the Swedish array network were found for this event, but useful infrasound data was obtained from the ARCES and Apatity arrays. We were able to determine an approximate source location of these signals, and it appeared to be in the White Sea somewhat to the northeast of the previous event.

Section 6.3 is entitled “A New Source of Seismo-Acoustic Events for the Study of Infrasound Propagation over Regional Distances”. As previously reported in various Semiannual Technical Summaries, industrial and military sources in northern Fennoscandia and NW Russia generate seismic and infrasound signals observed at regional distances. Similar seismic signals constrain origin times and explosion yield and, using correlation detectors at the ARCES array, have enabled us to detect and classify hundreds of events from a small number of sites which have in turn provided superb data sets for infrasound propagation studies. Thus, near-surface explosions at Hukkakero in northern Finland generate infrasound signals on the seismic sensors at ARCES, 175 km to the north, and we have made extensive studies of these events in the past.

We have recently identified a new site in northern Finland, where we first noted an event on October 2, 2009. The October 2 event occurred shortly after the end of the 2009 Hukkakero explosion sequence but, due to the event origin time and poor signal correlation with known events, was deemed unlikely to be from the same source location. Using seismic waveforms from stations of the Finnish national seismic network, in addition to ARCES, indicated an event location approximately 10 km to the west of the Hukkakero site. A consultation with colleagues at the Institute of Seismology at the University of Helsinki concluded that the source of the October 2 event was almost certainly the Kittilä Gold Mine, operated by Agnico-Eagle, at Suurikuusikko (67.90154 N, 25.39102 E).

Using an array-based waveform correlation detector with the seismic signal at ARCES from the October 2, 2009 event as a template, we obtained a total of 493 detections since July 2006. No convincing detections have been made prior to July 2006, and a consultation with the information provided by Agnico-Eagle confirms that this is consistent with the operational history of the mine.

The detection of infrasound signals at ARCES following many events in this sequence indicates that this source may be of great interest for the study of sound propagation of regional distances. The mine location is fortuitous in relation to the network of infrasound sensors in Norway, Sweden, Finland and Russia which provide an almost optimal coverage of the different directions from the source. Some of the stations are located either at the edge of or well within the so-called “Zone of Silence” within which the propagation of infrasound is currently very poorly understood. While initial indications are that the Suurikuusikko mine is a less efficient generator of infrasound than the military explosions at Hukkakero, the new data set has a great advantage in that the events occur throughout the year, and so will sample many different atmospheric profiles, and may contribute more to understanding the conditions under which infrasound is observed from explosions at a known location.

Section 6.4 summarizes our efforts to relocate the NDC Preparedness Exercise 2009 (NPE09) event with the use of near-regional data. The issued Reviewed Event Bulletin (REB) solution of the International Data Centre (IDC) for the event gives a location in Eastern Kazakhstan, close to the Kara-Zhyra open mine, which is situated in the Balapan sector of the former Soviet Semipalatinsk Test Site (STS). According to information received from the Kazakh NDC (KNDC), the event was the result of an open pit mining explosion, close to the border of the Western Kara-Zhyra mine. Complete ground truth information about the event is not available, but some characteristics of the ripple fired explosion are known and are reproduced in the paper.

A review of the REB observations showed rather large residuals for certain stations, both for arrival times and backazimuths. The worst case was KURK, which is a large, cross-shaped array situated at a distance of approximately 70 km from the event and which is deployed over variable site conditions. Due to the large array aperture, usual plane wave approximation cannot be used for events located so close. In addition, the signals of this event are quite incoherent between array sites far apart. We did attempt array processing by using only a part of the array, with reasonable results. Another problematic case was the Sn phase at ZALV, which turned out to be a clear case of phase misidentification and was consequently repicked. Minor changes were also made for other readings. The event was subsequently relocated using the (modified) REB information as well as additional regional data provided to us by KNDC and from KNET stations. Several different travel-time models were used in this connection.

The process of relocating the NPE09 event revealed several interesting aspects of possible path and structure interference in earthquake location and highlighted the importance of the availability of appropriate velocity models and SSSCs, in particular within the CTBTO monitoring framework.

Section 6.5 is a continued overview of NORSAR system responses, specifically addressing the Hagfors and FINES seismic arrays, as well as single three-component seismic stations in Åknes, western Norway, and on Hornsund, Spitsbergen. This series of contributions aims to recalculate and organize all of the system instrument responses of the seismic facilities operated or used routinely by NORSAR, from the time of the first installation to the present. All sources of information are being catalogued and archived. Furthermore, detailed documentation is being compiled, describing the methodology followed to obtain the necessary information, the calculation of the responses, as well as more practical issues, such as organizing and storing the results for future usage. Therefore, no information such as individual instrument poles and zeroes, serial numbers, sensitivity values, etc. are provided here; instead, the reader is referred to the relevant NORSAR internal documentation.

Frode Ringdal

2 Operation of International Monitoring System (IMS) Stations in Norway

2.1 PS27 — Primary Seismic Station NOA

The mission-capable data statistics were 100%, the same as for the previous reporting period. The net instrument availability was 98.329%.

There were no outages of all subarrays at the same time in the reporting period.

Monthly uptimes for the NORSAR on-line data recording task, taking into account all factors (field installations, transmissions line, data center operation) affecting this task were as follows:

2009		Mission Capable	Net instrument availability
July	:	100%	98.423%
August	:	100%	96.383%
September	:	100%	98.067%
October	:	100%	99.997%
November	:	100%	98.884%
December	:	100%	98.229%

B. Paulsen

NOA Event Detection Operation

In Table 2.1.1 some monthly statistics of the Detection and Event Processor operation are given. The table lists the total number of detections (DPX) triggered by the on-line detector, the total number of detections processed by the automatic event processor (EPX) and the total number of events accepted after analyst review (teleseismic phases, core phases and total).

	Total DPX	Total EPX	Accepted Events		Sum	Daily
			P-phases	Core Phases		
Jul	6,787	838	279	57	336	10.8
Aug	6,644	793	343	60	403	13.0
Sep	8,899	801	235	46	281	9.4
Oct	10,401	920	225	112	337	10.9
Nov	9,498	738	204	54	258	8.6
Dec	10,215	804	239	49	288	9.3
	52,444	4,894	1,525	378	1,903	10.3

Table 2.1.1. *Detection and Event Processor statistics, 1 July - 31 December 2009.*

NOA detections

The number of detections (phases) reported by the NORSAR detector during day 182, 2009, through day 365, 2009, was 52,444, giving an average of 285 detections per processed day (184 days processed).

B. Paulsen

U. Baadshaug

2.2 PS28 — Primary Seismic Station ARCES

The mission-capable data statistics were 99.995%, as compared to 99.927% for the previous reporting period. The net instrument availability was 99.444%.

The main outages in the period are presented in Table 2.2.1.

Day	Period
17 Dec	09.28-09.42

Table 2.2.1. *The main interruptions in recording of ARCES data at NDPC, 1 July - 31 December 2009.*

Monthly uptimes for the ARCES on-line data recording task, taking into account all factors (field installations, transmission lines, data center operation) affecting this task were as follows:

2009		Mission Capable	Net instrument availability
July	:	100%	100%
August	:	100%	100%
September	:	100%	100%
October	:	100%	100%
November	:	100%	100%
December	:	99.968%	99.5675

B. Paulsen

Event Detection Operation

ARCES detections

The number of detections (phases) reported during day 182, 2009, through day 365, 2009, was 212,469, giving an average of 1155 detections per processed day (184 days processed).

Events automatically located by ARCES

During days 182, 2009, through 365, 2009, 8,228 local and regional events were located by ARCES, based on automatic association of P- and S-type arrivals. This gives an average of 44.7 events per processed day (184 days processed). 70% of these events are within 300 km, and 92 % of these events are within 1000 km.

U. Baadshaug

2.3 AS72 — Auxiliary Seismic Station Spitsbergen

The mission-capable data for the period were 99.226%, as compared to 93.629% for the previous reporting period. The net instrument availability was 96.870%.

The main outages in the period are presented in Table 2.3.1.

Day	Period
23 Aug	21.43-00.00
24 Aug	00.00-06.45
12 Nov	20.33-00.00
13 Nov	00.00-10.54
27 Nov	21.57-00.00
28 Nov	00.00-08.20
28 Nov	10.14-10.30

Table 2.31. *The main interruptions in recording of Spitsbergen data at NDPC, 1 July - 31 December 2009.*

Monthly uptimes for the Spitsbergen on-line data recording task, taking into account all factors (field installations, transmissions line, data center operation) affecting this task were as follows:

2009		Mission Capable	Net instrument availability
July	:	99.998%	99.999%
August	:	98.787%	98.785%
September	:	99.996%	99.995%
October	:	99.996%	99.996%
November	:	96.524%	93.807%
December	:	99.992%	88.638%

B. Paulsen

Event Detection Operation

Spitsbergen array detections

The number of detections (phases) reported from day 182, 2009, through day 365 2009, was 391,901, giving an average of 2,130 detections per processed day (184 days processed).

Events automatically located by the Spitsbergen array

During days 182, 2009 through 365, 2009, 38,950 local and regional events were located by the Spitsbergen array, based on automatic association of P- and S-type arrivals. This gives an average of 211.7 events per processed day (184 days processed). 82% of these events are within 300 km, and 92% of these events are within 1000 km.

U. Baadshaug

2.4 AS73 — Auxiliary Seismic Station at Jan Mayen

The IMS auxiliary seismic network includes a three-component station on the Norwegian island of Jan Mayen. The station location given in the protocol to the Comprehensive Nuclear-Test-Ban Treaty is 70.9˚N, 8.7˚W.

The University of Bergen has operated a seismic station at this location since 1970. A so-called Parent Network Station Assessment for AS73 was completed in April 2002. A vault at a new location (71.0^{o}N, 8.5^{o}W) was prepared in early 2003, after its location had been approved by the PrepCom. New equipment was installed in this vault in October 2003, as a cooperative effort between NORSAR and the CTBTO/PTS. Continuous data from this station are being transmitted to the NDC at Kjeller via a satellite link installed in April 2000. Data are also made available to the University of Bergen.

The station was certified by the CTBTO/PTS on 12 June 2006.

J. Fyen

2.5 IS37 — Infrasound Station at Karasjok

The IMS infrasound network will, according to the protocol of the CTBT, include a station at Karasjok in northern Norway. The coordinates given for this station are 69.5˚N, 25.5˚E. These coordinates coincide with those of the primary seismic station PS28.

It has, however, proved very difficult to obtain the necessary permits for use of land for an infrasound station in Karasjok. Various alternatives for locating the station in Karasjok were prepared, but all applications to the local authorities to obtain the permissions needed to establish the station were turned down by the local governing council in June 2007.

In 2008, investigations were initiated to identify an alternative site for IS37 outside Karasjok. Two sites at Bardufoss, at 69.1^{o} N, 18.6^{o} E, are currently being pursued to select one of them for possible installation of IS37. The CTBTO PrepCom has approved a corresponding coordinate change for the station.

J. Fyen

2.6 RN49 — Radionuclide Station on Spitsbergen

The IMS radionuclide network includes a station on the island of Spitsbergen. This station has been selected to be among those IMS radionuclide stations that will monitor for the presence of relevant noble gases upon entry into force of the CTBT.

A site survey for this station was carried out in August of 1999 by NORSAR, in cooperation with the Norwegian Radiation Protection Authority. The site survey report to the PTS contained a recommendation to establish this station at Platåberget, near Longyearbyen. The infrastructure for housing the station equipment was established in early 2001, and a noble gas detection system, based on the Swedish “SAUNA” design, was installed at this site in May 2001, as part of PrepCom’s noble gas experiment. A particulate station (“ARAME” design) was installed at the same location in September 2001. A certification visit to the particulate station took place in October 2002, and the particulate station was certified on 10 June 2003. Both systems underwent substantial upgrading in May/June 2006. The equipment at RN49 is being maintained and operated under a contract with the CTBTO/PTS.

S. Mykkeltveit

3 Contributing Regional Seismic Arrays

3.1 NORES

NORES has been out of operation since lightning destroyed the station electronics on 11 June 2002.

B. Paulsen

3.2 Hagfors (IMS Station AS101)

Data from the Hagfors array are made available continuously to NORSAR through a cooperative agreement with Swedish authorities.

The mission-capable data statistics were 99.982%, as compared to 99.967% for the previous reporting period. The net instrument availability was 99.401%.

The main outages in the period are presented in Table 3.2.1.

Day	Period
02 Jul	10.49-10.53
02 Aug	06.30-06.33
04 Aug	01.10-01.13
04 Aug	17.50-17.53
08 Aug	18.30-18.33
03 Sep	19.30-19.34
14 Sep	18.31-18.34
15 Sep	01.11-01.14
23 Sep	10.31-10.34
26 Sep	05.11-05.14
28 Sep	07.51-07.54
29 Oct	03.11-03.15
19 Nov	14.52-14.55
23 Nov	14.12-14.15

Table 3.2.1. *The main interruptions in recording of Hagfors data at NDPC, 1 July - 31 December 2009.*

Monthly uptimes for the Hagfors on-line data recording task, taking into account all factors (field installations, transmissions line, data center operation) affecting this task were as follows:

2009		**Mission Capable**	**Net instrument availability**
July	:	99.992%	98.021%
August	:	99.970%	99.970%
September	:	99.954%	99.953%
October	:	99.992%	99.480%
November	:	99.986%	99.986%
December	:	99.997%	99.997%

B. Paulsen

Hagfors Event Detection Operation

Hagfors array detections

The number of detections (phases) reported from day 182, 2009, through day 365, 2009, was 126,206, giving an average of 686 detections per processed day (184 days processed).

Events automatically located by the Hagfors array

During days 182, 2009, through 365, 2009, 4,481 local and regional events were located by the Hagfors array, based on automatic association of P- and S-type arrivals. This gives an average of 24.4 events per processed day (184 days processed). 65% of these events are within 300 km, and 91% of these events are within 1000 km.

U. Baadshaug

3.3 FINES (IMS station PS17)

Data from the FINES array are made available continuously to NORSAR through a cooperative agreement with Finnish authorities.

The mission-capable data statistics were 97.738%, as compared to 99.991% for the previous reporting period. The net instrument availability was 96.303%.

The main outages in the period are presented in Table 3.3.1.

Day	Period
13 Sep	03.14-09.38
13 Sep	09.42-09.45
07 Oct	07.24-10.43
08 Oct	07.05-07-15
08 Oct	07.24-07.33
08 Oct	07.44-07.48
15 Oct	13.21-00.00
16 Oct	00.00-03.46
18 Oct	13.32-1652
09 Nov	06.10-06.12
13 Dec	15.47-17.54
13 Dec	18.22-18.49
14 Dec	05.55-05.59
20 Dec	02.41-00.00
21 Dec	00.00-00.00
22 Dec	00.00-23.59

Table 3.3.1. *The main interruptions in recording of FINES data at NDPC, 1 July - 31 December 2009.*

Monthly uptimes for the FINES on-line data recording task, taking into account all factors (field installations, transmissions line, data center operation) affecting this task were as follows:

2009		Mission Capable	Net instrument availability
July	:	100%	100%
August	:	100%	100%
September	:	99.103%	95.080%
October	:	97.121%	94.491%
November	:	99.994%	98.875%
December	:	90.328%	89.417%

B. Paulsen

FINES Event Detection Operation

FINES detections

The number of detections (phases) reported during day 182, 2009, through day 365, 2009, was 42,613, giving an average of 237 detections per processed day (180 days processed).

Events automatically located by FINES

During days 182, 2009, through 365, 2009, 2,350 local and regional events were located by FINES, based on automatic association of P- and S-type arrivals. This gives an average of 13.1 events per processed day (180 days processed). 88% of these events are within 300 km, and 94% of these events are within 1000 km.

U. Baadshaug

3.4 Regional Monitoring System Operation and Analysis

The Regional Monitoring System (RMS) was installed at NORSAR in December 1989 and has been operated at NORSAR from 1 January 1990 for automatic processing of data from ARCES and NORES. A second version of RMS that accepts data from an arbitrary number of arrays and single 3-component stations was installed at NORSAR in October 1991, and regular operation of the system comprising analysis of data from the 4 arrays ARCES, NORES, FINES and GERES started on 15 October 1991. As opposed to the first version of RMS, the one in current operation also has the capability of locating events at teleseismic distances.

Data from the Apatity array was included on 14 December 1992, and from the Spitsbergen array on 12 January 1994. Detections from the Hagfors array were available to the analysts and could be added manually during analysis from 6 December 1994. After 2 February 1995, Hagfors detections were also used in the automatic phase association.

Since 24 April 1999, RMS has processed data from all the seven regional arrays ARCES, NORES, FINES, GERES (until January 2000), Apatity, Spitsbergen, and Hagfors. Starting 19 September 1999, waveforms and detections from the NORSAR array have also been available to the analyst.

Phase and event statistics

Table 3.5.1 gives a summary of phase detections and events declared by RMS. From top to bottom the table gives the total number of detections by the RMS, the number of detections that are associated with events automatically declared by the RMS, the number of detections that are not associated with any events, the number of events automatically declared by the RMS, and finally the total number of events worked on interactively (in accordance with criteria that vary over time; see below) and defined by the analyst.

New criteria for interactive event analysis were introduced from 1 January 1994. Since that date, only regional events in areas of special interest (e.g, Spitsbergen, since it is necessary to acquire new knowledge in this region) or other significant events (e.g, felt earthquakes and large industrial explosions) were thoroughly analyzed. Teleseismic events of special interest are also analyzed.

To further reduce the workload on the analysts and to focus on regional events in preparation for Gamma-data submission during GSETT-3, a new processing scheme was introduced on 2

February 1995. The GBF (Generalized Beamforming) program is used as a pre-processor to RMS, and only phases associated with selected events in northern Europe are considered in the automatic RMS phase association. All detections, however, are still available to the analysts and can be added manually during analysis.

	Jul 09	**Aug 09**	**Sep 09**	**Oct 09**	**Nov 09**	**Dec 09**	**Total**
Phase detections	126,546	164,949	177,069	168,350	171,859	145,566	954,339
- Associated phases	4,895	6,603	8,263	7,041	7,109	4,922	38,833
- Unassociated phases	121,651	158,346	168,806	161,309	164,750	140,644	915,506
Events automatically declared by RMS	959	1,320	1,625	1,436	1,621	971	7,932
No. of events defined by the analyst	76	69	103	97	96	65	506

Table 3.5.1. RMS phase detections and event summary 1 July - 31 December 2009.

U. Baadshaug
B. Paulsen

4 NDC and Field Activities

4.1 NDC Activitities

NORSAR functions as the Norwegian National Data Center (NDC) for CTBT verification. Six monitoring stations, comprising altogether 132 field sensors plus radionuclide monitoring equipment, will be located on Norwegian territory as part of the future IMS as described elsewhere in this report. The four seismic IMS stations are all in operation today, and all of them are currently providing data to the CTBTO on a regular basis. PS27, PS28, AS72, AS73 and RN49 are all certified. Data recorded by the Norwegian stations is being transmitted in real time to the Norwegian NDC, and provided to the IDC through the Global Communications Infrastructure (GCI). Norway is connected to the GCI with a frame relay link to Vienna.

Operating the Norwegian IMS stations continues to require significant efforts by personnel both at the NDC and in the field. Strictly defined procedures as well as increased emphasis on regularity of data recording and timely data transmission to the IDC in Vienna have led to increased reporting activities and implementation of new procedures for the NDC. The NDC carries out all the technical tasks required in support of Norway's treaty obligations. NORSAR will also carry out assessments of events of special interest, and advise the Norwegian authorities in technical matters relating to treaty compliance. A challenge for the NDC is to carry 40 years' experience over to the next generation of personnel.

Verification functions; information received from the IDC

After the CTBT enters into force, the IDC will provide data for a large number of events each day, but will not assess whether any of them are likely to be nuclear explosions. Such assessments will be the task of the States Parties, and it is important to develop the necessary national expertise in the participating countries. An important task for the Norwegian NDC will thus be to make independent assessments of events of particular interest to Norway, and to communicate the results of these analyses to the Norwegian Ministry of Foreign Affairs.

Monitoring the Arctic region

Norway will have monitoring stations of key importance for covering the Arctic, including Novaya Zemlya, and Norwegian experts have a unique competence in assessing events in this region. On several occasions in the past, seismic events near Novaya Zemlya have caused political concern, and NORSAR specialists have contributed to clarifying these issues.

International cooperation

After entry into force of the treaty, a number of countries are expected to establish national expertise to contribute to the treaty verification on a global basis. Norwegian experts have been in contact with experts from several countries with the aim of establishing bilateral or multilateral cooperation in this field. One interesting possibility for the future is to establish NORSAR as a regional center for European cooperation in the CTBT verification activities.

NORSAR event processing

The automatic routine processing of NORSAR events as described in NORSAR Sci. Rep. No. 2-93/94, has been running satisfactorily. The analyst tools for reviewing and updating the solutions have been continually modified to simplify operations and improve results. NORSAR is currently applying teleseismic detection and event processing using the large-aperture NOA array as well as regional monitoring using the network of small-aperture arrays in Fennoscandia and adjacent areas.

Communication topology

Norway has implemented an independent subnetwork, which connects the IMS stations AS72, AS73, PS28, and RN49 operated by NORSAR to the GCI at NOR_NDC. A contract has been concluded and VSAT antennas have been installed at each station in the network. Under the same contract, VSAT antennas for 6 of the PS27 subarrays have been installed for intra-array communication. The seventh subarray is connected to the central recording facility via a leased land line. The central recording facility for PS27 is connected directly to the GCI (Basic Topology). All the VSAT communication is functioning satisfactorily. As of 10 June 2005, AS72 and RN49 are connected to NOR_NDC through a VPN link.

Jan Fyen

4.2 Status Report: Provision of data from Norwegian seismic IMS stations to the IDC

Introduction

This contribution is a report for the period July - December 2009 on activities associated with provision of data from Norwegian seismic IMS stations to the International Data Centre (IDC) in Vienna. This report represents an update of contributions that can be found in previous editions of NORSAR's Semiannual Technical Summary. All four Norwegian seismic stations providing data to the IDC have now been formally certified.

Norwegian IMS stations and communications arrangements

During the reporting interval, Norway has provided data to the IDC from the four seismic stations shown in Fig. 4.2.1. PS27 —NOA is a 60 km aperture teleseismic array, comprised of 7 subarrays, each containing six vertical short period sensors and a three-component broadband instrument. PS28 — ARCES is a 25-element regional array with an aperture of 3 km, whereas AS72 — Spitsbergen array (station code SPITS) has 9 elements within a 1-km aperture. AS73 — JMIC has a single three-component broadband instrument.

The intra-array communication for NOA utilizes a land line for subarray NC6 and VSAT links based on TDMA technology for the other 6 subarrays. The central recording facility for NOA is located at the Norwegian National Data Center (NOR_NDC).

Continuous ARCES data are transmitted from the ARCES site to NOR_NDC using a 64 kbits/s VSAT satellite link, based on BOD technology.

Continuous SPITS data were transmitted to NOR_NDC via a VSAT terminal located at Platåberget in Longyearbyen (which is the site of the IMS radionuclide monitoring station RN49 installed during 2001) up to 10 June 2005. The central recording facility (CRF) for the SPITS array has been moved to the University of Spitsbergen (UNIS). A 512 bps SHDSL link has been established between UNIS and NOR_NDC. Data from the array elements to the CRF are transmitted via a 2.4 Ghz radio link (Wilan VIP-110). Both AS72 and RN49 data are now transmitted to NOR_NDC over this link using VPN technology.

A minimum of seven-day station buffers have been established at the ARCES and SPITS sites and at all NOA subarray sites, as well as at the NOR_NDC for ARCES, SPITS and NOA. In addition, each individual site of the SPITS array has a 14-day buffer.

The NOA and ARCES arrays are primary stations in the IMS network, which implies that data from these stations is transmitted continuously to the receiving international data center. Since October 1999, this data has been transmitted (from NOR_NDC) via the Global Communications Infrastructure (GCI) to the IDC in Vienna. Data from the auxiliary array station SPITS — AS72 have been sent in continuous mode to the IDC during the reporting period. AS73 — JMIC is an auxiliary station in the IMS, and the JMIC data have been available to the IDC throughout the reporting period on a request basis via use of the AutoDRM protocol (Kradolfer, 1993; Kradolfer, 1996). In addition, continuous data from all three arrays is transmitted to the US_NDC.

Uptimes and data availability

Figs. 4.2.2 and 4.2.3 show the monthly uptimes for the Norwegian IMS primary stations ARCES and NOA, respectively, for the reporting period given as the hatched (taller) bars in these figures. These barplots reflect the percentage of the waveform data that is available in the NOR_NDC data archives for these two arrays. The downtimes inferred from these figures thus represent the cumulative effect of field equipment outages, station site to NOR_NDC communication outage, and NOR_NDC data acquisition outages.

Figs. 4.2.2 and 4.2.3 also give the data availability for these two stations as reported by the IDC in the IDC Station Status reports. The main reason for the discrepancies between the NOR_NDC and IDC data availabilities as observed from these figures is the difference in the ways the two data centers report data availability for arrays: Whereas NOR_NDC reports an array station to be up and available if at least one channel produces useful data, the IDC uses weights where the reported availability (capability) is based on the number of actually operating channels.

Use of the AutoDRM protocol

NOR_NDC's AutoDRM has been operational since November 1995 (Mykkeltveit & Baadshaug, 1996). The monthly number of requests by the IDC for JMIC data for the period July - December 2009 is shown in Fig. 4.2.4.

NDC automatic processing and data analysis

These tasks have proceeded in accordance with the descriptions given in Mykkeltveit and Baadshaug (1996). For the reporting period NOR_NDC derived information on 506 supplementary events in northern Europe and submitted this information to the Finnish NDC as the NOR_NDC contribution to the joint Nordic Supplementary (Gamma) Bulletin, which in turn is forwarded to the IDC. These events are plotted in Fig. 4.2.5.

Data access for the station NIL at Nilore, Pakistan

NOR_NDC has for many years provided access to the seismic station NIL at Nilore, Pakistan, through a VSAT satellite link between NOR_NDC and Nilore. In late July 2009, the VSAT ground station equipment at Nilore failed, and it turned out that this equipment is obsolete and cannot be repaired. The service provider has proposed the installation of new equipment. Following some technical clarifications, NORSAR will submit to AFTAC a proposal for a new satellite communications system between NOR_NDC and Nilore.

Current developments and future plans

NOR_NDC is continuing the efforts towards improving and hardening all critical data acquisition and data forwarding hardware and software components, so as to meet the requirements related to operation of IMS stations.

The NOA array was formally certified by the PTS on 28 July 2000, and a contract with the PTS in Vienna currently provides partial funding for operation and maintenance of this station. The ARCES array was formally certified by the PTS on 8 November 2001, and a contract with the PTS is in place which also provides for partial funding of the operation and maintenance of this station. The operation of the two IMS auxiliary seismic stations on Norwegian territory (Spitsbergen and Jan Mayen) is funded by the Norwegian Ministry of Foreign Affairs. Provided that adequate funding continues to be made available (from the PTS and the Norwegian Ministry of Foreign Affairs), we envisage continuing the provision of data from all Norwegian seismic IMS stations without interruption to the IDC in Vienna.

The two stations PS27 and PS28 are both suffering from lack of spare parts. The PS27 NOA equipment was acquired in 1995 and it is now impossible to get spare GPS receivers. The PS28 ARCES equipment was acquired in 1999, and it is no longer possible to get spare digitizers. A recapitilization plan for both arrays was submitted to the PTS in October 2008, and installation of new equipment will start in 2010.

U. Baadshaug
S. Mykkeltveit
J. Fyen

References

Kradolfer, U. (1993): Automating the exchange of earthquake information. *EOS, Trans., AGU*, 74, 442.

Kradolfer, U. (1996): AutoDRM — The first five years, *Seism. Res. Lett.*, 67, 4, 30-33.

Mykkeltveit, S. & U. Baadshaug (1996): Norway's NDC: Experience from the first eighteen months of the full-scale phase of GSETT-3. *Semiann. Tech. Summ., 1 October 1995 - 31 March 1996*, NORSAR Sci. Rep. No. 2-95/96, Kjeller, Norway.

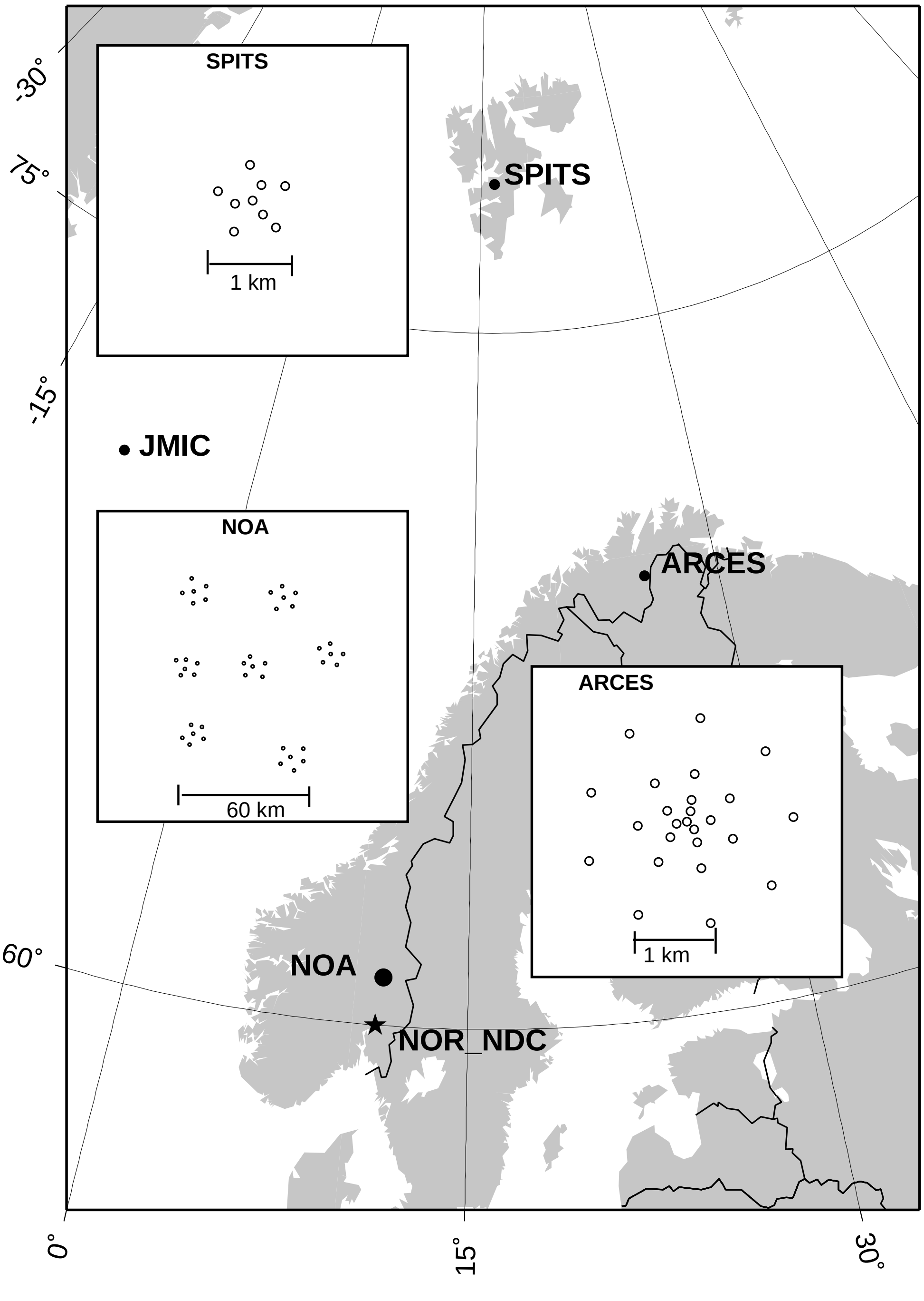

Fig. 4.2.1. The figure shows the locations and configurations of the three Norwegian seismic IMS array stations that provided data to the IDC during the period July - December 2009 The data from these stations and the JMIC three-component station are transmitted continuously and in real time to the Norwegian NDC (NOR_NDC). The stations NOA and ARCES are primary IMS stations, whereas SPITS and JMIC are auxiliary IMS stations.

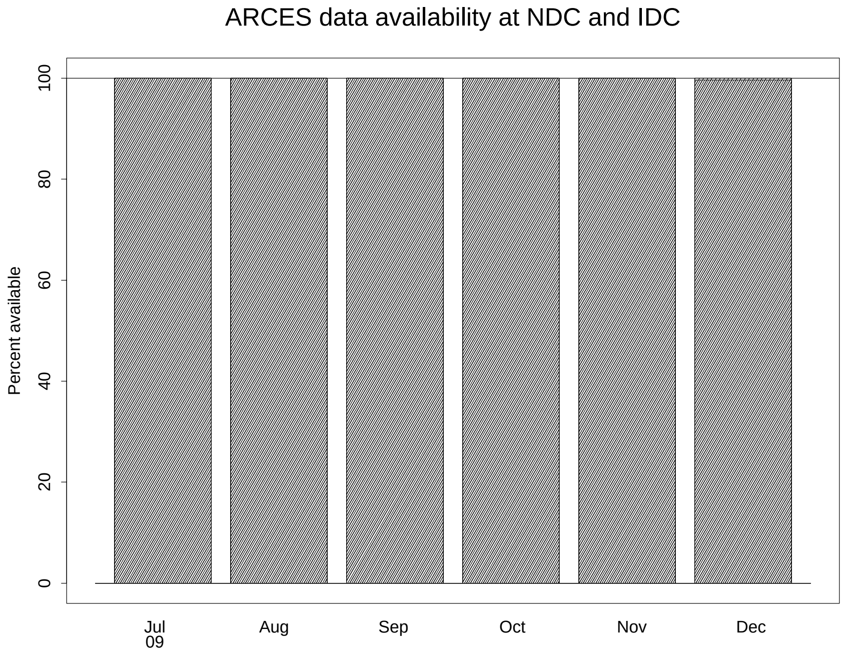

Fig. 4.2.2. The figure shows the monthly availability of ARCES array data for the period July - December 2009 at NOR_NDC and the IDC. See the text for explanation of differences in definition of the term "data availability" between the two centers. The higher values (hatched bars) represent the NOR_NDC data availability.

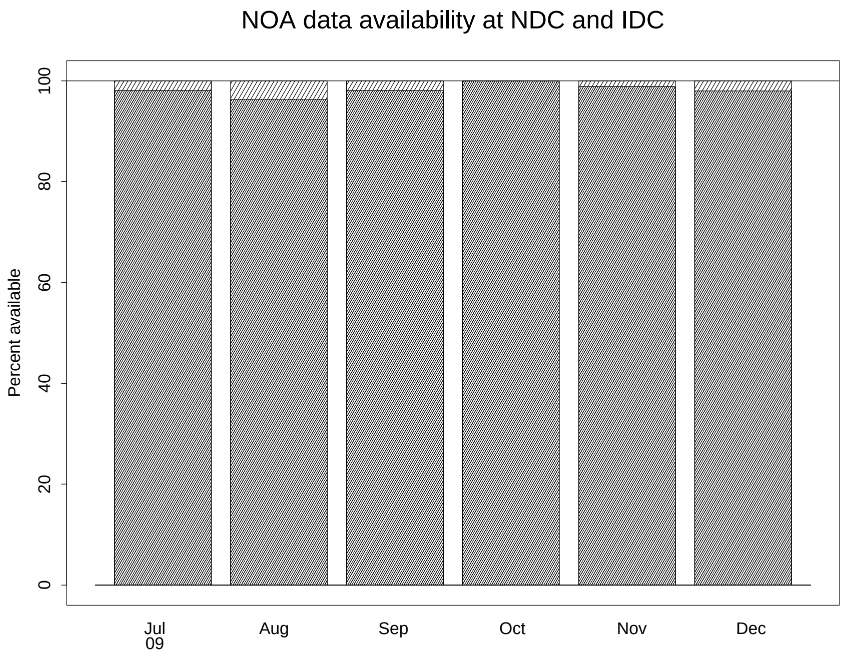

Fig. 4.2.3. The figure shows the monthly availability of NORSAR array data for the period July - December 2009 at NOR_NDC and the IDC. See the text for explanation of differences in definition of the term "data availability" between the two centers. The higher values (hatched bars) represent the NOR_NDC data availability.

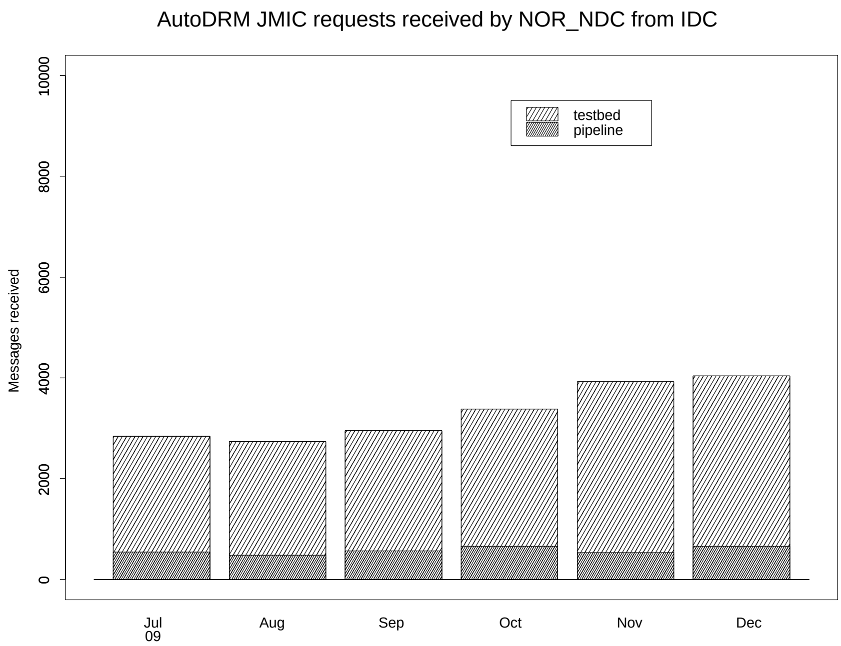

Fig. 4.2.4. The figure shows the monthly number of requests received by NOR_NDC from the IDC for JMIC waveform segments during July - December 2009.

Reviewed Supplementary events

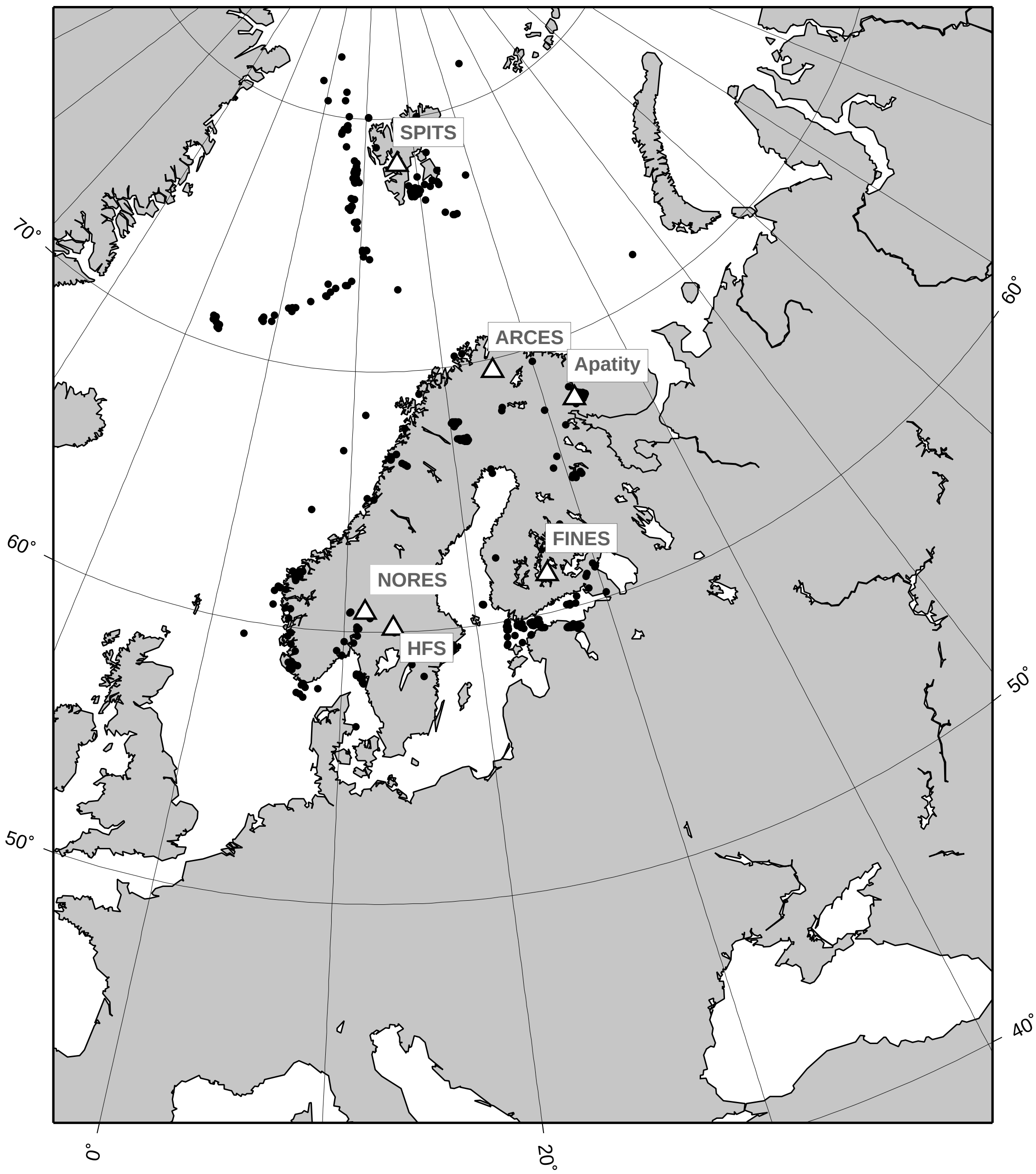

Fig. 4.2.5. The map shows the 506 events in and around Norway contributed by NOR_NDC during July - December 2009 as supplementary (Gamma) events to the IDC, as part of the Nordic supplementary data compiled by the Finnish NDC. The map also shows the main seismic stations used in the data analysis to define these events.

4.3 Field Activities

The activities at the NORSAR Maintenance Center (NMC) at Hamar currently include work related to operation and maintenance of the following IMS seismic stations: the NOA teleseismic array (PS27), the ARCES array (PS28) and the Spitsbergen array (AS72). Some work has also been carried out in connection with the seismic station on Jan Mayen (AS73), the radionuclide station at Spitsbergen (RN49), and preparations for the infrasound station at IS37. NORSAR also acts as a consultant for the operation and maintenance of the Hagfors array in Sweden (AS101).

NORSAR carries out the field activities relating to IMS stations in a manner generally consistent with the requirements specified in the appropriate IMS Operational Manuals, which are currently being developed by Working Group B of the Preparatory Commission. For seismic stations these specifications are contained in the Operational Manual for Seismological Monitoring and the International Exchange of Seismological Data (CTBT/WGB/TL-11/2), currently available in a draft version.

All regular maintenance on the NORSAR field systems is conducted on a one-shift-per-day, five-day-per-week basis. The maintenance tasks include:

- Operating and maintaining the seismic sensors and the associated digitizers, authentication devices and other electronics components.
- Maintaining the power supply to the field sites as well as backup power supplies.
- Operating and maintaining the VSATs, the data acquisition systems and the intra-array data transmission systems.
- Assisting the NDC in evaluating the data quality and making the necessary changes in gain settings, frequency response and other operating characteristics as required.
- Carrying out preventive, routine and emergency maintenance to ensure that all field systems operate properly.
- Maintaining a computerized record of the utilization, status, and maintenance history of all site equipment.
- Providing appropriate security measures to protect against incidents such as intrusion, theft and vandalism at the field installations.

Details of the daily maintenance activities are kept locally. As part of its contract with CTBTO/PTS NORSAR submits, when applicable, problem reports, outage notification reports and equipment status reports. The contents of these reports and the circumstances under which they will be submitted are specified in the draft Operational Manual.

P.W. Larsen
K.A. Løken

5 Documentation Developed

Debski, W., J. Schweitzer, G. Lizurek, T. Kværna, P. Wiejacz, L. Rudinski & J. Suchcicki (2009): A new joint Polish-Norwegian broadband seismic station at Hornsund (Svalbard). Geophys. Res. Abstracts, 11.

Gibbons, S.J., J. Schweitzer, F. Ringdal, T. Kværna & S. Mykkeltveit (2009): Improvements to seismic monitoring of the European Arctic using three-component array processing at SPITS. Geophys. Res. Abstracts, 11.

Gibbons, S.J. (2010): A new source of seismo-acoustic events for the study of infrasound propagation over regional distances. In: Semiannual Technical Summary, 1 July - 31 December 2009, NORSAR Sci. Rep. 1-2010, Kjeller.

Gubbins, D. & S.J. Gibbons (2009): Kinematic dynamo action in a sphere with weak differential rotation. Geophys. J. Int., 177 (1), 71-80.

Kværna, T. (2010): Infrasound signals from recent rocket launches in the White Sea. In: Semiannual Technical Summary, 1 July - 31 December 2009, NORSAR Sci. Rep. 1-2010, Kjeller.

Kværna, T. & F. Ringdal (2010): Seismic event in the eastern Barents Sea, 11 November 2009. In: Semiannual Technical Summary, 1 July - 31 December 2009, NORSAR Sci. Rep. 1-2010, Kjeller.

Pirli, M. (2010): NORSAR System Responses Manual, 2nd Edition, NORSAR, Kjeller, 180 pp.

Pirli, M. & J. Schweitzer (2010): Location of the NDC Preparedness Exercise 2009 event with the use of near-regional data. In: Semiannual Technical Summary, 1 July - 31 December 2009, NORSAR Sci. Rep. 1-2010, Kjeller.

Pirli, M. & J. Schweitzer (2010): Continued overview of array and station system responses contributing to NORSAR's Data Center. In: Semiannual Technical Summary, 1 July - 31 December 2009, NORSAR Sci. Rep. 1-2010, Kjeller.

Ringdal, F., T. Kværna, S.J. Gibbons, S. Mykkeltveit, J. Fyen, M. Roth, P.W. Larsen & J. Schweitzer (2009): Basic research on seismic and infrasonic monitoring of the European Arctic. Geophys. Res. Abstracts, 11.

Ringdal, F., D. Harris, D. Dodge & S. Gibbons (2009): Adaptive waveform correlation detectors for arrays: Algorithms for autonomous calibration. In: Proceedings, Monitoring Research Review 2009 on Ground-based Nuclear Explosion Monitoring Technologies, Tucson, Arizona, 21-23 September 2009.

Ringdal, F., D. Harris, T. Kværna & S. Gibbons (2009): Expanding coherent array processing to larger apertures using empirical matched field processing. In: Proceedings, Monitoring Research Review 2009 on Ground-based Nuclear Explosion Monitoring Technologies, Tucson, Arizona, 21-23 September 2009.

Ringdal, F., T. Kværna, S. Gibbons, S. Mykkeltveit & J. Schweitzer (2009): Basic research on seismic and infrasonic monitoring of the European Arctic. In: Proceedings, Monitoring Research Review 2009 on Ground-based Nuclear Explosion Monitoring Technologies, Tucson, Arizona, 21-23 September 2009.

6 Summary of technical reports / papers published

6.1 Seismic event in the eastern Barents Sea, 11 November 2009

6.1.1 Introduction

On 11 November 2009, at 04.18 GMT, signals from a seismic event in the eastern Barents Sea were recorded by seismic stations in the Nordic countries as well as in NW Russia. This part of the Barents Sea has no known history of significant earthquake activity. However, over the past decades, NORSAR has recorded several seismic events at various locations in this region as listed in the NORSAR reviewed regional seismic bulletin. Furthermore, the explosions associated with the Kursk submarine accident in 2000 and a number of explosions in the following years carried out by the Russian Navy have been recorded and are listed in the regional bulletin (see also Kvaerna, 2001).

The area is of interest in nuclear monitoring primarily because of the proximity to the former Soviet nuclear test site at Novaya Zemlya. Mapping the seismicity of the eastern Barents Sea is also important in assessing seismic hazard for production platforms and pipelines in connection with offshore oil and gas fields, such as the large Shtokman field (see Fig. 6.1.1).

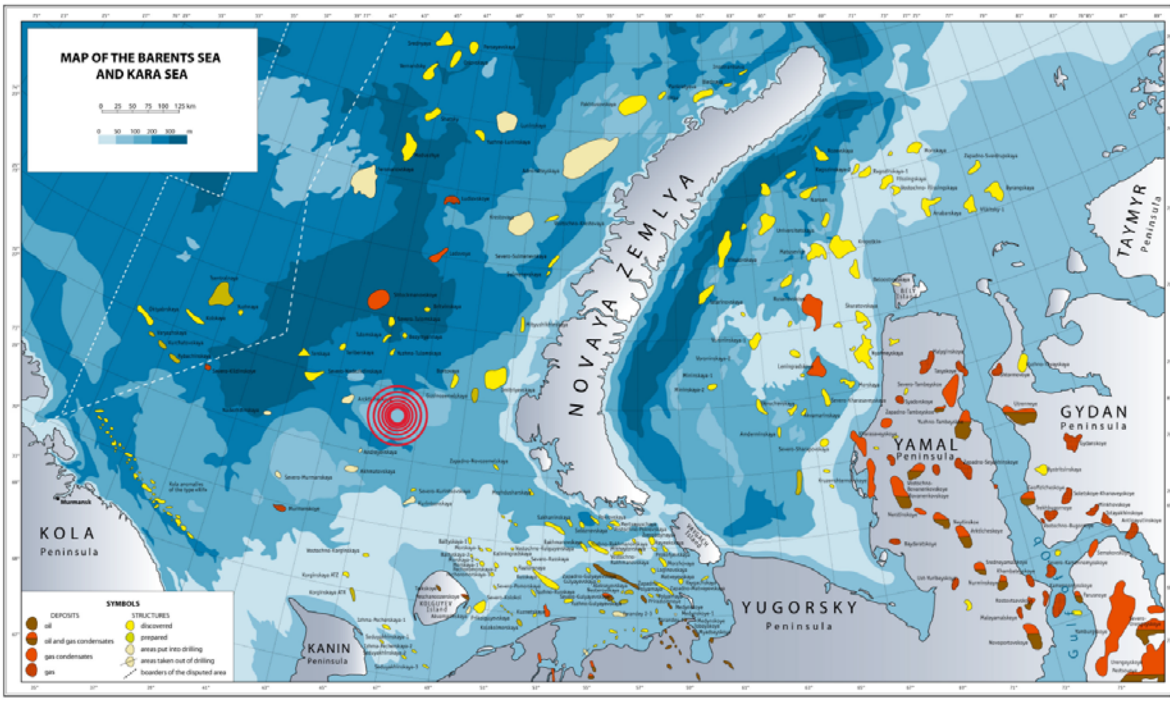

Fig. 6.1.1. Location of the seismic event on 11 November 2009 (red concentric circles). Known hydrocarbon reservoirs are also indicated.

The event parameters as published in the NORSAR bulletin are as follows:

Origin Date/time:	2009/11/11 04:18:21 GMT
Location:	71.58N, 46.09E, Depth 0 (fixed)
Magnitude:	3.2

6.1.2 Observations at ARCES

We have analyzed data from the ARCES array in northern Norway recorded for this event. Fig. 6.1.2 shows filtered recordings (2-16 Hz) of the three-component center seismometer of ARCES. The characteristics of the traces are similar to previous events from this region, with clear Pn and Sn phases, whereas the Pg and Lg phases are not discernible, at least not in this frequency band. We also note that the direction of the event is nearly due east of ARCES, and the consequently the radial component (se) of the Pn-phase is about as strong as the vertical component, while the Sn phase is by far the most prominent on the transverse (sn) component. This is an important confirmation of the advantages of using the transverse component of the seismogram to increase the probability of detecting S-type phases.

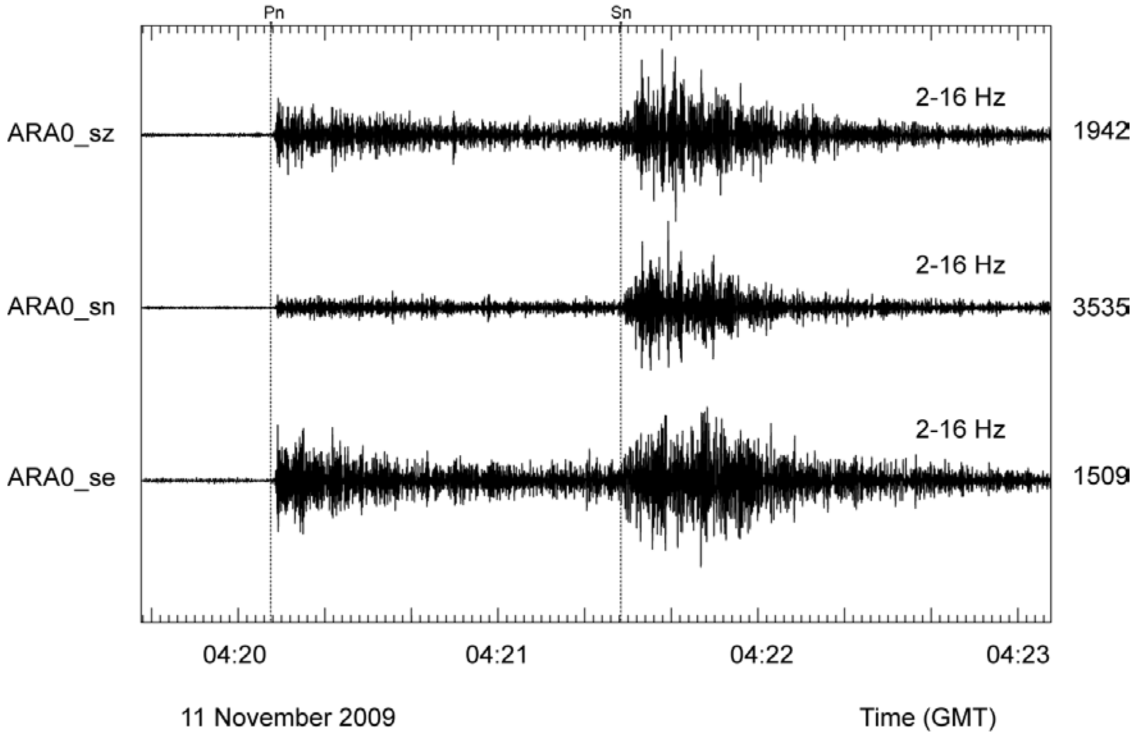

Fig. 6.1.2. Recordings by the three-component center seismometer of the ARCES array of the seismic event in the Barents Sea on 11 November 2009. The traces have been filte ed in the 2-16 Hz frequency band.

The event on 11 November 2009 is also important for another reason. As noted by Ringdal et al. (2008), the available high-frequency data at the time of their study did not include recordings of distant events to the east and north-east of the ARCES array, and the high-frequency propagation from the Novaya Zemlya region to ARCES could therefore not be assessed. The present event (at a distance of 800 km) is the first seismic event occurring in the region near Novaya Zemlya after the high-frequency element was installed at ARCES.

We have therefore made a special analysis of the associated ARCES high frequency recordings. Fig. 6.1.3 shows recordings by the ARCES vertical high-frequency element of the event. The recorded trace (bottom) have been filtered in six different frequency bands as indicated on the figure. We note the high SNR for both the Pn and the Sn phases, even in the highest frequency band plotted (20-40 Hz). The Pg and Lg phases are not easily noticed in any of the frequency bands. Fig. 6.1.4 shows spectra of the Pn and Sn phases as well as the noise spectrum. We note again the high-frequency characteristics of the Pn and Sn phases.

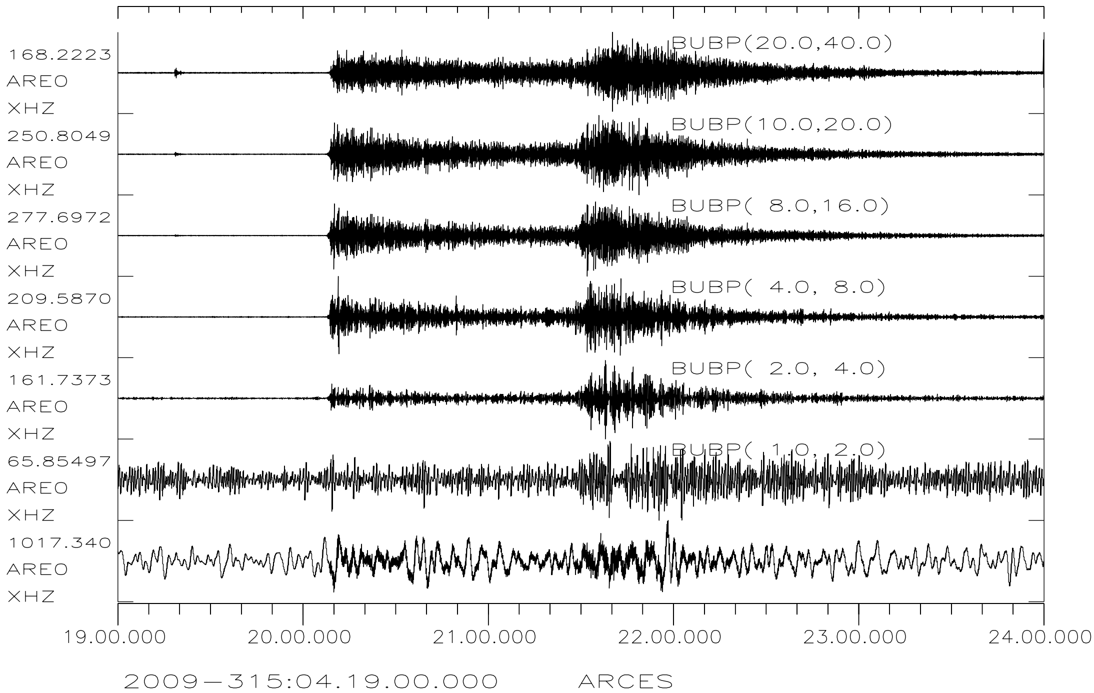

Fig. 6.1.3. Recordings by the ARCES vertical high-frequency element of the seismic event on 11 November 2009. The trace have been filte ed in six different frequency bands as indicated. Note the high SNR for both the Pn and the Sn phases, even in the highest frequency band plotted (20-40 Hz). The Pg and Lg phases are not noticeable in any of the frequency bands.

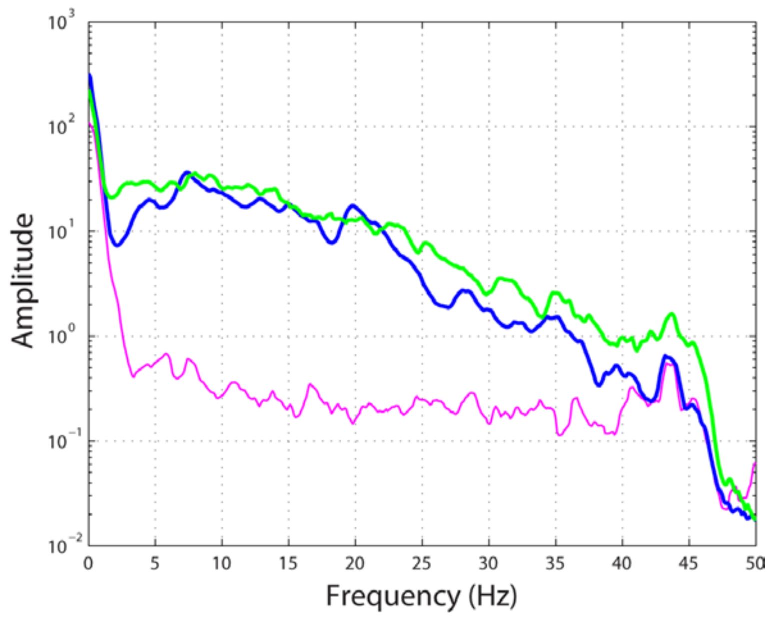

Fig. 6.1.4. Spectra from the ARCES vertical high-frequency element of the Pn (blue) and Sn (green) phases of the 11 November 2009 event. The noise spectrum (magenta) preceding the event is also shown.

6.1.3 Comparison with previous events

After the ARCES high-frequency element was installed, there have been a number of seismic events in or near the mining regions of NW Russia. However, the distance from ARCES to these events are 300 km or less, whereas the epicentral distance of the 11 November 2009 event was as large as 800 km. Nevertheless, it could be of interest to compare the latter event to some of the presumed underwater explosions at about 300 km distance.

One way to make such a comparison is to plot spectrograms as shown in Fig. 6.1.5. Again, a remarkably high signal energy for the Pn and Sn phases is noticeable at high frequencies. Figure 6.1.6 is similar to Fig. 6.1.5, and shows spectrograms from a series of events in the Barents Sea on 19 October 2008. We note that the presumed explosions in 2008 have their dominant energy at much lower frequencies than the event in 2009, even though the latter event is at a much larger distance from ARCES. The spectral scalloping evident in the 2008 plot is typical of many underwater explosions, and is associated with multiple reflections from the bottom and surface of the water.

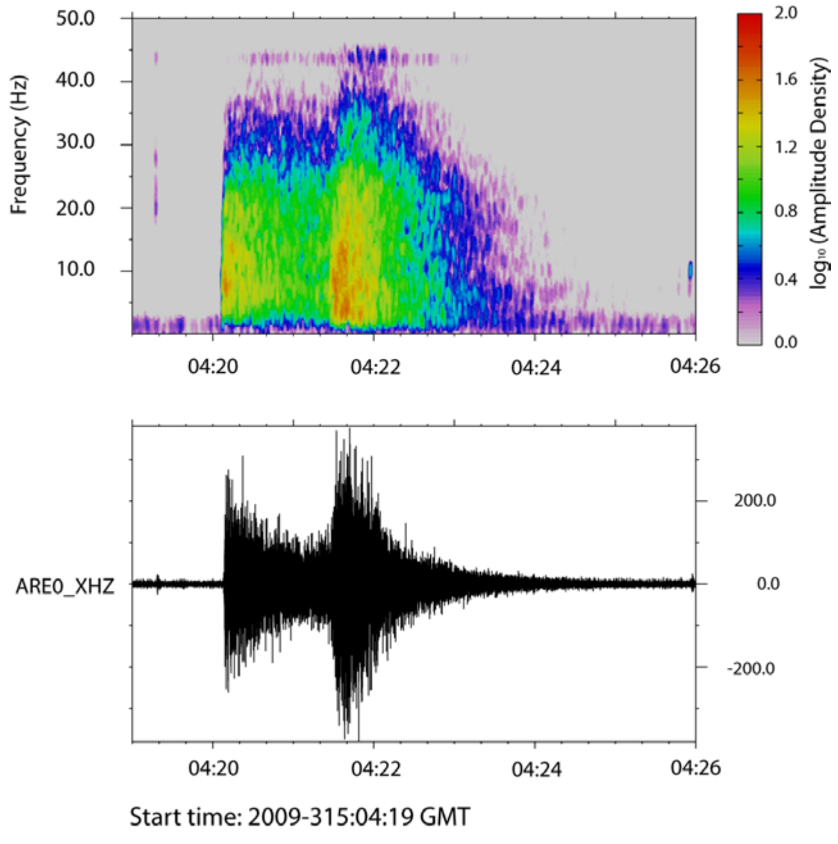

Fig. 6.1.5. Spectrograms from the ARCES vertical high-frequency element of the seismic event on 11 November 2009. The trace have been high-pass filte ed at 2.2 Hz. Note the significan energy for both the Pn and the Sn phases, even up to 40 Hz.

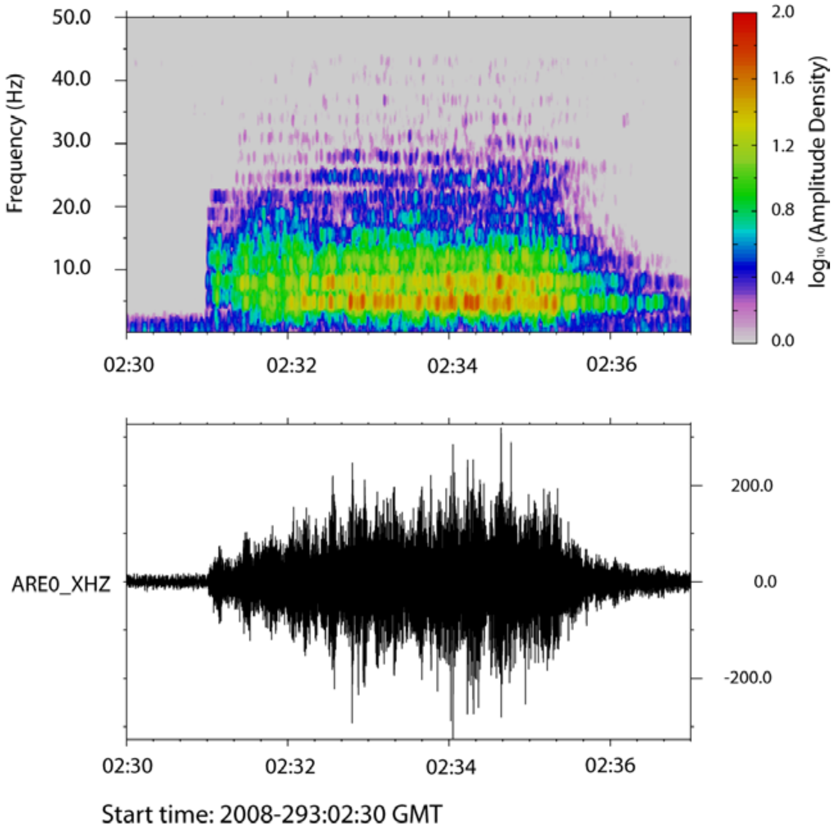

Fig. 6.1.6. Spectrograms from the ARCES vertical high-frequency element of a sequence of co-located presumed underwater explosions near the northern coast of the Kola Peninsula on 19 October 2008. The trace have been high-pass filte ed at 2.2 Hz. Note the significant dif ferences from the plot in Fig. 6.1.5.

6.1.4 Cepstral analysis

We have applied the software described by Öberg et al. (2004) to compare the cepstral peaks associated with various categories of events in the Barents Sea region. We have not used the high-frequency element for this purpose, and consequently we have a number of candidate events. Fig. 6.1.7 and 6.1.8 show the two events described earlier. The cepstral peak is significantly higher for the 2008 event than for the 2009 event. We know from previous studies that cepstral peaks are usually more pronounced for underwater explosions than for earthquakes, although it is difficult to discriminate reliably using this criterion only.

In order to further illustrate the ARCES cepstral analysis, we include some plots of previous presumed earthquakes and explosions in the Barents region. Fig. 6.1.9 shows two known underwater explosions (associated with the Kursk accident) and one presumed underwater explosion, while Fig. 6.1.10 shows two presumed earthquakes. The cepstral peaks are much more prominent for the three explosions than for the two earthquakes.

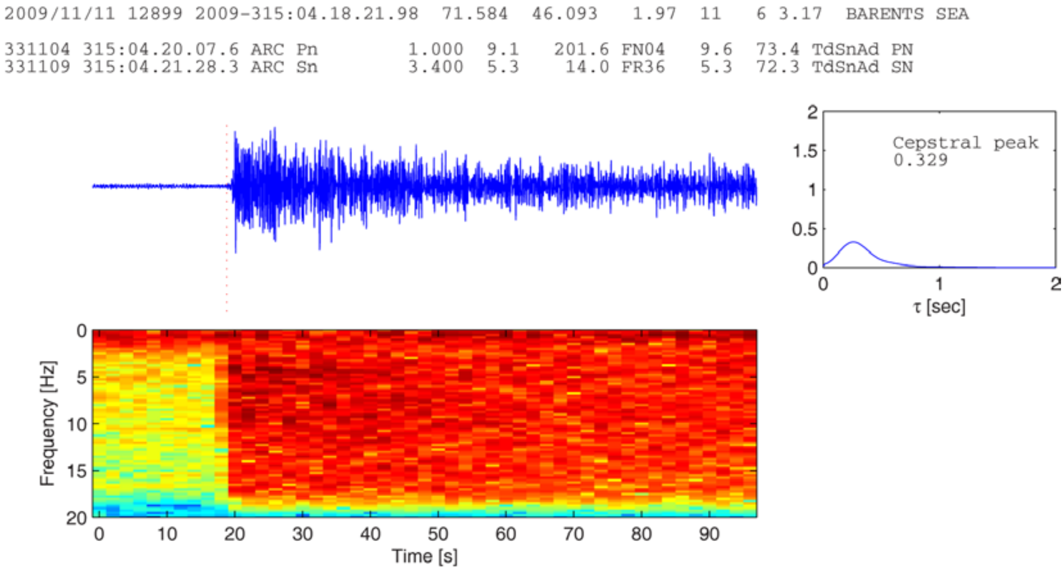

Fig. 6.1.7. Spectrograms from the ARCES vertical central seismometer of the seismic event on 11 November 2009 along with a plot showing the associated cepstral peak.

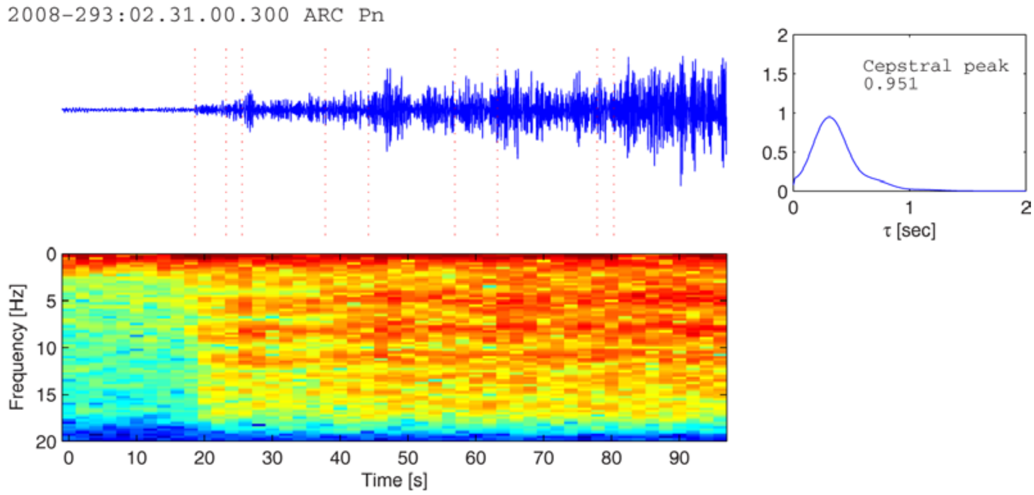

Fig. 6.1.8. Spectrograms from the ARCES vertical central seismometer of a sequence of co-located presumed underwater explosions near the northern coast of the Kola Peninsula on 19 October 2008, along with a plot showing the associated cepstral peak.

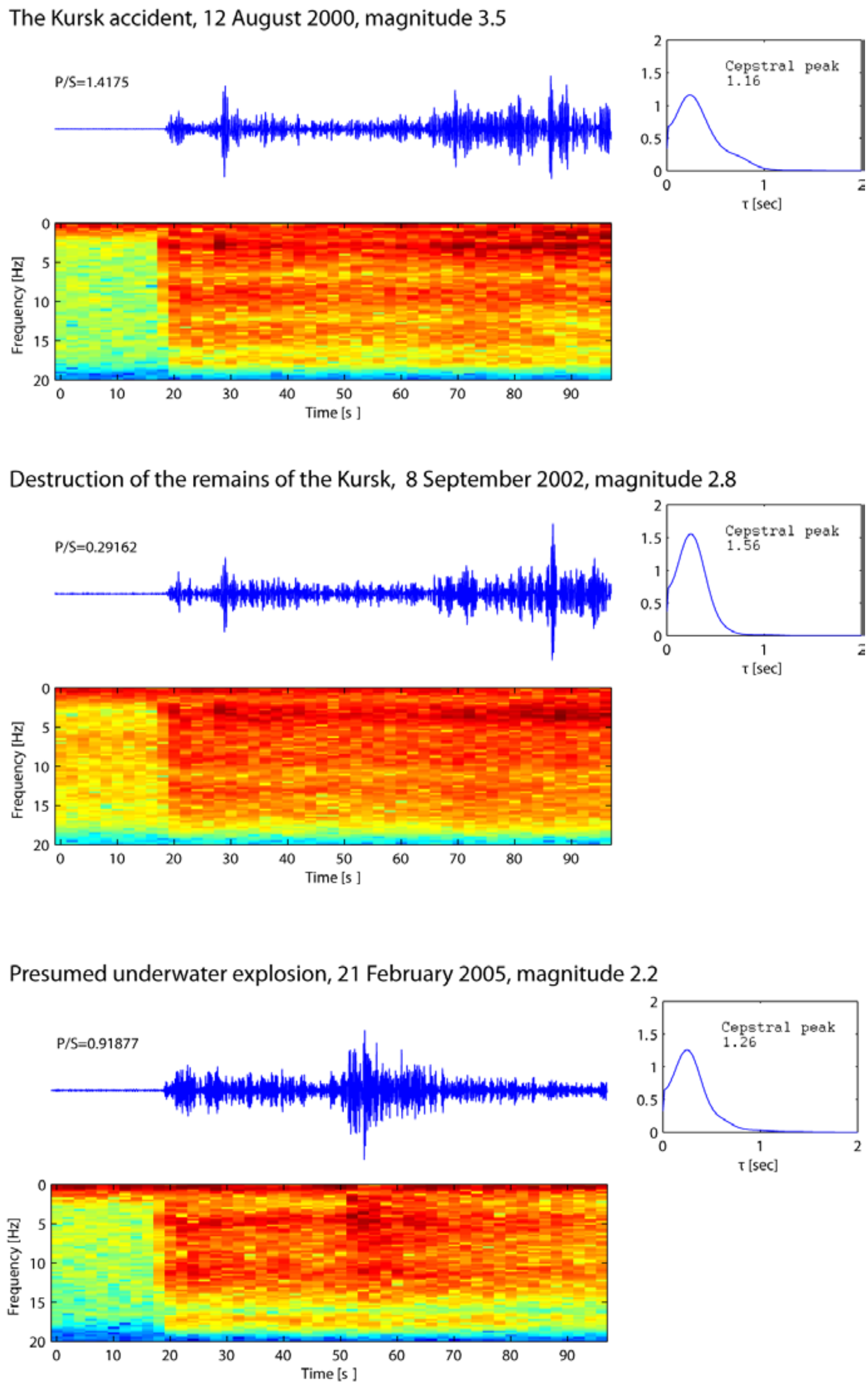

Fig. 6.1.9. Spectrograms from the ARCES vertical central seismometer of three underwater explosions in the Barents Sea, along with plots showing the associated cepstral peaks.

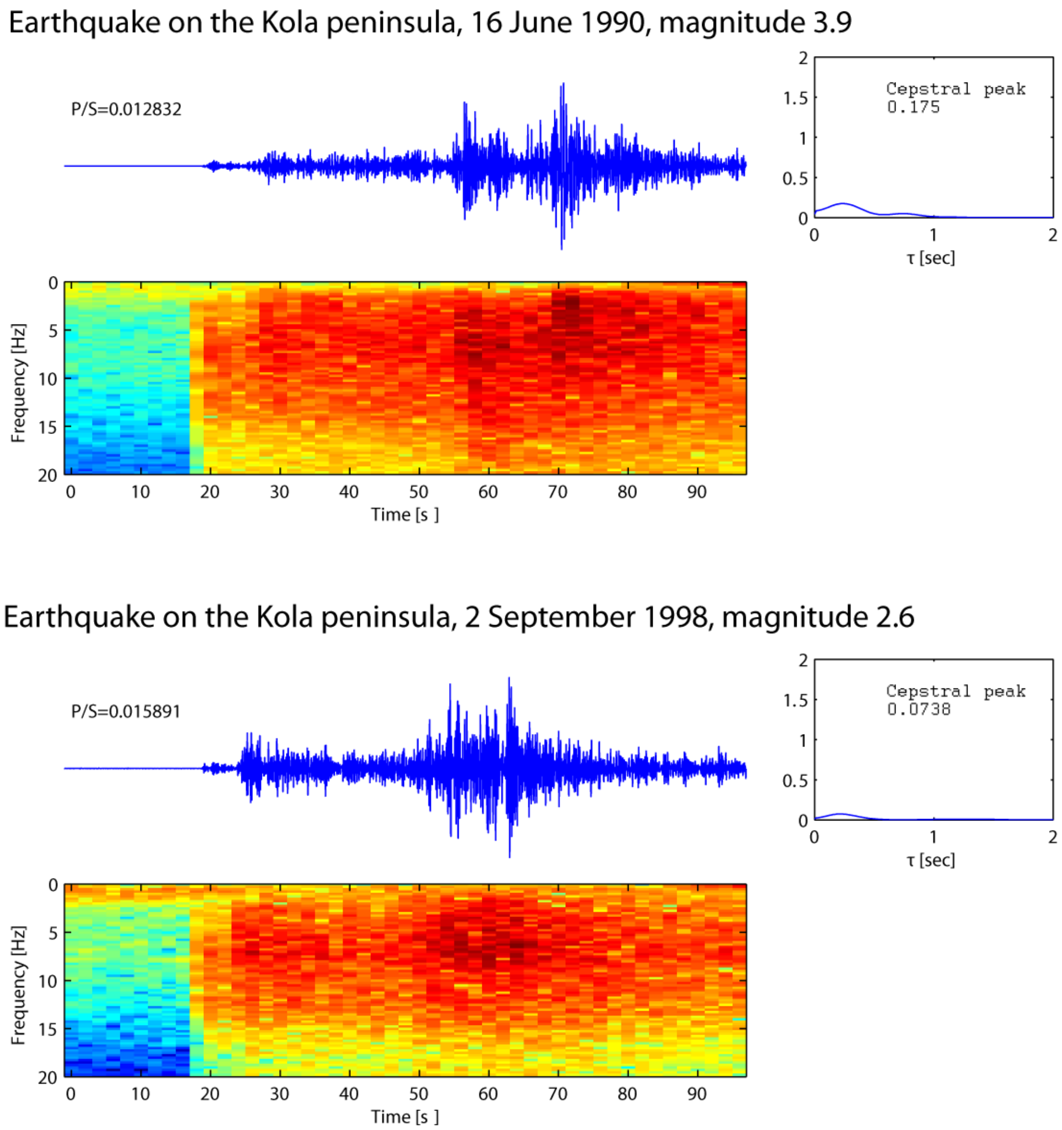

Fig. 6.1.10. Spectrograms from the ARCES vertical central seismometer of two presumed earthquakes located in the northern part of the Kola peninsula, along with plots showing the associated cepstral peaks

6.1.5 Conclusions

Seismic events in the eastern Barents Sea are rare, and the event on 11 November 2009 is therefore of considerable interest. It is the first recorded seismic event in this region since the new high-frequency system was installed at the ARCES array on 23 March 2008. Our analysis of this event confirms the preliminary results of Ringdal et al. (2008) that there is a remarkably efficient propagation from distant events recorded at ARCES at frequencies up to 30 Hz and above.

This result is similar to what has been previously observed at the Spitsbergen array for paths from Novaya Zemlya crossing the Barents Sea. The Spitsbergen studies showed that energy exceeding 20 Hz can be recorded with good signal-to-noise ratio even for small events at epicentral distances as large as 1000 km and we see a similar result in this study, although the event is at a slightly shorter distance (800 km).

As discussed by Ringdal et al. (2008), there are several advantages of high-frequency recordings in a nuclear monitoring context. Although the best filter band for event detection over paths across the Barents region generally appears to be either 4-8 Hz or 8-16 Hz, the most remarkable result shown in our previous as well as the current study is the strong SNR even at the highest frequencies (up to 40 Hz). While such frequencies would not be used for detection purposes, the high frequency data could be very important for signal characterization, as also pointed out by Bowers et. al. (2001) in their paper discussing the level of deterrence to possible CTBT violations in the Novaya Zemlya region provided by data from the Spitsbergen array. In fact, it appears from the present study that similar advantages are provided by the ARCES array. Another example would be to assist in identifying ripple-fired mining explosions or underwater explosions.

As to the source type of the 11 November 2009 event, we are not at this time in a position to give a firm conclusion. The cepstral analysis would indicate that the event is more likely an earthquake than an underwater explosion, but the reliability of the cepstral peak as a discriminant cannot be reliably assessed in this region, due to lack of a sufficient data base.

As more data is accumulated by the ARCES and Spitsbergen high-frequency systems, we may in the future be in a position to carry out a detailed study of the propagation characteristics for additional paths in the region, and make a systematic study of the benefits from combining the high-frequency observations from Spitsbergen and ARCES. This would be expected to contribute to a better understanding of various discriminants for the Barents region. The usefulness of the horizontal components for high-frequency S-phase detection, already demonstrated for the Spitsbergen array, is also an area that needs further study for ARCES.

References

Bowers, D., P. D. Marshall, and A. Douglas (2001). The level of deterrence provided by data from the SPITS seismometer array to possible violations of the Comprehensive Test Ban in the Novaya Zemlya region, *Geophys. J. Int.*, 146, pp. 425-438.

Kværna, T. (2001). Experimental threshold monitoring of the area surrounding the site of the Kursk submarine accident. *In NORSAR Scientifi Report No. 1-2001: Semiannual Technical Summary, NORSAR, Kjeller, Norway.*

Ringdal, F., Kværna, T., and Gibbons, S. J. (2008). Initial studies of high-frequency signals recorded at ARCES infrasound sensors. *In NORSAR Scientific Report No. 2-2008 Semiannual Technical Summary, NORSAR, Kjeller, Norway.*

Öberg, D., Kværna, T. and Ringdal, F. (2004). Discriminants for seismic monitoring. *In NORSAR Scientific Report: Semiannual echnical Summary No. 1-2004, NORSAR, Kjeller, Norway.*

Tormod Kværna
Frode Ringdal

6.2 Infrasound signals from recent rocket launches in the White Sea

6.2.1 Event on 15 July 2009

International news media reported in July 2009 on an unsuccessful launch of the new Russian intercontinental Bulava missile. The missile was launched from a submarine in the White Sea on 15 July. Figure 6.2.1 below shows an excerpt from the internet publication Aviation Week on 17 July, where it is stated that the technical problems resulted in a self-destruction of the missile at the initial stage of the flight.

AVIATION WEEK

Click to Print

Close

By Alexey Komarov
Moscow

The 11th test flight of an R-30 Bulava (SS-NX-30) solid-propellant ballistic missile, from the Borey-class flagship submarine Yury Dolgoruky in the White Sea on July 15 resulted in self-destruction of the missile at an initial stage of flight.

According to the Russian Defense Ministry statement the first stage of the missile malfunctioned and the weapon self-destructed. Special investigation commission has already established to find the failure cause, a ministry representative told reporters.

It was the sixth failure for the Bulava. After previous unsuccessful launch on December 2008 tests were suspended until the origin of malfunction had been determined. Officials from the investigation committee blamed low-quality components as a major source of problems.

Earlier this year, Deputy Defense Minister Vladimir Popovkin said the ministry expects to complete trials by the end of 2009. Consequently, more than four missiles were planned to be built and tested this year, with the missiles put into service almost immediately.

The Yury Dolgoruky, a Typhoon submarine in NATO classification, is designed to carry up to 16 Bulavas and is also undergoing trials. Another two subs of the class, Alexander Nevsky and Vladimir Monomach, are being constructed at the Severodvinsk Shipyard. Military experts believe up to 40% of Russia's defense budget for this year was allocated for Bulavas and submarine construction and tests.

Meanwhile, Russian firings of the in-service Sineva missile were successful. One of the Sineva launches used a flattened trajectory according to the government press agency Novosti. Sineva firings were carried out from Delta IV-class boats.

Photo: Russian Federation MoD

The McGraw-Hill Companies

Fig. 6.2.1 Excerpt from the internet publication Aviation Week on 17 July 2009

Infrasound signals associated with this rocket launch were recorded at NORSAR's infrasound station at ARCES and the four stations in Sweden and Finland operated by the Swedish Institute of Space Physics (IRF). Figure 6.2.2 shows clear observations at all stations in the time period 17:55 - 18:25 UTC in 15 July 2009. The pattern of signal pulses are quite similar among the different stations.

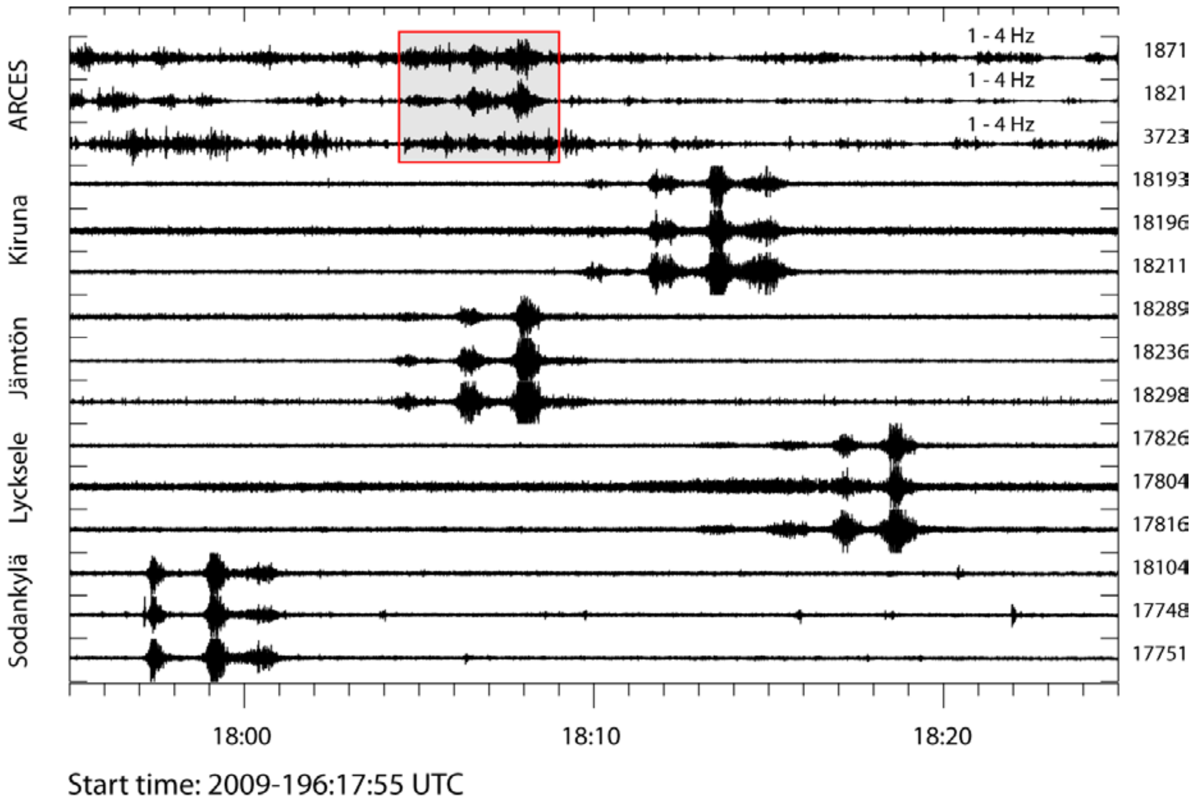

Fig. 6.2.2 Infrasound signals observed in the time period 17:55 to 18:25 UTC on 15 July 2009 at infrasound stations in Norway (ARCES), Sweden (Kiruna, Jämtön and Lycksele) and Finland (Sodankylä). The red rectangle indicates the time period with signals at the ARCES infrasound sensors. The locations of the infrasound sensors are shown in Figure 6.2.4.

Figure 6.2.3 shows azimuthal vespagrams for the different stations for a 10-minute interval centered around the main signal energy. The vespagrams provide information about changes in back-azimuths as a function of time. As seen from Figure 6.2.3, the back-azimuths are relatively constant within the wavetrains of each station. The directional estimates from the different stations are given in Table 6.2.1. We have applied these for location of the event, which we found to be in the White Sea (see Figure 6.2.4). NORSAR's event location has the coordinates:

65.92^{o}N 36.81^{o}E

We have been provided location estimates from Prof. L. Liszka of IRF based on analysis of the two largest signal pulses observed at the 4 stations operated by IRF. These are:

65.77^{o}N 36.89^{o}E
65.69^{o}N 37.08^{o}E

The approximate origin time of the event is estimated to 17:30 UTC.

The strong signal pulses at each station most likely correspond to different stratospheric arrivals. However, both the take-off of the missile and the self-destruction may have lead to the generation of distinct signal pulses at different times, but we are unable to resolve this from our data.

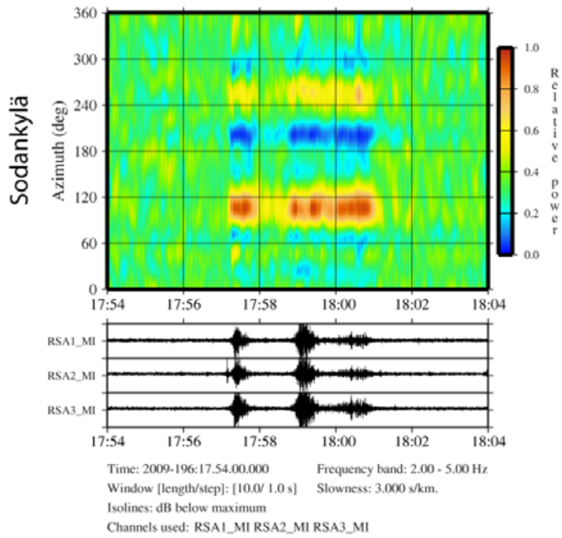

Fig. 6.2.3. Waveforms and vespagrams for a 10-minute segment around the infrasound signals from the event in the White Sea in 15 July 2009. The most energetic areas in the vespagrams (red) indicate the back-azimuth of the arriving signals. The secondary maxima are caused by side-lopes of the recording arrays. A constant sound velocity of 333 m/s is used in the calculation of the vespagrams.

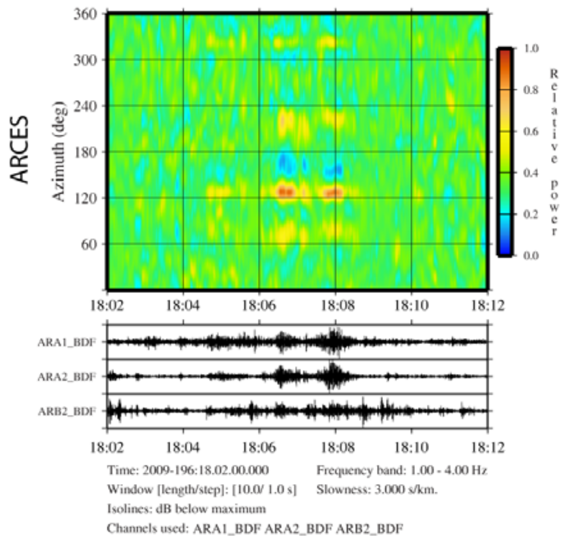

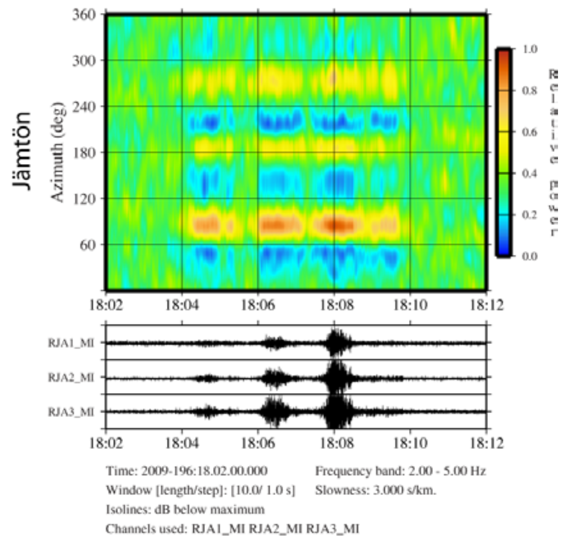

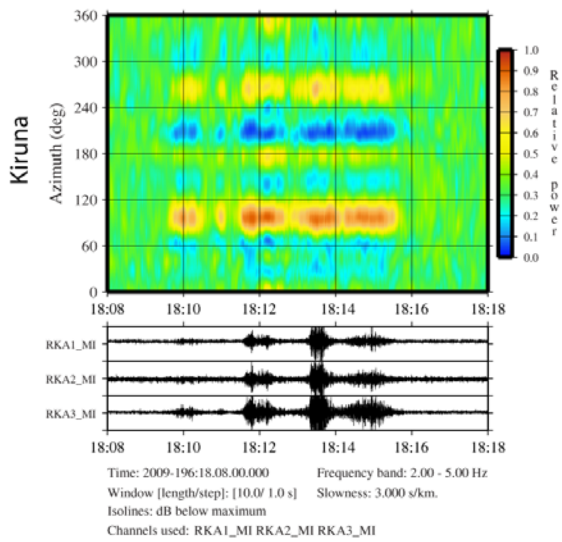

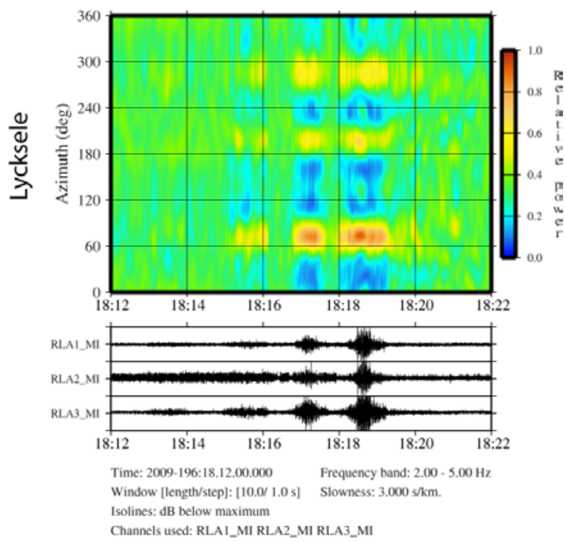

Table 6.2.1. Distances and back-azimuths to the event located in the White Sea on 15 July 2009. The event location estimate is 65.92°N, 36.81°E

Station	Latitude (N)	Longitude (E)	Distance (km)	Back-azimuth (°)
Sodankylä	67.42	26.39	489	105.5
ARCES	69.54	25.51	624	126.3
Jämtön	65.86	22.51	651	83.5
Kiruna	67.86	20.42	747	95.3
Lycksele	64.61	18.75	853	73.5

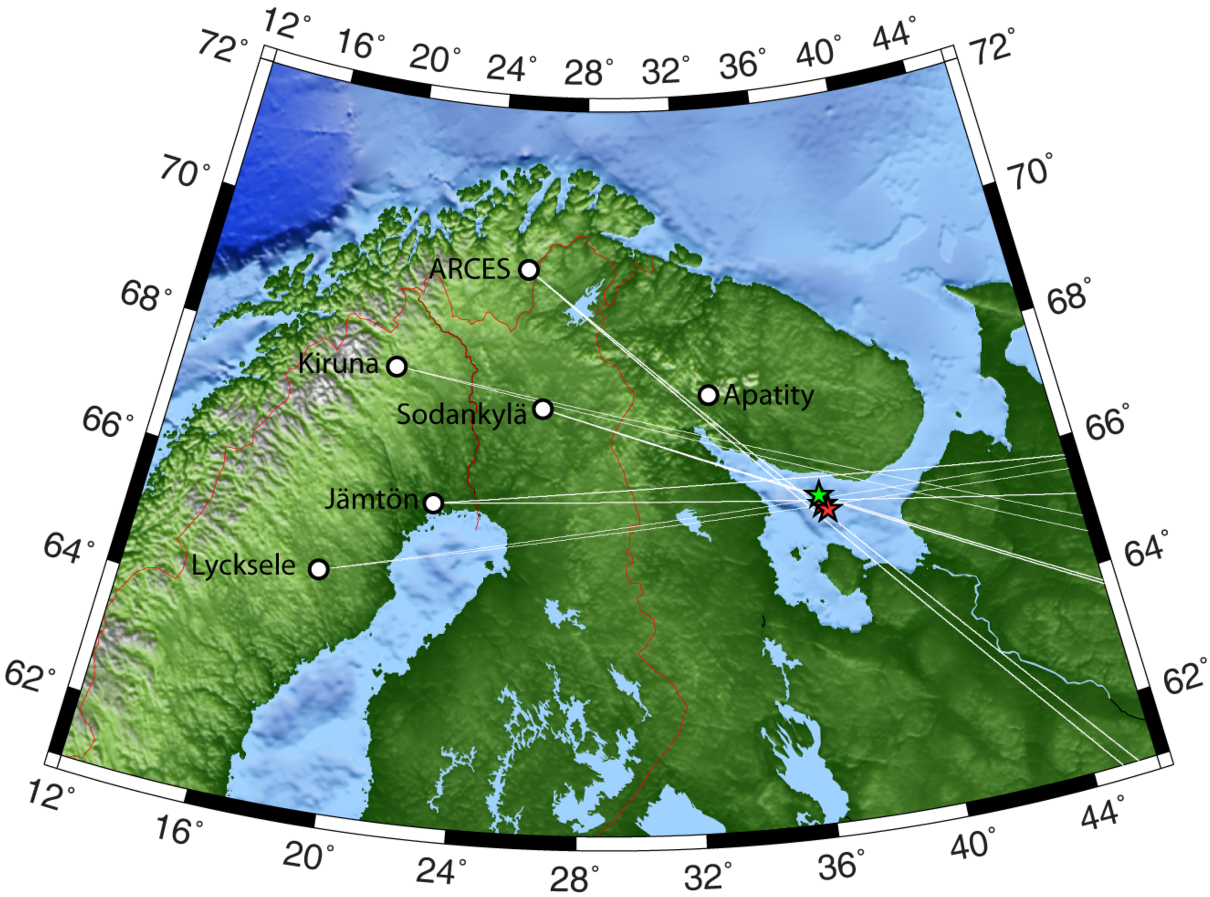

Fig. 6.2.4 Map of infrasound stations in Norway, Sweden, Finland and NW Russia. The station in Apatity was out of operation on 15 July 2009. The white great-circles show estimated back-azimuths from the different stations. Our location is shown by a green star. The red stars show locations provided by Prof. L. Liszka of the Swedish Institute of Space Physics.

6.2.2 Event on 9 December 2009

Around 6:50 UTC on 9 December 2009, strange light phenomena were observed in northern Norway. Figure 6.2.5 shows a photograph taken near Tromsø.

Fig. 6.2.5 Photograph take near Tromsø, northern Norway, of the light phenomena observed around 6:50 UTC on 9 December 2009. The picture is copied from the web page of the newspaper Nordlys at the internet address http://www.nordlys.no/nyheter/bildeserier/article4750399.ece?start=6

These observations caused a lot of attention in the news media, and after a while it became evident that the phenomena were caused by another failure of a Russian Bulava missile. According to the Russian Defence Ministry there was an engine failure in the third stage of the flight that caused the problem. According to recent information provided by the Norwegian Ministry of Defence, they believe that the missile exploded at an altitude between 100 and 300 km above the Novaya Zemlya region, and that the missile was launched from a submarine in the north-eastern part of the White Sea.

Infrasound signals believed to originate from this rocket launch were observed at ARCES as well as at the infrasound station in Apatity on the Kola peninsula. No infrasound signals were found at the stations of the IRF network.

Figure 6.2.6 shows infrasound observations at the ARCES array. From f-k analysis we estimate a back azimuth of about 117^{o} for this signal (see Figure 6.2.7).

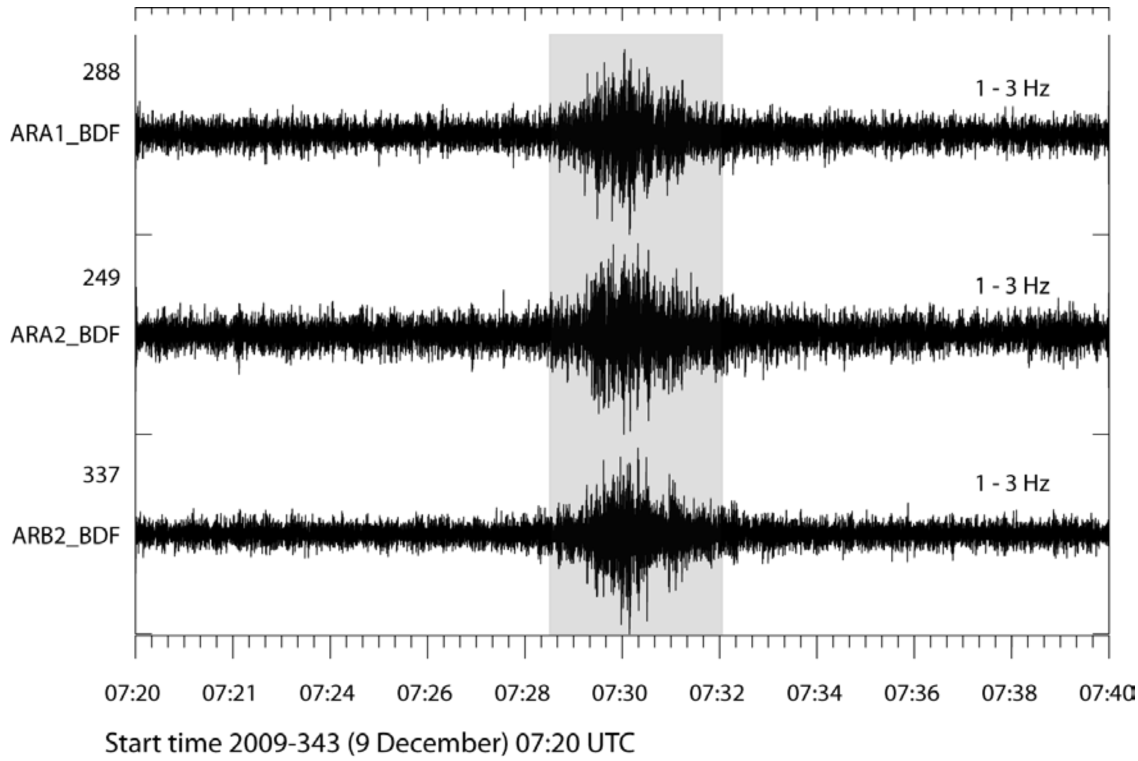

Fig. 6.2.6. Observations at the ARCES infrasound station on 9 December 2009 at about 07:30 UTC. The data are bandpass filtered between 1 and 3 Hz.

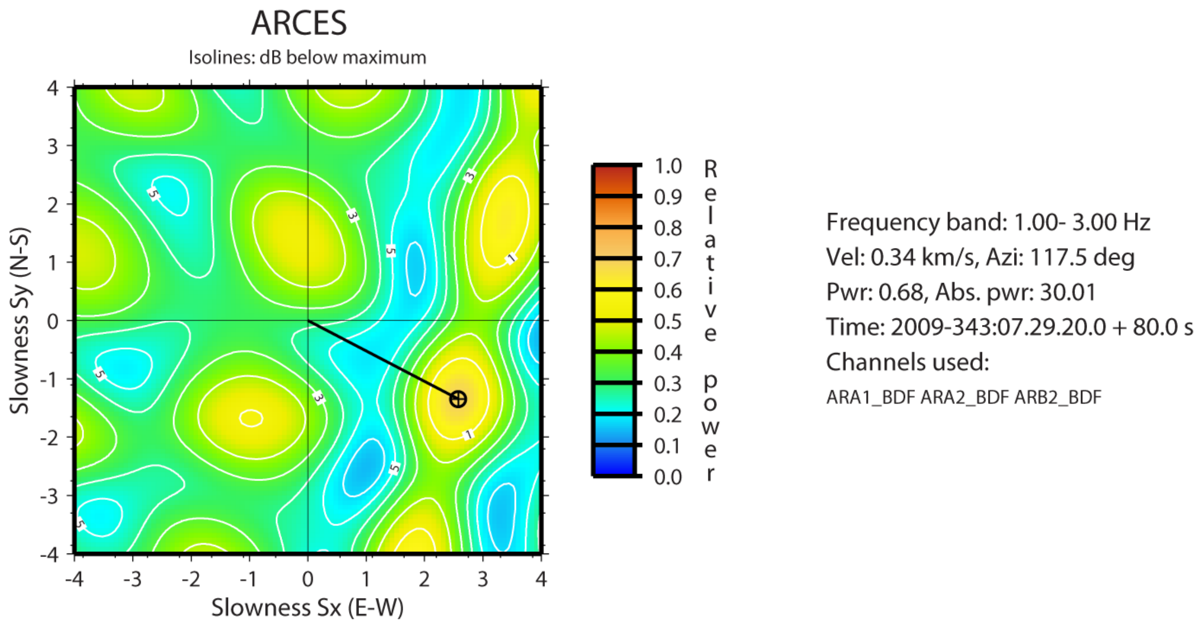

Fig. 6.2.7 F-k analysis of the ARCES infrasound signal shown within the grey-shaded area of Figure 6.2.6.

Clear signals were also observed at the Apatity array (see Figure 6.2.8), but unfortunately only two infrasound sensors were operating at this time. Standard f-k estimation could thus not be performed for back-azimuth estimation. However, by assuming a standard propagation velocity across the array (333 m/s) an azimuthal vespagram could be computed. With only two available sensors, this vespagram exhibit a mirrored image with two maxima (see Figure 6.2.9), and we have to select one of these. As we expect this signal to be associated with the Bulava missile, we selected the lowermost maximum having a back-azimuth ranging between 120 and 130 degrees.

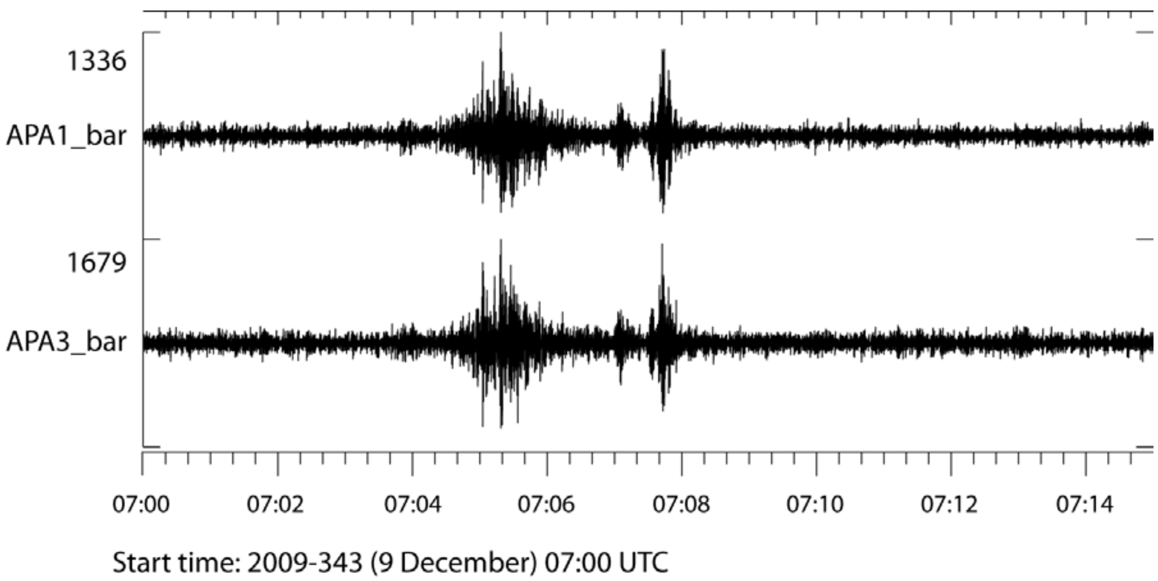

Fig. 6.2.8 Observations at the Apatity infrasound station on 9 December 2009. The signal energy arrives between 07:04 and 07:08 UTC.

Tracing the intersection between the estimated back-azimuths at the ARCES and Apatity infrasound stations, we indicate in Figure 6.2.10 a source region for the infrasound signal. The distances to the Apatity and ARCES stations are approximately 360 km and 730 km, respectively. Applying a standard celerity of 0.29 km/s for stratospheric arrivals we obtain a time difference of about 22 minutes between the Apatity and ARCES infrasound arrivals, which is approximately what we observe at the two stations (see Figures 6.2.6 and 6.2.8). The estimated origin time of the event is in the time interval 06:45 - 06.48 UTC, and the event is most likely associated with the launch of the Bulava missile from the submarine. We do not believe that the infrasound signals are associated with the explosion causing the light phenomena shown in Figure 6.2.5

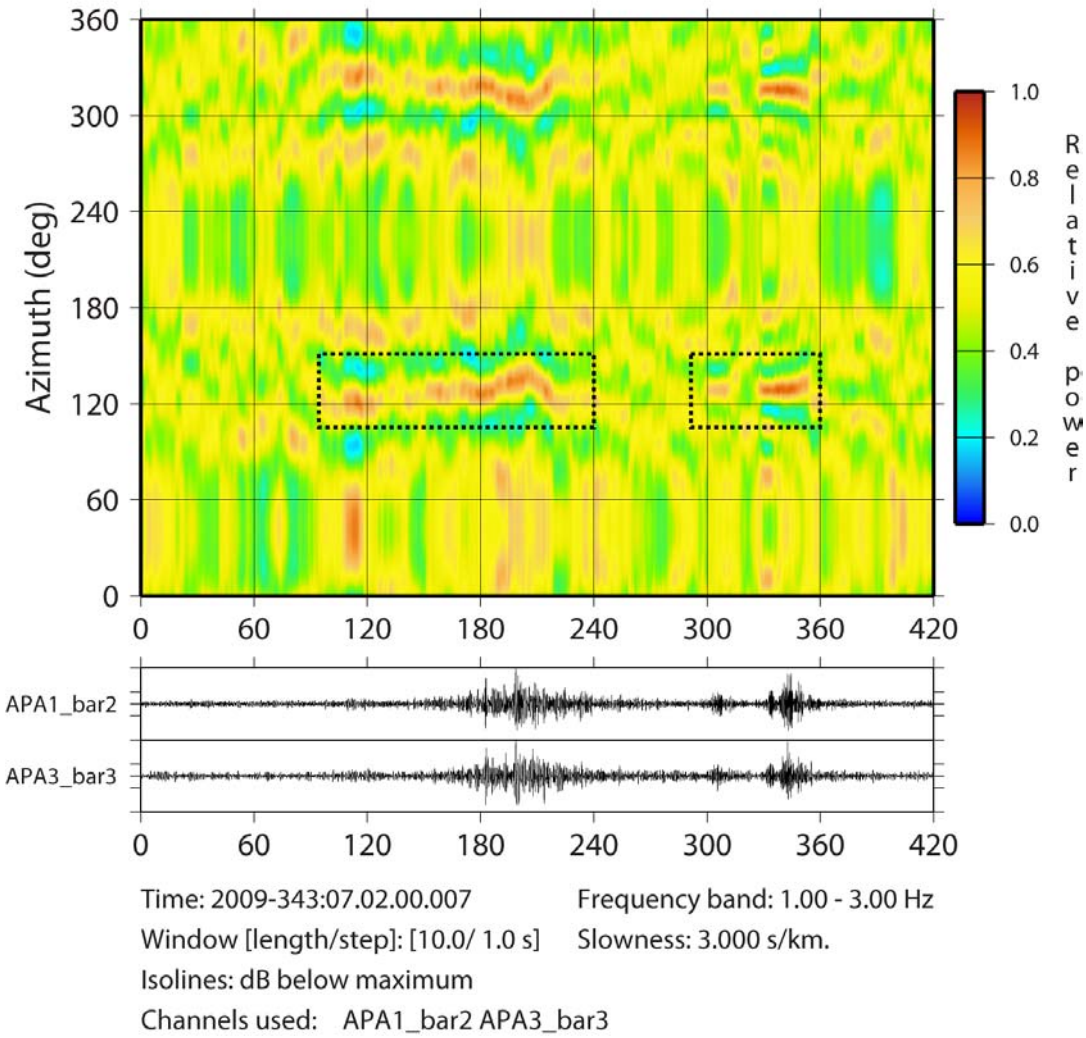

Fig. 6.2.9 Azimuthal vespagram using the two operational Apatity infrasound sensors for the time period 07:02 - 07:09 on 9 December 2009. A standard sound propagation velocity of 333 m/s was applied. The selected vespagram maxima are indicated by dotted rectangles, and these show variation in back-azimuths ranging between 120 and 130 degrees.

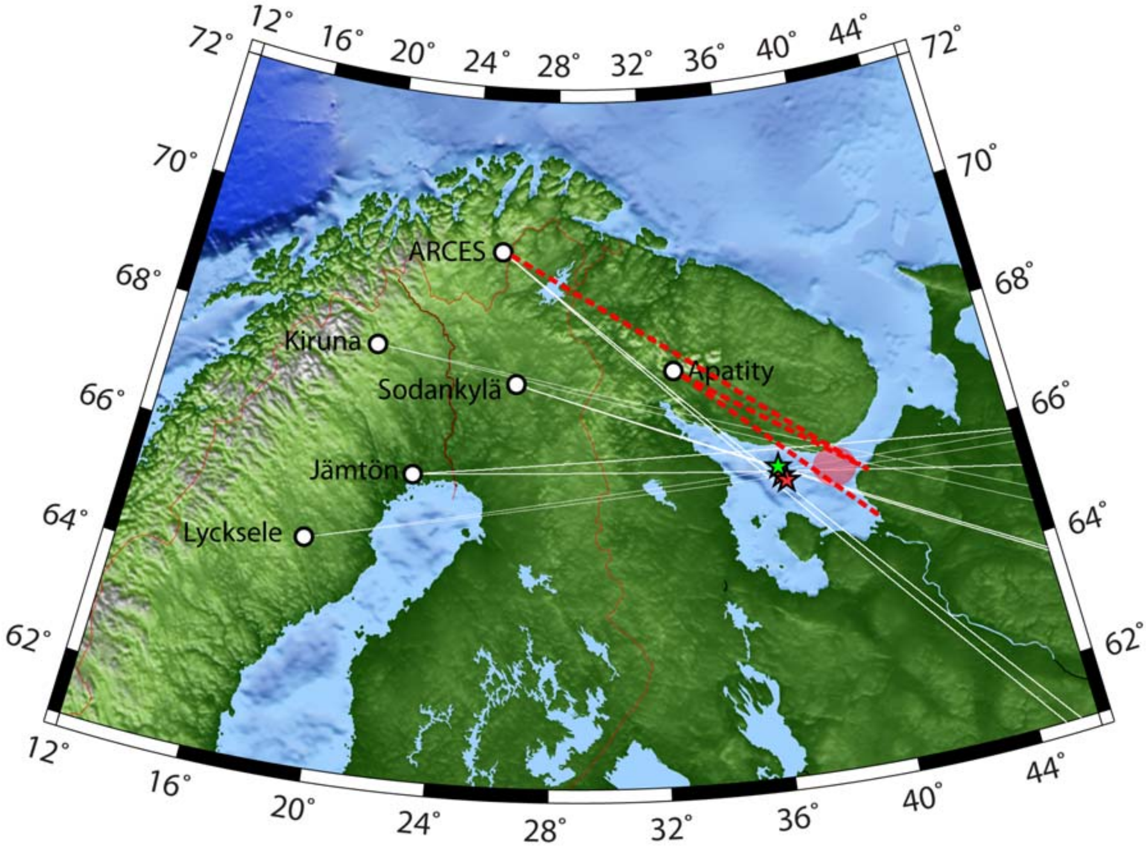

*Fig. 6.2.10 The dashed red lines show estimated back-azimuths from the ARCES and Apatity infrasound arrays for the 9 December 2009 event. The approximate source region of this event is indicated by the red ellipse.
For comparison, the red and green stars show the estimated locations of the 15 July 2009 event. See caption of Figure 6.2.4 for details.*

Acknowledgements

This research has been supported by the US Army SMDC under contract W9113M-05-C-0224. We are grateful to Professor Ludwik Liszka at the Swedish Institute of Space Physics, Umeå, Sweden, for providing access to the infrasound data from the IRF station network.
We thank colleagues at the Kola Regional Seismological Center for providing the infrasound data from the mircobarograph array at Apatity, Russia.

Tormod Kværna

6.3 A New Source of Seismo-Acoustic Events for the Study of Infrasound Propagation over Regional Distances

Since June 8, 2007, a seismic event alert system has been operational at NORSAR to provide early notification of, and robust preliminary location estimates for, earthquakes and other seismic events in the European Arctic. It is based on the NORSAR Event Warning System (NEWS: Schweitzer, 2003) but with parameters tuned specifically for seismic phases likely to be generated by events in the region of interest. On October 2, 2009, the system provided a trigger for an event at approximately 08.54.42 GMT in Central Lapland, Finland, at a distance of approximately 180 km south of the ARCES seismic array. Attention was drawn to this event because the seismic phases at ARCES were followed after approximately 10 minutes by infrasonic phases from the same direction, and because the uncertainty ellipses associated with the event location estimate include a site of military explosions at Hukkakero (67.934 N, 25.832 E) which has raised significant interest in recent years due to the generation of infrasound (Gibbons et al., 2007).

Hukkakero is the site of between 20 and 50 near-surface explosions every year for the destruction of expired ammunition. The events occur on consecutive days in August and September and provide a useful data set for the study of infrasound propagation for a number of reasons:

1. The location of the events is known. All explosions are known to take place within approximately 300 meters of the coordinates stated.
2. The sources are almost identical both in terms of yield (approximately 20000 kg per explosion) and source-time function (there are no multiple or ripple-fired explosions as are common in open-cast mining: see, for example, Gibbons et al., 2005).
3. The similarity of the waveforms makes the events amenable to detection using waveform correlation detectors (Gibbons and Ringdal, 2006). This means that every event can be detected with an almost negligible false alarm rate and also that the origin times of explosions can be constrained very accurately.

The October 2 event occurred shortly after the end of the 2009 Hukkakero explosion sequence but, due to the event origin time and poor signal correlation with known events, was deemed unlikely to be from the same source location. Using seismic waveforms from stations of the Finnish national seismic network, in addition to ARCES, indicated an event location approximately 10 km to the west of the Hukkakero site. A consultation with colleagues at the Institute of Seismology at the University of Helsinki concluded that the source of the October 2 event was almost certainly the Kittilä Gold Mine, operated by Agnico-Eagle, at Suurikuusikko (67.90154 N, 25.39102 E). Figure 6.3.1 displays the location of the sources together with waveforms from one event from each of the two sites.

Agnico-Eagle Mines Limited provide information about the operations at the Suurikuusikko mine on their website[1] and Figure 6.3.2 displays a view of the site showing a large region already excavated and an even larger volume of rock to be mined in the future. We conclude that this mine has probably been the site of large number of explosions in recent years and that this is likely to continue for a long time into the future. The magnitude estimate for the seismic event on October 2, 2009, was just in excess of 1.0 and, while such events are routinely

1. http://www.agnico-eagle.com/English/OperatingMines/Kittila/OperationsUpdate/default.aspx

detected and included in the fully automatic seismic event bulletins at NORSAR, they are not large enough to be reviewed manually and included in the published analyst bulletin. We therefore use a correlation detector to try to catch as many occurrences as possible of seismic events at this mine.

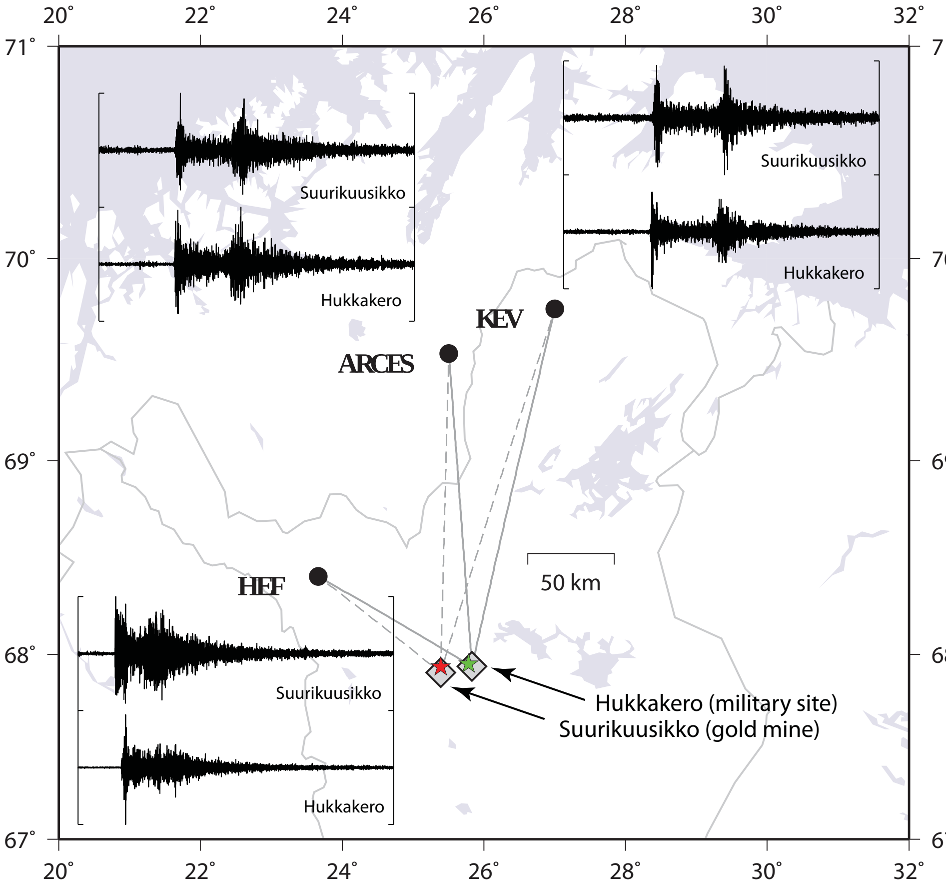

Fig. 6.3.1. Locations of the Hukkakero military explosion site (67.934 N, 25.832 E) and the Suurikuusikko gold mine (67.902 N, 25.391 E) in relation to the ARCES seismic array and the HEF and KEV 3-component stations of the Finnish seismic network. Two minutes of data are displayed for each trace beginning at the estimated event origin time and all waveforms are bandpass filte ed 3-16 Hz. The green and red stars denote event location estimates for a Hukkakero and a Suurikuusikko event respectively using the network displayed.

Gibbons and Ringdal (2006) demonstrated that seismic arrays have a tremendous advantage over single stations for correlation detectors. Firstly, there is a great suppression of the background noise made possible by a stacking of the correlation coefficient traces. Secondly, we can perform a post-processing of detections by examining the alignment of the cross-correlation coefficients from the different channels and large numbers of false alarms can be eliminated in this way.

Fig. 6.3.2. Aerial view of the Suurikuusikko mine in September 2007. The circular road indicates the final xtent of the open pit. View to the North. Photo courtesy of Agnico-Eagles Mines Limited.

Figure 6.3.3 displays all of the detections attained using a correlation detector with signal at ARCES from the October 2, 2009, event as a template since 2006. A total of 493 detections have been made in the period shown. No convincing detections have been made prior to July 2006, and a consultation with the information provided by Agnico-Eagle confirms that this is consistent with operational history of the mine. The detections displayed in Figure 6.3.3 have yet to be screened manually for false alarms, but have been filtered using the criteria described by Gibbons and Ringdal (2006). Figure 6.3.4 shows the same detections displayed as a function of the local time at the ARCES array, and the concentration of detections at particular times of day and the absence of detections at night time suggests that false alarm rate is very small.

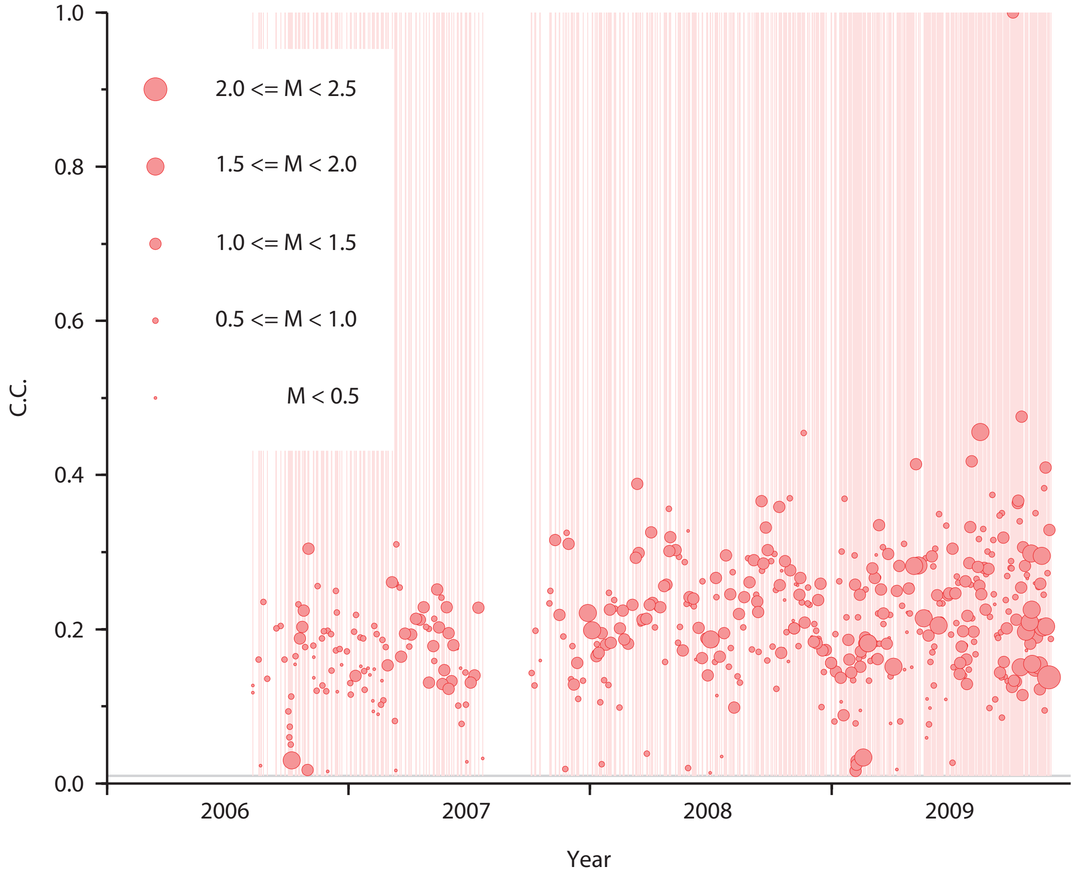

Fig. 6.3.3. Correlation detections on the ARCES array using a template of the signal from the October 2, 2009, event. In addition to a detection threshold based on the cross-correlation coefficient the detection list is screened using additional criteria of alignment of correlation traces as described in detail by Gibbons and Ringdal (2006). The correlation detector was run on archived data from years prior to 2006 and only very few detections were made with marginal values of the detection statistic. All detections prior to July 2006 were demonstrated to be false alarms. The magnitude estimates are made by comparing the amplitudes of the filte ed waveforms at ARCES with those generated from the largest of these events on November 25, 2009, which was assigned a network magnitude of 2.4.

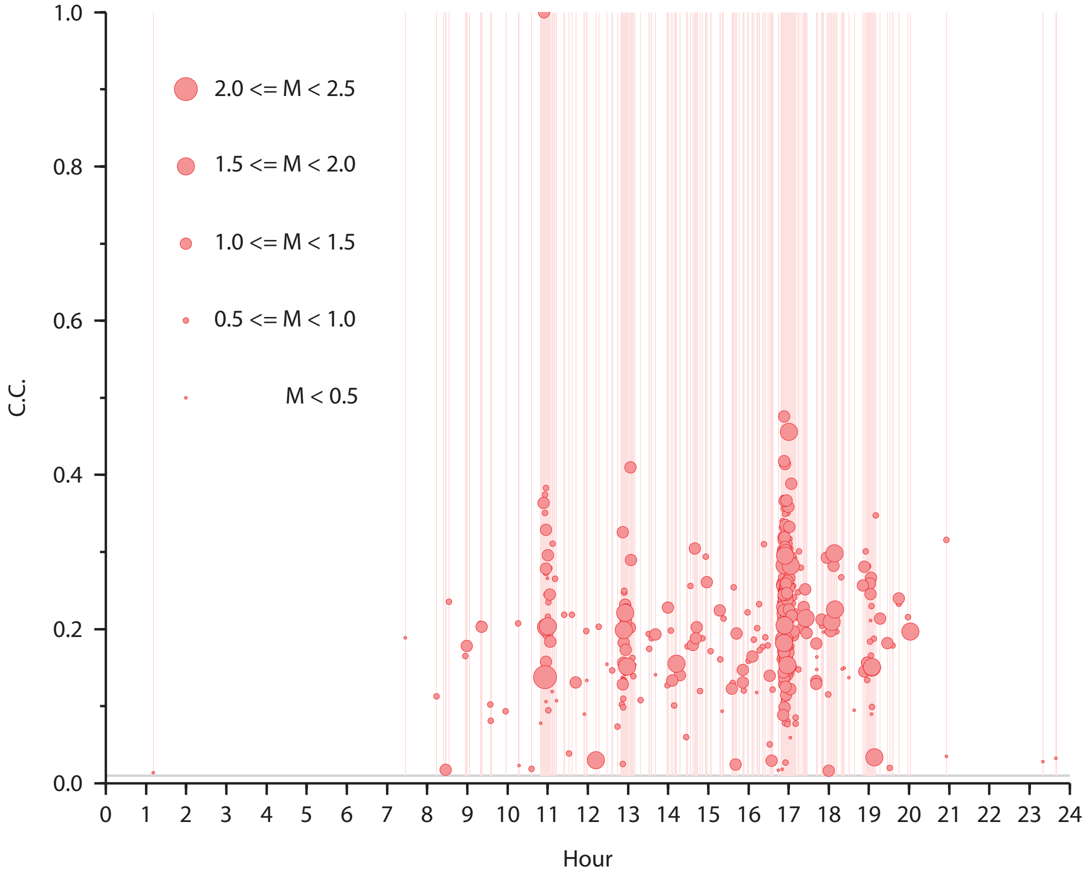

Fig. 6.3.4. Correlation detections on the ARCES array using a template of the signal from the October 2, 2009, event as a function of local time at the receiver. There are very clear clusters of events close to 1100, 1300, 1700 and 1900 hours. There are almost no detections between 2000 and 0800 hours which also suggests that the false alarm rate among these detections is probably very low.

The detection of infrasound signals at ARCES following many events in this sequence indicates that this source may be of great interest for the study of sound propagation of regional distances. The mine location is fortuitous in relation to the network of infrasound sensors in Norway, Sweden, Finland and Russia (Figure 6.3.5) which provide an almost optimal coverage of the different directions from the source. Some of the stations are located either at the edge of or well within the so-called “Zone of Silence” within which the propagation of infrasound is currently very poorly understood. While initial indications are that the Suurikuusikko mine is a less efficient generator of infrasound than the military explosions at Hukkakero, the new data set has a great advantage in that the events occur throughout the year, and so will sample many different atmospheric profiles, and may contribute more to understanding the conditions under which infrasound is observed from explosions at a known location.

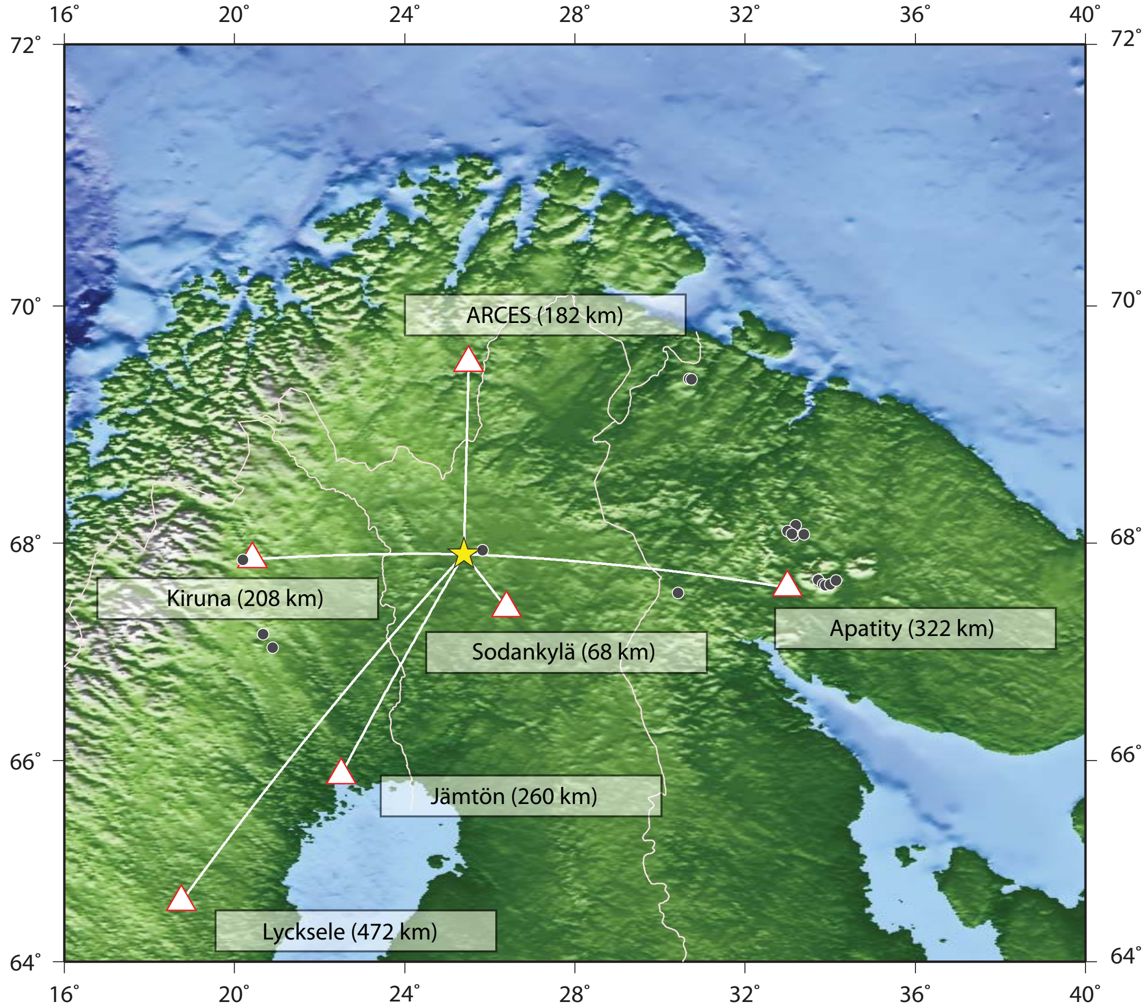

Fig. 6.3.5. Location of the Suurikuusikko gold mine in Central Lapland in relation to the ARCES and Apatity seismic/infrasonic arrays and the microphone arrays at Kiruna, Lycksele, Jämtön and Sodankylä. The coordinates 67.90154 N, 25.39102 E for the mine are taken from the website of the Geological Survey of Finland, GTK[2].

The Sodankylä microphone array is located at only 68 km from the source (to the south). This station is located within the so-called Zone-of-Silence although it is accepted that infrasound can propagate to these distances in the lower atmosphere (the troposphere) given favourable wind and temperature profiles. Very clear infrasound signals have been observed for very many of these events at Sodankylä (see Figure 6.3.6) and it will be the subject of future research to understand the conditions under which infrasound is and is not detected at this and the other stations shown.

2. http://en.gtk.fi/ExplorationFinland/Commodities/Gold/suurikuusikko.html

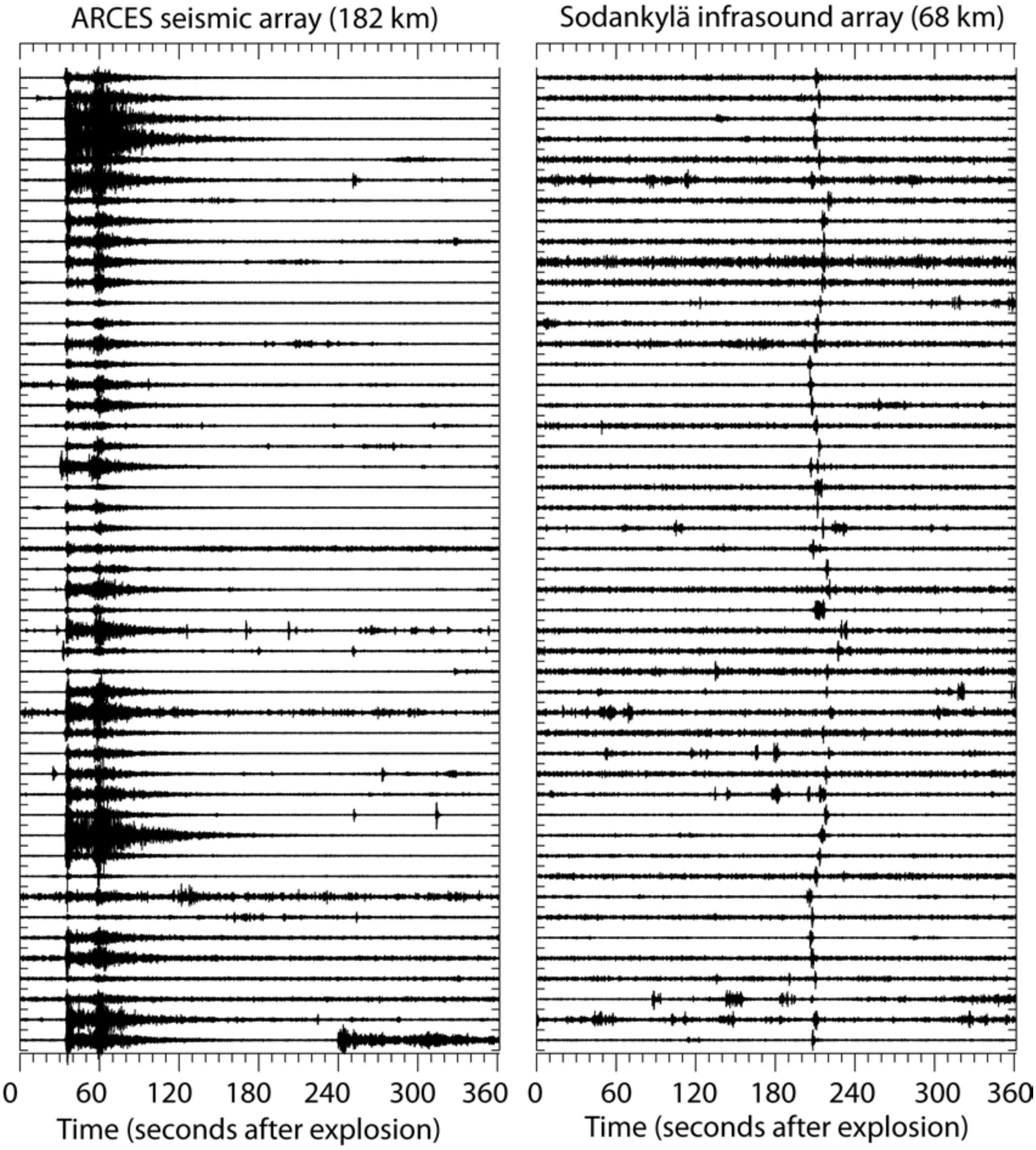

Fig. 6.3.6. Waveforms at the ARCES seismic array (ARA0_sz channel, bandpass filte ed 4-16 Hz) and the Sodankylä microphone array (SDA1_MI channel, bandpass filte ed 2-5 Hz) for the 50 events with the greatest coherence of the associated infrasound signals. The ARCES waveforms are drawn to a common scale, demonstrating the variation in the event magnitudes. Each channel of the Sodankylä data is scaled individually.

Acknowledgements

Maps were created using GMT software (Wessel and Smith, 1995). We are grateful to Agnico-Eagle Mines Limited for permission to use the photograph of the Suurikuusikko mine and to Ludwik Liszka of the Swedish Institute of Space Physics for providing data from the Sodankylä array.

References

Gibbons, S. J., Kværna, T. and Ringdal, F. (2005). Monitoring of seismic events from a specific source region using a single regional array: a case study. *Journal of Seismology*, **9**, 277-294.

Gibbons, S. J. and Ringdal, F. (2006). The detection of low magnitude seismic events using array-based waveform correlation, *Geophysical Journal International*, **165**, 149-166.

Gibbons, S. J., Ringdal, F. and Kværna, T. (2007). Joint seismic-infrasonic processing of recordings from a repeating source of atmospheric explosions. *Journal of the Acoustical Society of America*, **122**, EL158-EL164.

Schweitzer, J. (2003). NORSAR's Event Warning System (NEWS), NORSAR Scientific Report No. 1-2003, Semiannual Technical Summary 1 July - 31 December 2002. 27-32.

Wessel, P. and Smith, W. H. F. (1995). New version of the Generic Mapping Tools, *EOS Transactions of the American Geophysical Union*, **76**, 329.

S. J. Gibbons

6.4 Location of the NDC Preparedness Exercise 2009 event with the use of near-regional data

6.4.1 Introduction

This contribution focuses on our efforts to relocate the NDC Preparedness Exercise 2009 (NPE09) event with the use of near-regional data. The starting information about the selected event, as received from the German NDC, is presented in Box 6.4.1.

Box 6.4.1. NPE09 event information as distributed via E-mail by the German NDC.

```
Event parameters from SEL3:

     EventID                        5727516
     Date                        2009/11/28
     Origin Time                07:20:31.21
     Epicenter     Latitude     50.1853° N
                   Longitude    77.4514° E
     Depth                           0.0 km
     Magnitude                       ML 3.4
     Region            Eastern Kazakhstan


The event was defined by two primary seismic stations at regional distances
and a primary station at PKP distance. It is also associated with a detection
at infrasound station I46RU. This event is included in the SEL1, SEL2, and
SEL3.

The closest operational radionuclide station is MNP45. The results of the
ATM forward modeling indicate that a signal from this event may be expected
about three days after origin time.
```

The issued Reviewed Event Bulletin (REB) solution of the International Data Centre (IDC) for the NPE09 event is presented in Box 6.4.2. In the REB the event is located in Eastern Kazakhstan, close to the Kara-Zhyra open mine, which is situated in the Balapan sector of the former Soviet Semipalatinsk Test Site (STS). According to information from Zlata Sinyova of the Kazakh NDC (KNDC), the event was the result of an open pit mining explosion, close to the border of the Western Kara-Zhyra mine. Complete ground truth information about the event is not available. However some characteristics of the ripple fired explosion are known and are listed below.

- Area equal to 10975 m^2
- Detonation at 171 boreholes with average depth of 13 m
- Boreholes arranged in 10 rows
- Delay time between detonations: 0.035 s
- Mass of explosive material (possibly Igdanit): 54193 kg

According to the KNDC, the Kara-Zhyra mine has the following geographic coordinates:

- Western Kara-Zhyra mine: 50.0183°N, 78.7265°E
- Eastern Kara-Zhyra mine: 50.0231°N, 78.7449°E

The mine is clearly visible in Google™ Earth where also the locations of known, past nuclear tests can be seen.

Box 6.4.2. The REB solution for the NPE09 event.

```
EVENT  5727516 EASTERN KAZAKHSTAN
   Date       Time        Err   RMS Latitude Longitude  Smaj  Smin  Az Depth   Err Ndef Nsta Gap
mdist  Mdist Qual   Author
 OrigID
2009/11/28 07:20:38.58   0.99  1.34  49.9622   78.7531  22.2   8.2  43   0.0f         9    4 162
3.95   6.06 m i uk IDC_REB
5736538

Magnitude  Err Nsta Author      OrigID
ML     3.1 0.2    3 IDC_REB    5736538
mb1    3.1 0.3    3 IDC_REB    5736538
mb1mx  3.0 0.2   30 IDC_REB    5736538
mbtmp  3.1 0.3    3 IDC_REB    5736538

Sta      Dist  EvAz Phase         Time       TRes  Azim AzRes   Slow   SRes Def   SNR       Amp
Per Qual Magnitude    ArrID
KURK     0.68 347.9 Pg       07:20:46.169  -5.9 152.9 -14.8   25.2    6.1 ___ 174.8      14.6
0.33 a__             55040383
KURK     0.68 347.9 Lg       07:20:57.504  -3.6 176.5   8.8   32.2   -1.7 ___  35.3      20.1
0.33  __             55160858
KURK     0.68 347.9 Rg       07:21:01.504  -2.1  97.6 -70.1   29.0   -8.1 ___  14.2      36.5
0.49  __             55160859
MKAR    3.95 142.0 Pn       07:21:40.650  -0.2 328.5   3.8   11.2   -2.5 TA_  39.7 0.9 0.33 a__
ML 2.9 55037946
mb1    2.9
mbtmp  2.9
MKAR     3.95 142.0 Pg       07:21:48.886   1.4 320.2  -4.4   14.1   -4.1 TA_  22.6       1.9
0.33  __             55141662
MKAR     3.95 142.0 Sn       07:22:31.068   3.5 322.2  -2.4   12.9  -11.8 ___   2.8       0.8
0.33  __             55141660
MKAR     3.95 142.0 Lg       07:22:43.496  -0.7 323.7  -1.0   27.3   -4.4 TA_  15.7       4.6
0.33  __             55141658
I46RU     5.48   40.9  I          07:50:10.000  -145.  220.6   -5.1   325.8   -24.2  _A_     2.9
a__           55038570
ZALV     5.48  40.9 Pn       07:22:00.975  -0.4 232.4   6.7   14.2    0.5 TA_  25.1       1.7
0.33 a__ ML     3.6 55037891
mb1    3.8
mbtmp  3.8
ZALV     5.48  40.9 Sn       07:23:22.313  16.2 228.1   2.4   20.9   -3.8 ___   4.3       0.2
0.33  __             55141659
ZALV     5.48  40.9 Lg       07:23:33.184   0.6 225.0  -0.7   28.7   -3.0 TA_   6.5       0.5
0.33 a__             55037892
BVAR     6.06 303.6 Pn       07:22:08.269  -0.2 120.2   3.1   14.0    0.3 TA_   3.6       0.3
0.33  __ ML     2.9 55141661
mb1    2.7
mbtmp  2.7
BVAR     6.06 303.6 Sn       07:23:16.107  -0.7 110.5  -6.6   22.4   -2.3 TA_  10.0       1.0
0.33 a__             55040591
BVAR     6.06 303.6 Lg       07:23:47.758  -3.3 116.4  -0.6   30.0   -1.8 TA_   6.0       0.7
0.33 a__             55040592
```

The IMS primary and auxiliary seismic stations within a 40° epicentral distance from the event can be seen in Fig. 6.4.1, copied from the NPE09 related web-page of the German NDC.

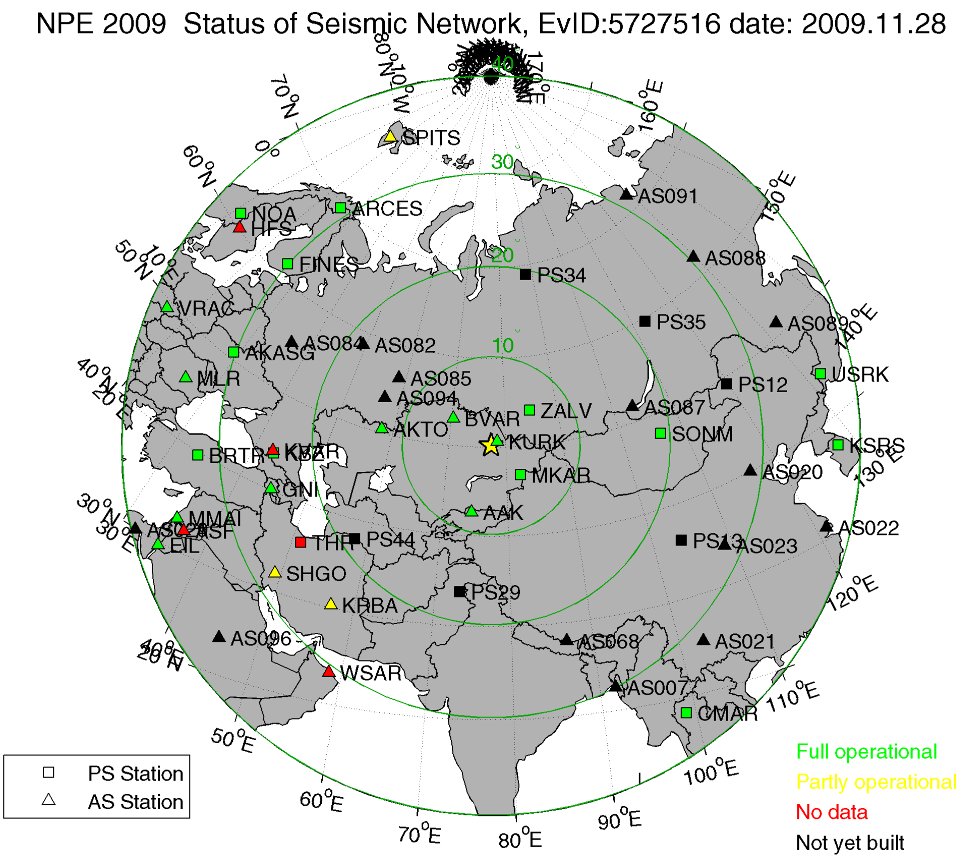

Fig. 6.4.1. Map of IMS primary (PS) and auxiliary (AS) seismic stations up to a distance of 40° from the selected NPE09 event (yellow star). From the NPE09 related web-page of the German NDC (http://www.seismologie.bgr.de/NPE).

6.4.2 Analysis and discussion

The REB solution

The REB NPE09 solution shown in Box 6.4.2 uses data from the seismic arrays Kurchatov (KURK), Makanchi (MKAR), Zalesovo (ZALV) and Borovoye (BVAR), and the infrasound station I46RU collocated with ZALV (for station locations see Fig. 6.4.1). A first inspection of the solution shows rather large residuals for certain stations, both for arrival times and backazimuth results. In order to look further into this matter, all available readings from the stations in the REB solution for events in the region since 01/01/2001 were retrieved, and the mean and median residuals for the entire dataset were compared to those reported in the REB NPE09 solution. The comparison results can be seen in the series of tables that follow (Tables 6.4.1 – 6.4.4). Except for the REB NPE09 and the mean ($_{me}$) and median ($_{md}$) residuals for each phase, the tables provide the number of observations (N) included in the retrieved dataset and which entry of the REB appears to be problematic (T - time, B - backazimuth, S - slowness, N - number).

Table 6.4.1. Comparison between REB entry for NPE09 and REB (2001 - 2009) mean and median onset time, backazimuth and slowness residuals for the KURK array.

phase	NPE09 Tres	REB $Tres_{me}$	REB $Tres_{md}$	NPE09 Bres	REB $Bres_{me}$	REB $Bres_{md}$	NPE09 Sres	REB $Sres_{me}$	REB $Sres_{md}$	REB N	NPE09 problematic
Pg	-5.9	0.1	-0.3	-14.8	0.7	1.2	6.1	-1.3	-1.1	67	TAS
Lg	-3.6	-2.8	-2.3	8.8	2.7	3.5	-1.7	-2.7	-2.1	953	T--
Rg	-2.1			-70.1			-8.1			2	-AS

Table 6.4.2. Comparison between REB entry for NPE09 and REB (2001 - 2009) mean and median onset time, backazimuth and slowness residuals for the MKAR array.

phase	NPE09 Tres	REB $Tres_{me}$	REB $Tres_{md}$	NPE09 Bres	REB $Bres_{me}$	REB $Bres_{md}$	NPE09 Sres	REB $Sres_{me}$	REB $Sres_{md}$	REB N	NPE09 problematic
Pn	-0.2	0.4	0.3	3.8	-1.4	-1.2	-2.5	-0.3	-0.3	6890	--s?
Pg	1.4	1.0	0.7	-4.4	1.4	1.8	-4.1	-2.1	-2.0	672	--s?
Sn	3.5	-0.2	0.0	-2.4	1.0	1.1	-11.8	-1.6	-1.0	2049	T-S
Lg	-0.7	-2.2	-1.7	-1.0	2.6	1.6	-4.4	-4.1	-3.6	2755	---

Table 6.4.3. Comparison between REB entry NPE09 and REB (2001 - 2009) mean and median onset time, backazimuth and slowness residuals for the ZALV array.

phase	NPE09 Tres	REB $Tres_{me}$	REB $Tres_{md}$	NPE09 Bres	REB $Bres_{me}$	REB $Bres_{md}$	NPE09 Sres	REB $Sres_{me}$	REB $Sres_{md}$	REB N	NPE09 problematic
Pn	-0.4	-0.1	-0.1	6.7	2.6	2.1	0.5	-0.9	-0.9	1176	---
Sn	16.2	-2.4	-2.2	2.4	1.6	1.3	-3.8	-1.9	-1.6	348	T--
Lg	0.6	2.1	-1.0	-0.7	2.9	1.5	-3.0	-5.9	-5.9	789	---

Table 6.4.4. Comparison between REB entry NPE09 and REB (2001 - 2009) mean and median onset time, backazimuth and slowness residuals for the BVAR array.

phase	NPE09 Tres	REB $Tres_{me}$	REB $Tres_{md}$	NPE09 Bres	REB $Bres_{me}$	REB $Bres_{md}$	NPE09 Sres	REB $Sres_{me}$	REB $Sres_{md}$	REB N	NPE09 problematic
Pn	-0.2	0.9	0.7	3.1	-5.7	-6.1	0.3	-0.1	-0.5	2165	---
Sn	-0.7	0.3	-0.1	-6.6	-3.9	-4.3	-2.3	-1.6	-1.8	863	---
Lg	-3.3	-4.3	-3.6	-0.6	-4.5	-5.3	-1.8	-5.2	-5.3	1064	---

The REB NPE09 solution residuals were plotted together with all reported residuals as function of the epicentral distance (not shown). Whenever an REB NPE09 residual was laying outside the cloud of the other observations, a marker (T for time, A for backazimuth and S for slowness) was used in column "problematic" of the tables above. Lower case characters with question mark (see Table 6.4.2) denote residuals laying at the borders of the observation cloud. In the case of the Rg phase at KURK, only two observations can be found in the entire dataset, so no statistics can be provided. From the tables it becomes clear that several observations at KURK, MKAR and the Sn arrival time at ZALV do not fit the solution satisfactorily. It is evident that these observations need to be reviewed, as they can be the results of either wrong interpretation of readings or insufficiently modelled lateral heterogeneities.

Review of the REB solution

In the light of the above, we first tried relocating the event based solely on the stations used in the REB solution. We have currently no utilities for applying the Source-Specific Station Corrections (SSSCs) used to produce the REB NPE09 solution, so no SSSCs were applied. We tried several global and regional models in our disposal, *i.e*, the global models AK135 (Kennett *et al.*, 1995) and IASP91 (Kennett and Engdahl, 1991), the global 5°x5° model CRUST5.1 (Mooney *et al.*, 1998) and velocity models for the STS region we found in literature (Belyashova *et al.*, 2001; Mikhailova *et al.*, 2002). All data analysis was performed using NORSAR's EP software package, while event location was performed using the HYPOSAT algorithm (Schweitzer, 2001; 2002).

A review of the REB observations made immediately clear the reasons for the large residuals reported in that solution. The worst case was KURK (Table 6.4.1), which is a large, cross-shaped array situated in a distance of approximately 70 km from the event and which is deployed over variable site conditions. Due to the large array aperture, usual plane wave approximation cannot be used for events located so close. In addition, the signals of this event are quite incoherent between farther apart array sites. However, we did attempt array processing by using only a part of the array, with reasonable results. The other obvious problematic case was the Sn phase at ZALV (Table 6.4.3), which is a clear case of phase misidentification and was consequently repicked. Minor changes were made also for other readings, after the application of different filters and the construction of a variety of array beams.

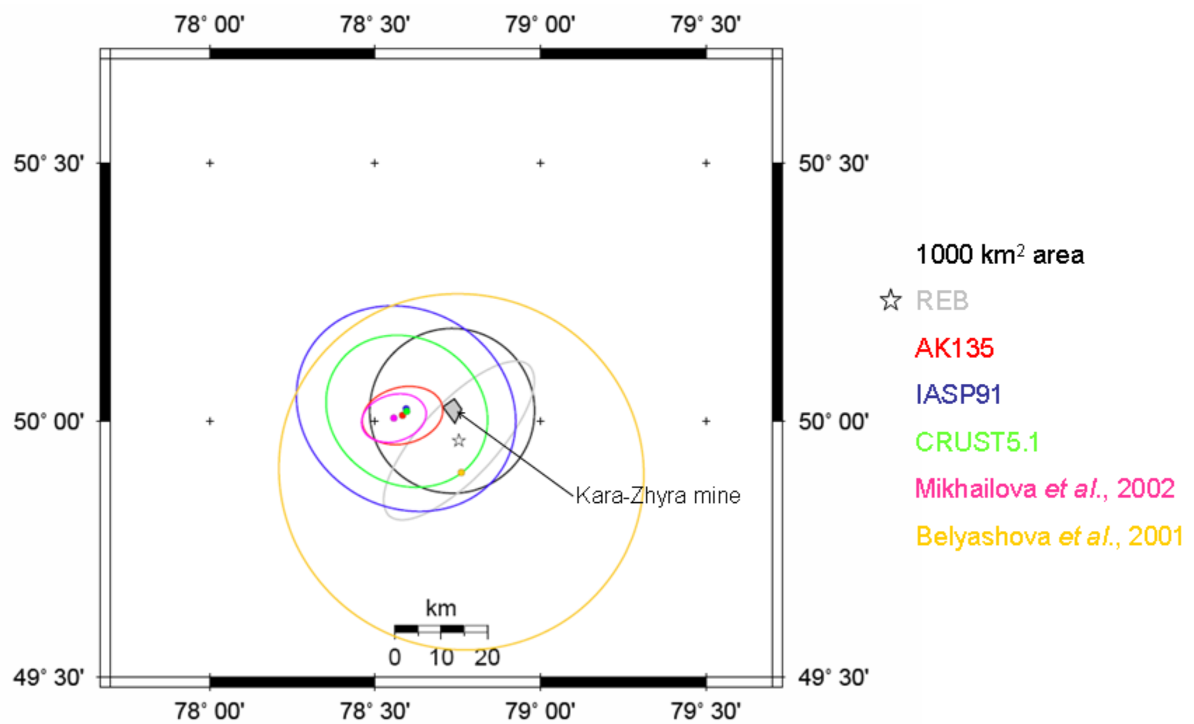

Fig. 6.4.2. Epicenters (circles) and error ellipses for the relocation of the NPE09 event by using only the data appearing in the REB solution. The REB solution (star), the Kara-Zhyra mine (gray polygon) and the 1000 km² area (black circle) around the mine are also displayed.

The results of our reanalysis and corresponding location uncertainty in the form of 95% confidence-level error ellipses with the use of the velocity models mentioned above can be seen on the map of Fig. 6.4.2, together with the REB NPE09 location and the approximate location of the Kara-Zhyra mine. All locations correspond to a fixed depth of 0.0 km.

The models fitting the data best are the one based on the travel-time curves calculated by Mikhailova *et al.* (2002) and AK135. With the exception of the solution based on the travel-time curves calculated by Belyashova *et al.* (2001), the rest of our relocations are situated more or less in the same place, but outside the area of the mine, while the "best" solutions have error ellipses that do not include any part of the area occupied by the mine.

Relocation of the NPE09 event with more near-regional data

The next step in our analysis was to try to include in our relocation as many near-regional data as possible, in an attempt to decrease the azimuthal gap in the event location process. Zlata Sinyova of the KNDC kindly provided the full set of array data for the Karatau (KKAR) and the Akbulak (ABKAR) arrays, while KNET station USP, AAK and EKS2 data were retrieved from IRIS (Fig. 6.4.3). Moreover, Pg and Sg onsets were picked for all 20 elements of the KURK array, to be used as a network. Several attempts were made to relocate the event using AK135 and the regional models for the STS region. Among the varying factors were the number of stations used and the definition of the associated phases (e.g., Sn vs Sg/Lg). The final location for the NPE09 event by the use of near-regional data that we are suggesting herein can be seen in Fig. 6.4.4.

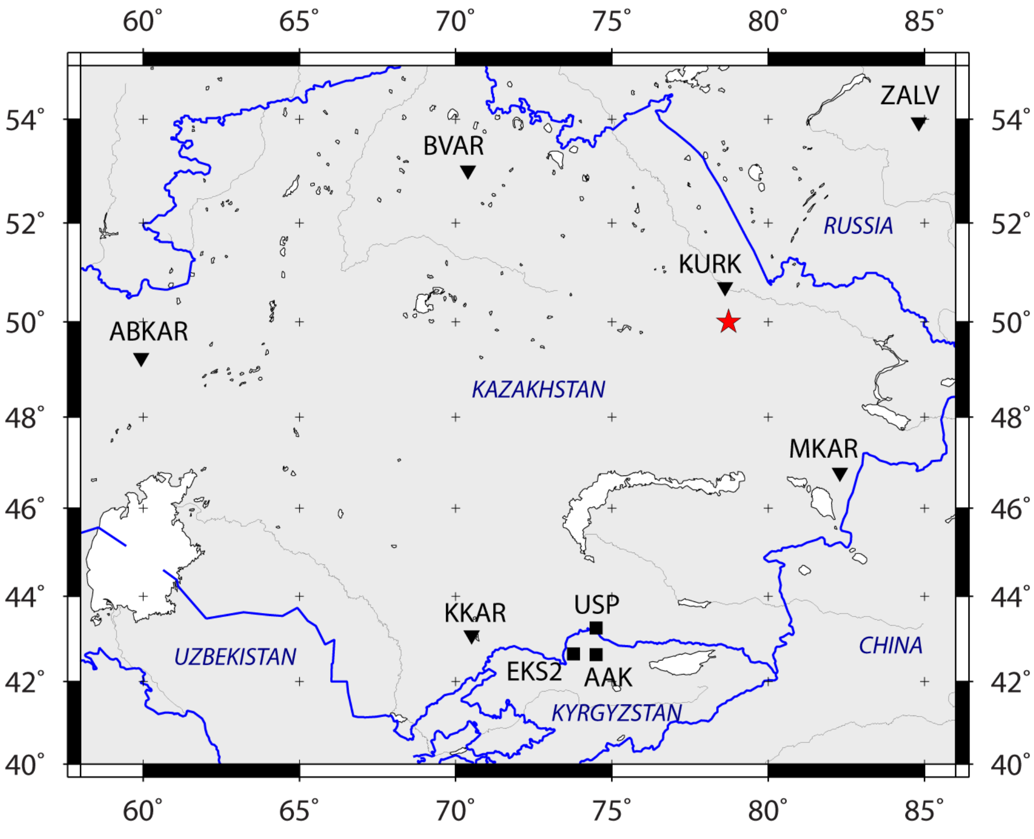

Fig. 6.4.3. Map of the stations used to relocate the NPE09 event. Squares show the 3C stations and inverted triangles the seismic arrays. The source area is located at the red star.

Table 6.4.5. The final solution with the use of near-regional data.

	Parameter value	**Uncertainty**
Origin time	28/11/2009 07:20:36.868	0.213 s
Latitude	50.0125°N	0.0117°
Longitude	78.6944°E	0.0448°
Depth	0.0 km	Fixed
RMS	0.911 s	
95% error ellipse major semi-axis	2.96 km	
95% error ellipse minor semi-axis	1.13 km	
95% error ellipse azimuth	89.1°	
95% error ellipse area	10.5 km^2	
N of defining observations	8	
N of defining onset times	55	
Maximum azimuthal gap	100.9°	
Velocity model	Mikhailova *et al.*, 2002	

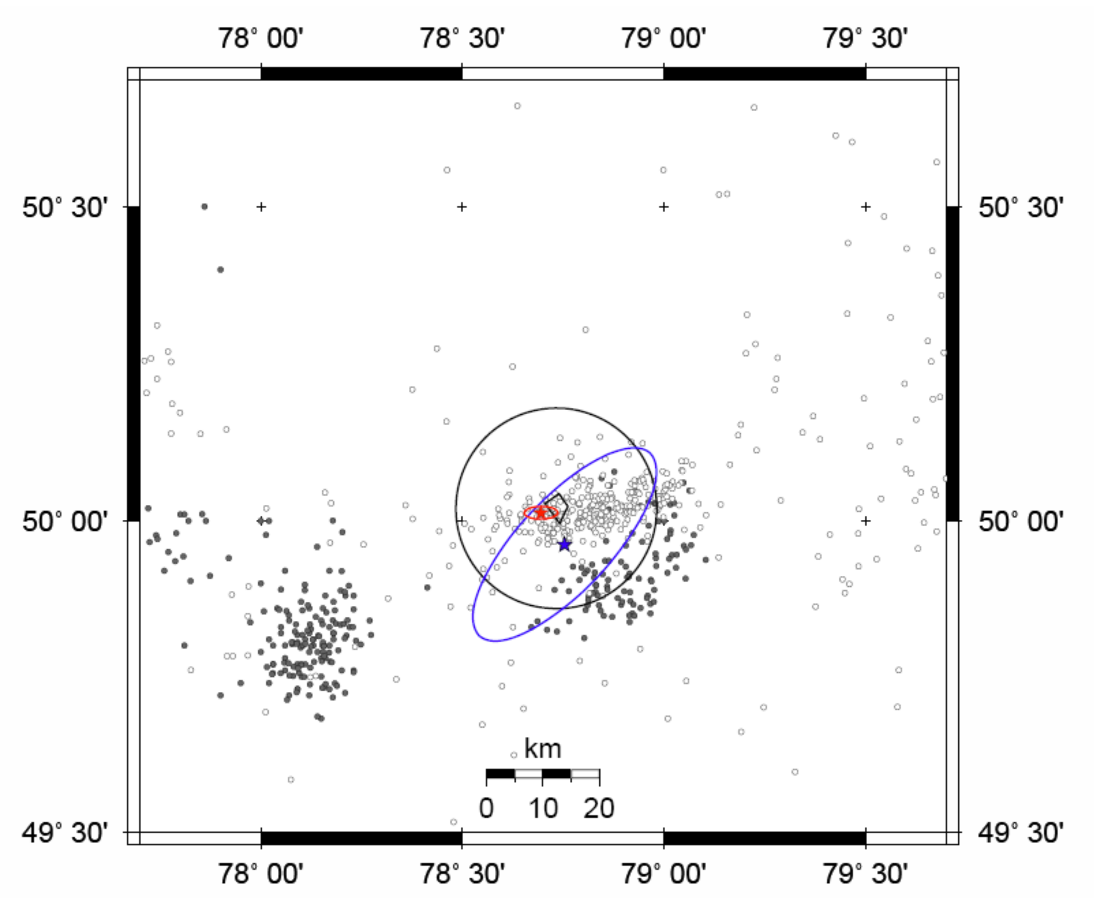

Fig. 6.4.4. Our final relocation of the NPE09 event (red star), the REB solution (blue star) and corresponding 95% confidence level error ellipses. The location of the Kara-Zhyra mine (polygon) and an area of 1000 km^2 around it, as well as the locations of the seismic events in the ISC On-line Bulletin (ISC, 2001) are displayed. Filled circles are ISC events prior to 1991, when testing was being conducted at Balapan, while open circles are events after 1991 and presumably correspond mainly to mining activity.

Table 6.4.6. Event location input data and corresponding residuals.

station	dist (°)	azi (°)	phase	onset time	res	used
KUR10	0.539	344.27	Pg	07:20:46.422	-0.661	T--D
KUR10	0.539	344.27	Sg	07:20:55.300	1.232	T--D
KUR09	0.556	345.24	Pg	07:20:46.771	-0.628	T--D
KUR09	0.556	345.24	Sg	07:20:55.613	1.003	T--D
KUR08	0.574	346.13	Pg	07:20:47.119	-0.625	T--D
KUR08	0.574	346.13	Sg	07:20:55.779	0.576	T--D
KUR07	0.592	346.96	Pg	07:20:47.495	-0.580	T--D
KUR07	0.592	346.96	Sg	07:20:56.482	0.712	T--D
KUR11	0.597	357.53	Pg	07:20:47.477	-0.752	T--D
KUR11	0.597	357.53	Sg	07:20:55.784	-0.251	T--D
KUR12	0.602	355.64	Pg	07:20:47.696	-0.608	T--D
KUR12	0.602	355.64	Sg	07:20:56.075	-0.089	T--D
KUR13	0.608	353.87	Pg	07:20:47.745	-0.656	T--D
KUR13	0.608	353.87	Sg	07:20:56.163	-0.176	T--D
KUR06	0.614	347.81	Pg	07:20:47.826	-0.648	T--D
KUR06	0.614	347.81	Sg	07:20:56.459	0.004	T--D
KUR14	0.615	352.06	Pg	07:20:47.925	-0.594	T--D
KUR14	0.615	352.06	Sg	07:20:56.477	-0.056	T--D
KUR15	0.622	350.27	Pg	07:20:48.048	-0.578	T--D
KUR15	0.622	350.27	Sg	07:20:56.273	-0.443	T--D
KUR16	0.639	346.89	Pg	07:20:48.195	-0.717	T--D
KUR16	0.639	346.89	Sg	07:20:57.527	0.320	T--D
KUR05	0.649	349.26	Pg	07:20:48.417	-0.691	T--D
KUR05	0.649	349.26	Sg	07:20:57.402	-0.141	T--D
KUR17	0.649	345.31	Pg	07:20:48.371	-0.723	T--D
KUR17	0.649	345.31	Sg	07:20:57.589	0.070	T--D
KUR18	0.656	343.76	Pg	07:20:48.425	-0.779	T--D
KUR18	0.656	343.76	Sg	07:20:58.993	1.284	T--D
KUR19	0.666	342.14	Pg	07:20:48.570	-0.820	T--D
KUR19	0.666	342.14	Sg	07:20:58.475	0.448	T--D
KUR04	0.667	349.93	Pg	07:20:48.775	-0.674	T--D
KUR04	0.667	349.93	Sg	07:20:58.159	0.029	T--D
KUR20	0.677	340.68	Pg	07:20:48.649	-0.925	T--D
KUR20	0.677	340.68	Sg	07:21:01.263	2.920	T--D
KUR03	0.685	350.43	Pg	07:20:49.176	-0.598	T--D
KUR03	0.685	350.43	Sg	07:20:58.931	0.245	T--D
KUR02	0.705	351.17	Pg	07:20:49.649	-0.491	T--D
KUR02	0.705	351.17	Sg	07:20:59.528	0.214	T--D
KUR01	0.723	351.71	Pg	07:20:50.071	-0.410	T--D
KUR01	0.723	351.71	Sg	07:21:00.116	0.215	T--D
MKAR	3.996	142.20	Pn	07:21:40.650	0.291	T--D
MKAR	3.996	142.20	Pg	07:21:48.886	-1.213	T--D
MKAR	3.996	142.20	Sn	07:22:30.337	1.779	T--D
MKAR	3.996	142.20	Sg	07:22:43.496	0.734	T--D
ZALV	5.454	41.30	Pn	07:22:01.013	1.461	T--D
ZALV	5.454	41.30	Sn	07:23:00.608	-2.269	T--D
BVAR	6.018	303.34	Pn	07:22:08.269	1.572	T--D
BVAR	6.018	303.34	Sn	07:23:16.136	0.508	T--D
USP	7.341	204.92	Pn	07:22:25.216	0.608	T--D
USP	7.341	204.92	Sn	07:23:47.417	-0.184	T--D
AAK	7.928	203.26	Pn	07:22:32.218	-0.377	T---
EKS2	8.103	206.84	Pn	07:22:33.980	-0.869	T---
KKAR	8.923	222.43	Pn	07:22:45.317	-0.192	T--D
KKAR	8.923	222.43	Sn	07:24:27.170	2.219	T--D
ABKAR	12.205	273.67	Pn	07:23:29.779	0.967	T---

The focal parameters, corresponding uncertainties and general information about the final NPE09 solution suggested in this contribution are summarized in Table 6.4.5. Phase information, input parameter values, corresponding residuals and information about defining observations can be found in Table 6.4.6.

The velocity model based on the travel-time curves by Mikhailova *et al.* (2002) used up to a distance of 13° and thus covering all employed stations, is the one that provides in general the best fit to the available data. However, S-phases and especially Lg are not modelled satisfactorily at all distances. For distances up to 5°, modelling the high amplitude S-phase as Sg provides the best fit, while for larger distances residuals are smaller if the phase is identified as Lg. HYPOSAT cannot extract an Lg velocity from an applied velocity model, but an Lg group velocity value can be assigned through the parameter file (Schweitzer, 2002). The group velocity value of 3.54 km/s, which corresponds to the travel-time curves calculated by Mikhailova *et al.* (2002), produces rather high residuals. Taking these into consideration, we decided to treat the S-phase readings as Sg up to about 5° and as Lg for the rest of the stations, without including the latter in the location process. All other available onset readings were used. In addition, whenever more than one onset reading from the same station was available, we also inverted for the travel-time differnce between these onsets. Such cases are indicated with a “D” in Table 6.4.6. In our final inversion we did not use any slowness vector observation since they are in this case (source - station geometry) of little importance to the solution.

The final solution shows some quite large travel-time residuals at some stations (for P or S onsets). These residuals might be caused by insufficient modelling of lateral heterogeneities by a simple horizontally layered velocity model. Reports can be found in literature (see *e.g.*, Ringdal et al., 1992; Bonner *et al.*, 2001 and references therein) of two distinct shear-wave velocity zones at the Balapan Test Site, a relatively high velocity area to the SW and a lower velocity area to the NE, their NW-SE trending boundary roughly coinciding with the Chinrau fault. Such information, combined with observed contrasts in Lg amplitudes and spectral and waveform differences for teleseismic P-phases between the NE and SW regions of the Balapan Test Site are highly suggestive of structural complexities that are presumably unaccounted for by the velocity model.

6.4.3 Concluding remarks

The NDC Preparedness Exercise 2009 event was relocated with the use of near-regional seismic data. The suggested location is in good agreement with the information we have about the nature of the event, namely that it corresponds to a mining explosion in the Western Kara-Zhyra open pit mine.

The process of relocating the NPE09 event revealed several interesting aspects of possible path and structure interference in earthquake location and highlighted the importance of the availability of appropriate velocity models and SSSCs, in particular within the CTBTO monitoring framework.

Myrto Pirli

Johannes Schweitzer

Acknowledgements

Zlata Sinyova of the KNDC kindly provided the data from the KKAR and ABKAR arrays, as well as a great wealth of information on the event and velocity models for the region. KNET station data were retrieved from IRIS (http://www.iris.edu/data/).

References

Belyashova, N.N., V.I. Shacilov, N.N. Mikhailova, I.I. Komarov, Z.I. Sinyova, A.V. Belyashov & M.N. Malakhova (2001). On the use of calibration explosions at the former Semipalatinsk Test Site for compiling a travel-time model of the crust and upper mantle. Pure Appl. Geophys. **158**, 193-209.

Bonner, J.L., C.D. Pearson, S.W. Phillips & S.R. Taylor (2001). Shallow velocity structure at the Shagan River Test Site in Kazakhstan. Pure Appl. Geophys. **158**, 2017-2039.

ISC (2001). On-line Bulletin, http://www.isc.ac.uk, Internatl. Seis. Cent., Thatcham, United Kingdom.

Kennett, B.L.N. & E.R. Engdahl (1991). Travel times for global earthquake location and phase identification. Geophys. J. Int. **105**, 429-465.

Kennett, B.L.N., E.R. Engdahl & R. Buland (1995). Constraints of seismic velocities in the Earth from travel times. Geophys. J. Int. **122**, 108-124.

Михайлова Н.Н., И.Л. Аристова и Т.И. Германова (2002). Годограф сейсмических волн по результатам регистрации сигналов от химических взрывов на Семипалатинском испытательном полигоне. Вестник НЯЦ РК **выпуск 2**, **сентябрь 2002**, 46-54. (Mikhailova, N.N., I.L. Aristova & T.I. Germanova (2002). Seismic waves travel-time curve basing on the results of signal detection from chemical explosions detonated at Semipalatinsk Test Site. Bull. NNC RK **Release 2**, **September 2002**, 46-54.)

Mooney, W.D., G. Laske & G. Masters (1998). CRUST5.1: A global crustal model at 5°x5°. J. Geophys. Res. **103**, 727-747.

Ringdal, F., P.D. Marshall & R.W. Alewine (1992). Seismic yield determination of Soviet underground nuclear explosions at the Shagan River test site. Geophys. J. Int., **109**, 65-77.

Schweitzer, J. (2001). HYPOSAT – An enhanced routine to locate seismic events. Pure Appl. Geophys. **158**, 277-279.

Schweitzer, J. (2002). PD11.1: User Manual for HYPOSAT (including HYPOMOD). In: Bormann, P. (Ed.) (2002). IASPEI New Manual of Seismological Observatory Practice, GeoForschungsZentrum Potsdam, Vol. 2, 15 pp.

6.5 Continued overview of array and station system responses contributing to NORSAR's Data Center

6.5.1 Introduction

This series of contributions (Pirli and Schweitzer, 2008a; 2008b; 2009; present paper), presenting the system response of seismic stations and arrays contributing to NORSAR's Data Center, is continued with the responses of two seismic arrays situated in neighboring countries, but contributing on a regular basis to NORSAR's database, and two new three-component, broadband seismic stations. The Hagfors array in Sweden and the FINES array in Finland are part of a long collaboration between NORSAR and FOI (the Swedish Defence Research Agency) in Stockholm, and NORSAR and the University of Helsinki, respectively. The two single seismic stations are Åknes (AKN) and Hornsund (HSPB). The latter is also part of a collaborative activity between NORSAR and the Institute of Geophysics of the Polish Academy of Sciences (Schweitzer and The IPY Project Consortium Members, 2008).

6.5.2 Hagfors (HFS) array configurations

The Hagfors array operated initially in 1969 as a sub-station (HFS) of a larger installation known as the Hagfors Observatory (*e.g.*, GSE, 1990; FOI, 2005). This system became modernized in 1989 and later the HFS sub-array became known as Hagfors array instead of the larger deployment. Since June 8, 1994 NORSAR has been collecting data from the Hagfors array and using them in its routine analysis. The Hagfors array was certified as IMS auxiliary station AS101 in December 2002. The initial configuration consisted of 8 sites, distributed over an aperture of about 900 m (see Fig. 6.5.1, left-hand side), all of them equipped with short-period Geotech S-13 or 20171A vertical seismometers and Nanometrics RD-3 digitizers. In addition, site HFSC2 had a three-component long-period and a vertical broadband channel, carrying a 7505A/8700C sensor combination and an STS-1 vertical seismometer respectively.

Poles and zeros for the short-period and long-period sensors are provided by the standard damping seismometer formula (*e.g.*, Geotech Instruments, 1999):

$$p_{1,2} = \lambda_0\omega_0 \pm j\omega_0\sqrt{1-\lambda_0^2}\ , \tag{6.5.1}$$

where λ_0 is the damping factor and $\omega_0 = 2\pi f_0$. Not much information is available about these sensors and the λ_0 and f_0 values that were used, so for the short-period channels, after several tests we used the same settings as for the NORSAR array (Pirli, 2010; Pirli and Schweitzer, 2008a) and for the long-period channels values of $f_0 = 0.05$ Hz and $\lambda_0 = 0.406$ were the ones reconstructing better the calibration curves provided by FOI in 2005 and shown in Fig. 6.5.2. Channel sensitivity information (see Table 6.5.1) is provided by Lund and Lennartsson (2005), so the system can be tuned accordingly.

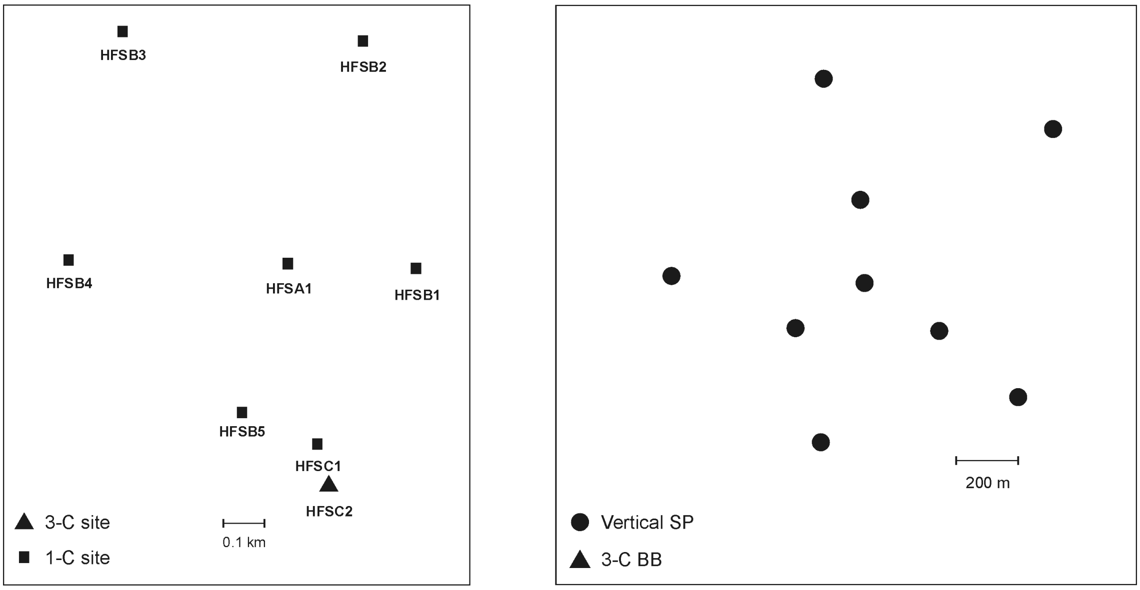

Fig. 6.5.1. Geometry of the initial (left, GSETT3, 1995) and current (right) Hagfors array.

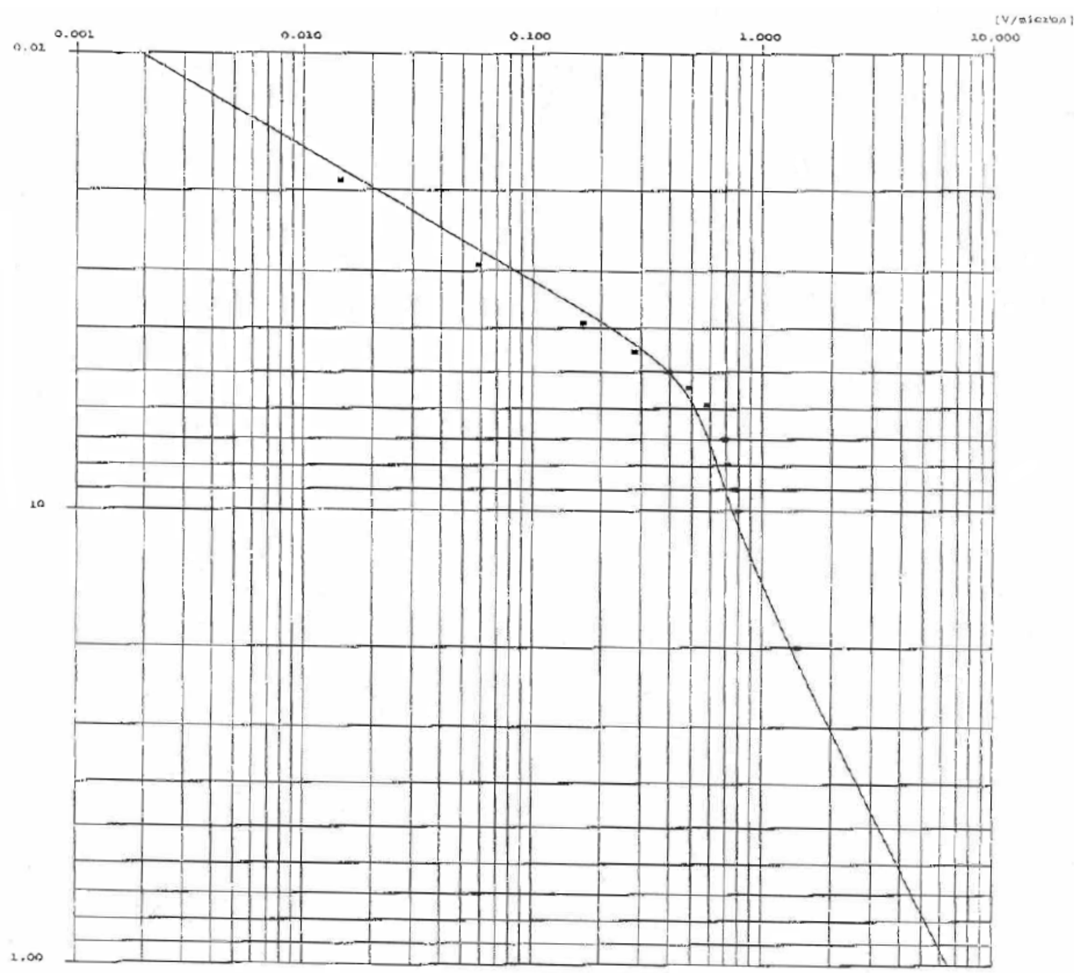

Fig. 6.5.2. Calibration curves for the vertical component (7505A sensor) of the long-period channel displacement amplitude response [V/micron] vs. frequency [Hz]. Information was faxed to J. Schweitzer from FOI SYSTEMTEKNIK in 2005.

The velocity transfer function of the STS-1 seismometer is described by the formula (Streckeisen, 1986):

$$T(\omega) = \frac{-\omega^2 S}{-\omega^2 + 2i\omega\omega_1 h_1 + \omega_1^2} \cdot \frac{\omega_2^2}{-\omega^2 + 2i\omega\omega_2 h_2 + \omega_2^2}, \qquad (6.5.2)$$

where $\omega_1 = 2\pi/360$ rad/s, $h_1 = 1/\sqrt{2}$, $\omega_2 = 2\pi/0.1$ rad/s, $h_2 = 0.6235$ and S = 2400 V/m/s.

The RD-3 digitizers employ the following filters:

- Low-pass analog 5th order Butterworth filter (f_{3db} = 20 Hz)
- Low-pass digital FIR filter (symmetric, 150 coefficients, f_{3db} = 17 Hz)
- High-pass digital IIR filter (f_c = 0.008 Hz)

To achieve the overall channel sensitivity values reported by Lund and Lennartsson (2005), a gain factor of 2 is assigned to the low-pass Butterworth filter (Nanometrics, 1992), while an additional gain stage of a factor of 30 is introduced for all channels of this configuration. The displacement amplitude and phase response for all channels of this configuration, as well as the rest of the Hagfors systems described later in this section, are shown in Fig. 6.5.3.

In August 2001 and while the initial HFS was in operation, a new configuration was tested. The new array comprised 10 sites, nine of which carried only vertical short-period GS-13 sensors, the tenth having been equipped with a three-component, broadband STS-2 seismometer. Digitizers were Nanometrics Europa T, including an HRD-24 A/D unit and authentication for CTBTO compatibility. The two systems, which were stored under separate database entries at NORSAR, were kept operating in parallel because of the rather small amplitudes achieved by the new system, due to the needed pre-amplifiers not having been delivered (Bergkvist and Lennartsson, 2004). The pre-amplifiers with a gain factor of 30.23 were installed in late autumn 2003, while the final HFS configuration was shaped in 2004 when the IIR filter of the digitizer for the broadband channel was switched from 10 mHz to 1 mHz. The present day geometry of HFS is shown on the right-hand side of Fig. 6.5.1.

The poles and zeros of the GS-13 seismometers are also computed by formula (6.5.1), while the sensitivity is 2000 V/m/s. Regarding the poles and zeros of the STS-2 seismometer, information on how to calculate their values, as well as the sensitivity for each component can be found in our description of the response of the JMIC station (Pirli, 2010; Pirli and Schweitzer, 2009) and from Streckeisen (2003; 2006) and Wielandt (2002). The Europa T unit contains an HRD-24 digitizer which employs the following filter cascade:

- Low-pass analog 3rd order Bessel filter (f_{3db} = 1500 Hz)
- Digital FIR 1, decimating by factor 5, 34 coefficients
- Digital FIR 2, decimating by factor 3, 30 coefficients
- Digital FIR 7, decimating by factor 5, 36 coefficients
- Digital FIR 10, decimating by factor 5, 256 coefficients
- High-pass IIR digital filter (f_c = 10 mHz)

Overall channel sensitivity for the current system is in the order of 23 count/nm/s (Bergkvist and Lennartsson, 2004). The displacement amplitude and phase responses for all different configurations are shown in Fig. 6.5.3, while a summary of all these systems and corresponding

Respid flags given in parentheses (Pirli, 2010; Pirli and Schweitzer, 2008a) are listed in Table 6.5.1.

Table 6.5.1. The different instrument configurations of the Hagfors array

Time	Installation Name	Components	Calib [nm/count]	Calper [s]
1992-2003	Initial SP (HFSSP1, HFSSP2, HFSSP3)	S-13 RD-3 digitizer LP Butterworth, analog LP FIR, digital HP IIR, digital	0.0265500*	1.00
1992-2003	Initial SP (HFSSP4)	20171A RD-3 digitizer LP Butterworth, analog LP FIR, digital HP IIR, digital	0.0262300*	1.00
2001-2003	New SP, Non amplified (HFSSP5)	GS-13 Europa T digitizer LP Bessel, analog LP FIR, digital HP IIR, digital	0.2019800*	1.00
2003-…	Current SP amplified (HFSSP6)	GS-13 Pre-amplifier, 30.23x Europa T digitizer LP Bessel, analog LP FIR, digital HP IIR, digital	0.0066814*	1.00
1992-2003	LP channel (HFSLP1, HFSLP2, HFSLP3)	7505A & 8700C RD-3 digitizer LP Butterworth, analog LP FIR, digital HP IIR, digital	0.3454400*	20.00
1992-2003	Initial BB (HFSBB1)	STS-1 RD-3 digitizer LP Butterworth, analog LP FIR, digital HP IIR, digital	0.0060000	1.00
2003-2004	New BB, 10 mHz (HFSBB2, HFSBB3, HFSBB4)	STS-2 Europa T digitizer LP Bessel, analog LP FIR, digital HP IIR, digital, 10 mHz	0.0069643*	1.00
2004-…	Current BB, 1 mHz (HFSBB5, HFSBB6, HFSBB7)	STS-2 Europa T digitizer LP Bessel, analog LP FIR, digital HP IIR, digital, 1 mHz	0.0069639*	1.00

* Indicative value

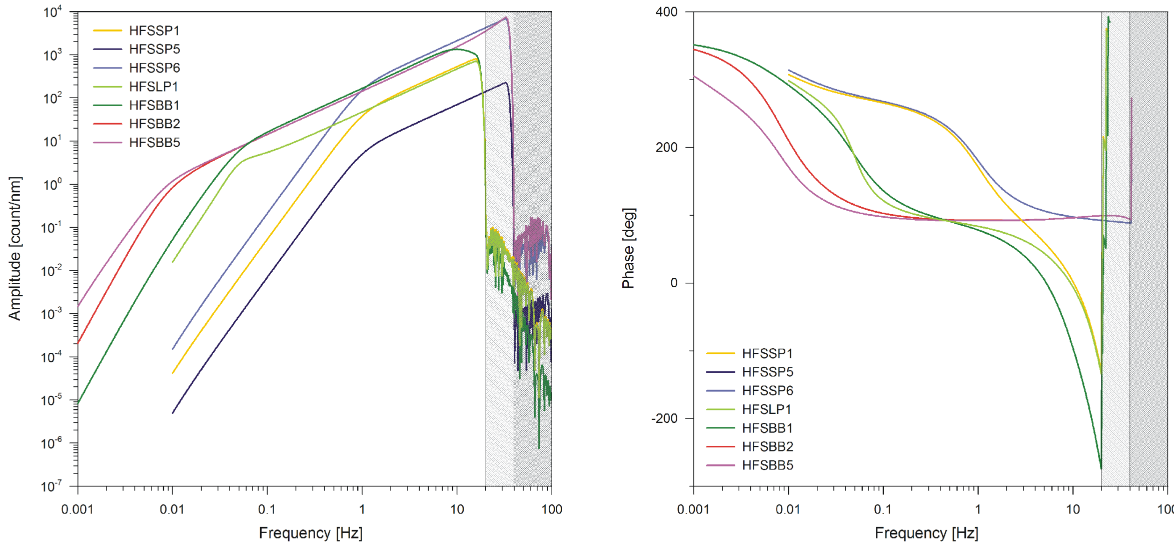

Fig. 6.5.3. Displacement amplitude and phase responses for the short-period (HFSSP1, HFSSP5, HFSSP6), long-period (HFSLP1) and broadband (HFSBB1, HFSBB2, HFSBB5) configurations of the Hagfors array. The shaded areas represent the range beyond the Nyquist frequency (20 Hz for the RD-3 and 40 Hz for the Europa T configurations).

6.5.3 FINES array configurations

The FINES array was installed in November 1985 at Sysmä, about 100 km NE of Helsinki, in cooperation between the Institute of Seismology of the University of Helsinki and NORSAR (*e.g.*, Ringdal *et al.*, 1987; Uski, 1990). The array, which was named FINESA at that time, comprised 10 short-period elements with a maximum intersensor separation of about 1.5 km (see Fig. 6.5.4). All sites were equipped with vertical S-13 seismometers, except for site FIA1 that also carried two horizontal sensors. The instrumentation included also RA-5 and LTA amplifiers and 12-bit DDS-1105 A/D converters by Kinemetrics (Korhonen *et al.*, 1987). Five additional elements were installed in autumn 1987, without modifying the instrumentation, except for the removal of the horizontal sensors (*e.g.*, Uski, 1990). Regarding the response of this configuration, S-13 poles and zeros are calculated by Equation 6.5.1 and the data coil generator constant is equal to 629 V/m/s. The settings of the amplifiers and digitizer, so that the latter has a scaling of 0.181 nm/count at 1 Hz, is shown in the calibration flowchart of Fig. 6.5.5 (Korhonen *et al.*, 1987).

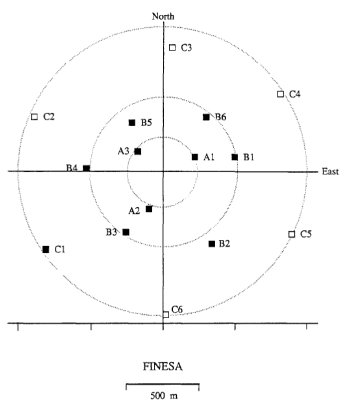

Fig. 6.5.4. Geometry of the FINESA array. Open squares denote elements added in autumn 1987, while the central recording unit is located at site A1 (from Uski, 1990).

We know from the NORSAR array (Pirli, 2010; Pirli and Schweitzer, 2008a) that the amplifiers contained several filters, however the only information we have from Korhonen *et al.* (1987) is about an analog anti-alias filter, directly before the digitizer, with 3db points at 0.7 and 14.5 Hz and slopes of 6 and 30 db/octave respectively. The filter was reconstructed and the resulting displacement response curves (see Fig. 6.5.7) fit the calibration curves of Korhonen *et al.* (1987) (not shown here). For this, the amplifiers were treated as simple gain stages.

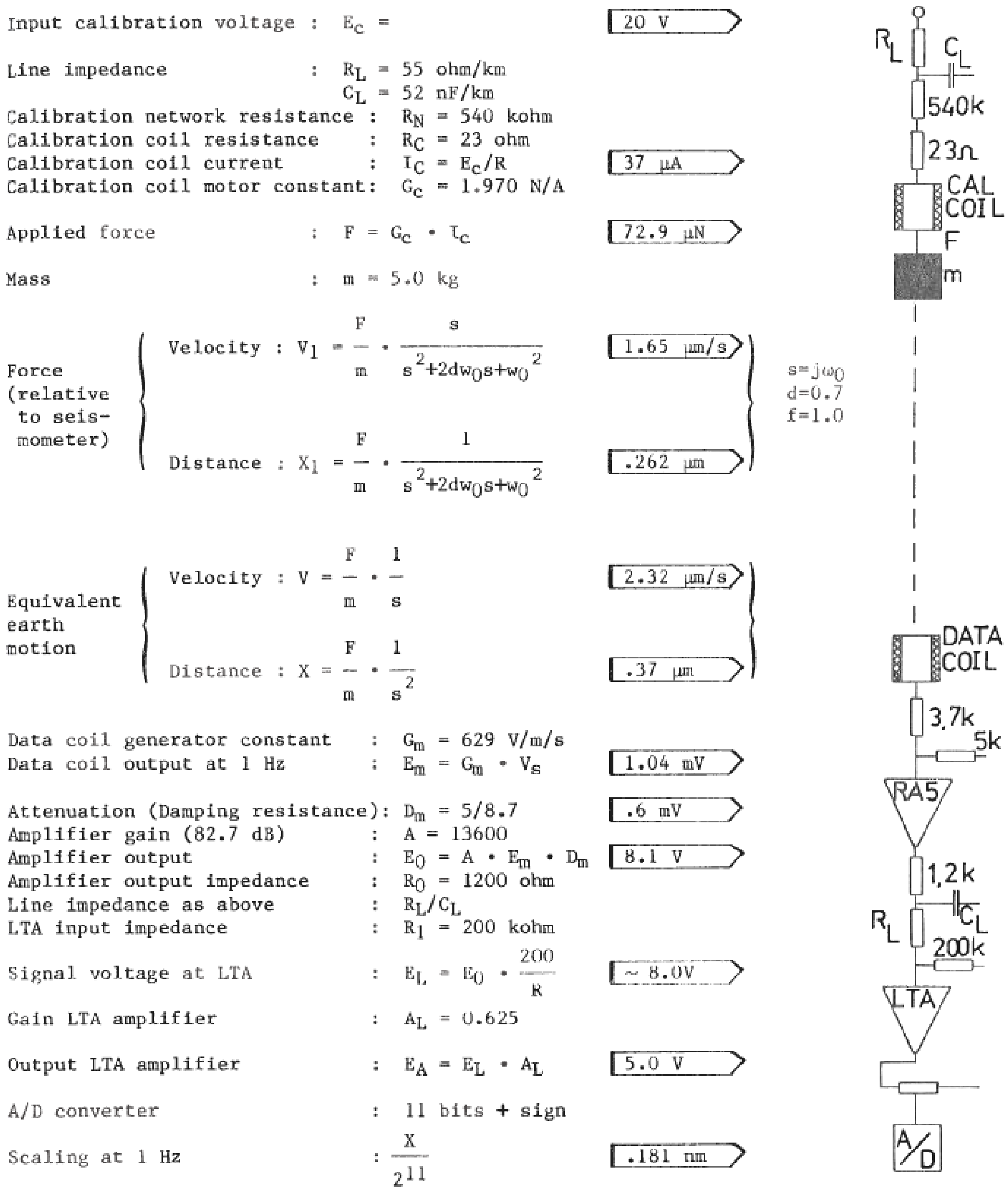

Fig. 6.5.5. FINESA array calibration flowchart (from Korhonen et al., 1987). The entire instrumentation chain, including the A/D converter, is presented.

In 1989, the LTA amplifiers were removed and the Kinemetrics digitizers were exchanged with 16-bit Motorola based (Force Computers) Data Translation A/D converters (DT1405/5716A cards). The response of this configuration was calculated based on the poles and zeros and sensitivity information contained in Teikari and Suvilinna (1994). A channel attenuated by 30 db operated at site FIA0, which was installed in August 1990 (see left in Fig. 6.5.6) in addition to the standard short-period channels, while site FIA1 was once more equipped with horizontal sensors. The displacement response is shown in Fig. 6.5.7.

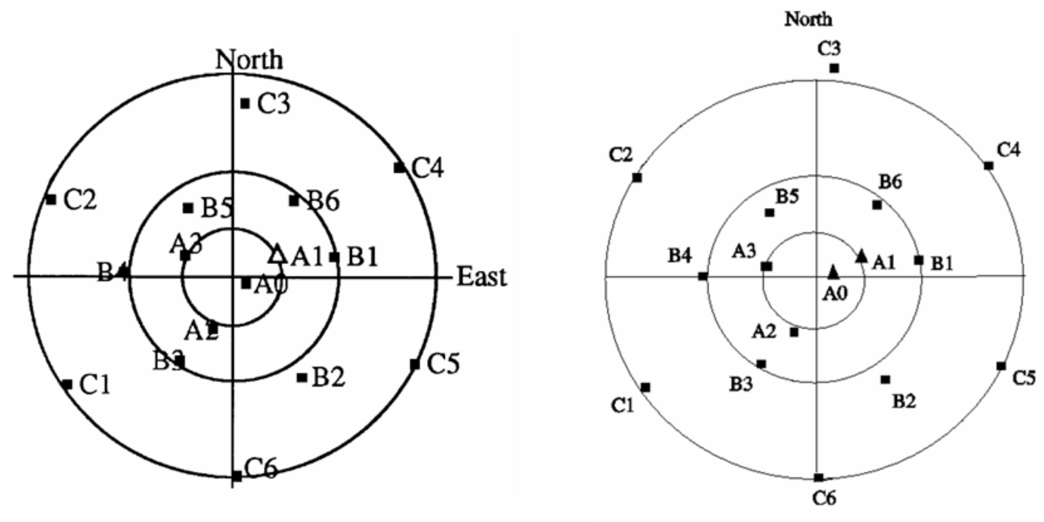

Fig. 6.5.6. (Left) Geometry of the upgraded FINESA array (from Tarvainen, 1994). The 3-component element is noted with an open triangle. (Right) Geometry of the FINES array (from Heikkinen, 2003). Triangles denote 3-component elements. Site FIA1 carries a broadband seismometer.

An extensive upgrade of the array took place in the early 1990s. It was completed in 1993 and the system was then renamed to FINES (Tarvainen, 1994; Tiira *et al.*, 1995). Horizontal channels were moved to site FIA0 from FIA1 and the equipment was modernized, exchanging the old 16-bit digitizers with 24-bit AIM24 units (Tiira *et al.*, 1995). Response information is again reconstructed by using the report of Teikari and Suvilinna (1994). No mention of an amplifier is made, but based on our knowledge of the AIM24 digitizer from the NORSAR array (Pirli 2010; Pirli and Schweitzer, 2008a) an additional gain factor of about 10.5 is needed to achieve the reported channel sensitivity. Thus, a gain-only amplifier stage is assumed. In 2000, a three-component broadband CMG-3T seismometer was added to site FIA1, completing the geometry of the FINES array, which is shown in Fig. 6.5.6 (right). No amplifier was used for the broadband channel, while sensor response information was provided by Güralp Systems Ltd. These responses are also plotted in Fig. 6.5.7.

The current instrumentation of the FINES array was shaped in 2007, when the AIM24 digitizers were exchanged with Nanometrics Europa T models. Initially, this took place for sites FIA0 through FIB4, while the change to the remaining sites was made in the spring of 2009. In the case of the short-period channels, the S-13 sensors and the Europa T digitizers are used together with a preamplifier from Nanometrics, with a gain factor of 51.236. The preamplifiers include an external damping resistor to be used with the damping circuit of the S-13s (Laporte, 2006; J. Kortström, pers. comm.). At FINES, the Europa T includes a Trident A/D converter, with a sensitivity of 1.0078 count/μV for the short-period channels and 4.8 count/μV for the broadband channels (J. Kortström, pers. comm.). No preamplifier is used for the broadband channels. The filter cascade employed by the digitizer to decimate from the input frequency of 30 kHz down to the desired sampling rate of 40 sps is the following:

- Digital FIR 1, decimating by 15, symmetric, 177 coefficients
- Digital FIR 2, decimating by 5, symmetric, 71 coefficients

- Digital FIR 3, decimating by 5, symmetric, 113 coefficients
- Digital FIR 4, decimating by 2, symmetric, 223 coefficients

The different configurations of the FINES array are listed in Table 6.5.2, together with their corresponding Respid flags.

Table 6.5.2. The different instrument configurations of the FINES array

Time	Installation Name	Components	Calib [nm/count]	Calper [s]
1985-1989	Initial SP (FINSP1, FINSP2, FINSP3)	S-13 RA-5 amplifier LTA amplifier anti-alias BB analog filter DDS-1105 digitizer	0.1810000	1.00
1989-1993	Second SP (FINSP4, FINSP5, FINSP6)	S-13 RA-5 amplifier anti-alias BB analog filter Motorola based digitizer	0.0245580	1.00
1990-1993	Attenuated SP (FINSL1)	S-13 RA-5 amplifier, -30 dB anti-alias BB analog filter Motorola based digitizer	0.7760200	1.00
1993-2007	Upgraded SP (FINSP7, FINSP8, FINSP9)	S-13 amplifier AIM24 digitizer LP FIR cascade, digital	0.0100370	1.00
2007-…	Current SP (FINSP10, FINSP11, FINSP12)	S-13 Nanometrics preamplifier Europa T digitizer LP FIR cascade, digital	0.0025756*	0.333
2000-2007	First BB (FINBB1, FINBB2, FINBB3)	CMG-3T AIM24 digitizer LP FIR cascade, digital	0.0250230*	1.00
2007-…	Current BB (FINBB4, FINBB5, FINBB6)	CMG-3T Europa T digitizer LP FIR cascade, digital	0.0273370*	1.00

* Indicative value

The displacement amplitude (in count/nm) and phase (in degrees) responses for the FINES array configurations listed in Table 6.5.2 are depicted in Fig. 6.5.7. Once again, only the vertical channels are pictured and shaded areas represent the range beyond the Nyquist frequency, which is 20 Hz for all channels.

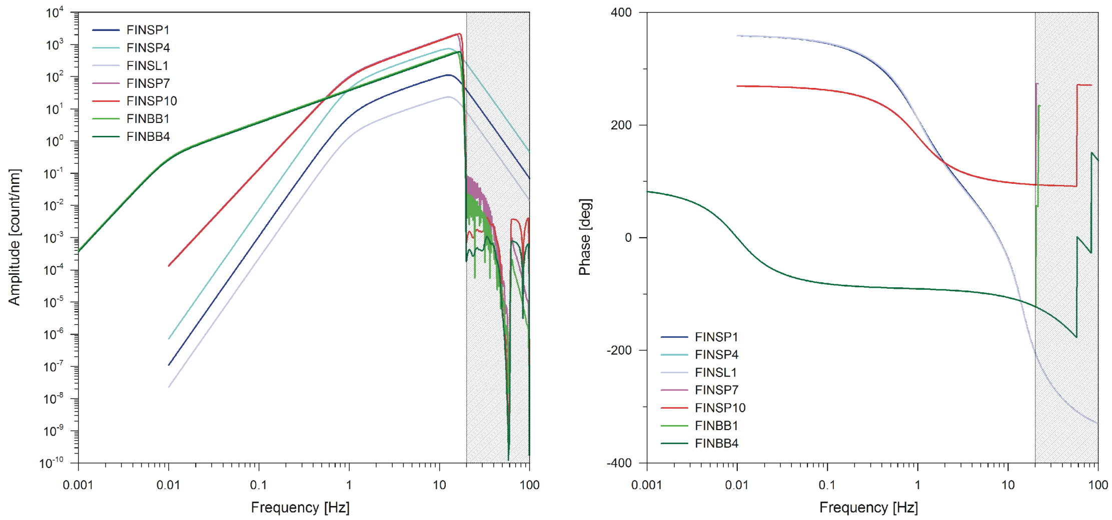

Fig. 6.5.7. Displacement amplitude (left) and phase (right) response for the FINES array configurations. Respids are used to link each curve to the corresponding configuration listed in Table 6.5.2. Shaded areas represent the range beyond the Nyquist frequency (20 Hz for all channels).

6.5.4 Åknes (AKN) station configurations

The AKN broadband, three-component station was installed on the rockslope at Åknes, close to Stranda, Møre og Romsdal, in the end of October 2009, to complement the rockslide monitoring network operating there. The station is equipped with a Güralp Systems CMG-3ESP seismometer and a CMG-DM24S6DCM unit, which combines a DM24 digitizer and EAM data communications module (Güralp Systems, 2009a). The response information of the instrumentation is provided by the manufacturer in the form of poles and zeros and sensitivity values. In the case of AKN, where the output sampling rate is 200 sps, the DM24 digitizer employs the following cascade of FIR filters to decimate down from the input rate of 512 kHz (Güralp Systems, 2006):

- FIR filter SINC-1, decimating by 8, asymmetric, 18 coefficients
- FIR filter SINC-2-stage-3, decimating by 2, asymmetric, 3 coefficients
- FIR filter SINC-2-stage-4, decimating by 2, symmetric, 7 coefficients
- filter FIR-1-set0, decimating by 4, asymmetric, 24 coefficients
- filter FIR-2-set0, decimating by 2, asymmetric, 63 coefficients
- filter DM24-tap0, decimating by 2, symmetric, 501 coefficients
- filter DM24-tap1, decimating by 5, symmetric, 501 coefficients

The AKN station configuration described above and the corresponding Respid flags are listed in Table 6.5.3. The displacement amplitude and phase response curves are shown in Fig. 6.5.8 for the AKN vertical channel. The response is plotted only up to the Nyquist frequency.

Table 6.5.3. The instrument configuration of the Åknes station

Time	Installation Name	Components	Calib [nm/count]	Calper [s]
2009-…	Current BB (AKNBH1, AKNBH2, AKNBH3)	CMG-3ESP CMG-DM24 digitizer LP FIR cascade, digital	0.26421*	1.00

* Indicative value

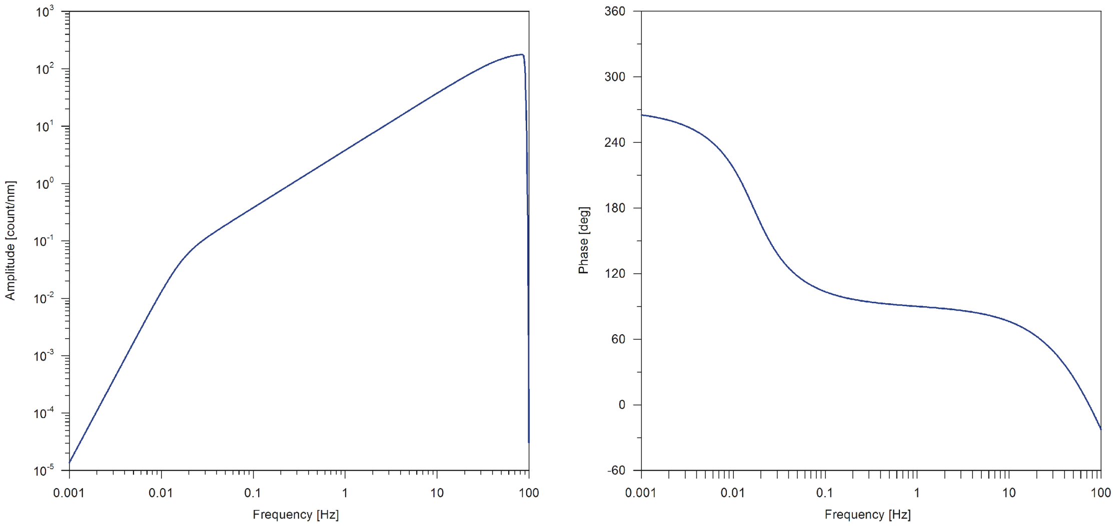

Fig. 6.5.8. Displacement amplitude (left) and phase (right) response for the vertical channel of the AKN broadband, three-component station. The response is plotted only up to the Nyquist frequency.

6.5.5 Hornsund (HSPB) station configurations

A new broadband, three-component seismic station (HSPBB) was installed close to the Polish Polar Station Hornsund, in September 2007, within the frame of the IPY project “The Dynamic Continental Margin Between the Mid-Atlantic-Ridge System (Mohns Ridge, Knipovich Ridge) and the Bear Island Region”, in a collaborative effort between the Institute of Geophysics of the Polish Academy of Sciences (IGF-PAS) and NORSAR (Schweitzer and The IPY Project Consortium Members, 2008). The original instrumentation of the station involved an STS-2 seismometer by Streckeisen and a Güralp Systems DM24 digitizer. The station outputted three different data streams, with sampling rates of 100, 10 and 1 sps.

A detailed description about the way to obtain response information for an STS-2 sensor has already been provided in our reports about the Jan Mayen station (Pirli, 2010; Pirli and Schweitzer, 2009). In the case of the HSPBB station, which is equipped with sensor # 60702, the sensitivity and pole and zero values are provided below.

Generator constant values for X, Y and Z: 1500 ± 15 V/m/s. The generator constant values and orientations of the three different sensors are:

- Sensor U: G/G0 = 1.0486 theta = 54.544° phi = 179.79°
- Sensor V: G/G0 = 1.0525 theta = 54.458° phi = 59.844°
- Sensor W: G/G0 = 1.0516 theta = 53.311° phi = 299.73°

where G/G0 is the normalized generator constant, which is equal to the actual constant divided by 1500 V/m/s. The poles and zeros (Hz) for the vertical component are the following:

Poles (11):	Zeros (4):
-4.55×10^2	$-461.8 \pm j\,429.1$
$-1.024 \times 10^4 \pm j\,2.725 \times 10^3$	-191.1
-424.5	-15.15
$-99.7 \pm j\,391.5$	
$-9.513 \times 10^3 \pm j\,1.147 \times 10^4$	
-15.46	
$-0.037 \pm j\,0.037$	

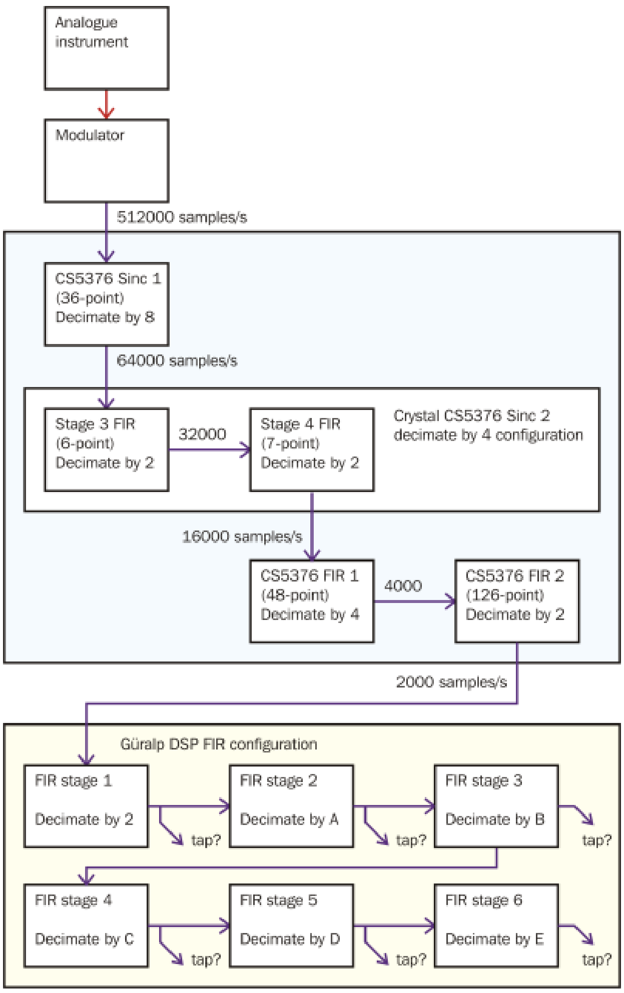

Fig. 6.5.9. The digital filter cascade employed by the Güralp DM24 mk3 digitizer to decimate from the 512 kHz input clock of the CS5375 chipset to the desired data sampling rate(s) (from Güralp Systems, 2009b). In the case of HSPBB a decimation of 5 from the sampling rate of 2 kHz (FIR stage 1) occurs, omitting the decimation by 2 stage shown in the figure.

The DM24 digitizer, with serial number # B794 (mk3), has the following sensitivity for the velocity channels:

- Z: 3.203 μV/count
- N-S: 3.200 μV/count
- E-W: 3.197 μV/count

To achieve the three different sampling rates mentioned earlier, the digitizer employs a particular cascade of FIR filters that has different taps. The standard and variable parts of the cascade for an mk3 system are shown in Fig. 6.5.9 (Güralp Systems, 2009b).

The TTL (tap table lookup) value contained in the GCF data header provides the needed information for the actual cascade used to output the desired sampling rate(s). This corresponds to FIR stages 1 to 6 in Fig. 6.5.9. Initially, only the 100 and 10 sps channels were outputted at Hornsund, and a TTL value of 76 was used. From 23rd September 2007, the 1 sps tap was also installed, with a TTL value of 77. TTL 77 and 76 differ only in the two last FIR stages, which were not used initially, so cascade 77 can be used for both configurations, and it is the following (Cirrus Logic, 2001; Güralp Systems, 2006):

- FIR filter CS5376 Stage 1, Sinc 1, decimating by 8 from the 512 kHz input clock, asymmetric, 18 coefficients
- FIR filter CS5376 Stage 3, Sinc 2, decimating by 8, asymmetric, 3 coefficients
- FIR filter CS5376 Stage 4, Sinc 2, decimating by 2, asymmetric, 7 coefficients
- FIR filter CS5376 Stage 5, FIR1, decimating by 4, asymmetric, 24 coefficients
- FIR filter CS5376 Stage 5, FIR2, decimating by 2, asymmetric, 63 coefficients
- FIR filter DM24 Stage 1, SWA-D24-3D08, decimating by 5 from 2 kHz, symmetric, 501 coefficients
- FIR filter DM24 Stage 2, SWA-D24-3D07, decimating by 4, symmetric, 501 coefficients, tap for 100 sps
- FIR filter DM24 Stage 3, SWA-D24-3D08, decimating by 5, symmetric, 501 coefficients
- FIR filter DM24 Stage 4, SWA-D24-3D06, decimating by 2, symmetric, 501 coefficients, tap for 10 sps
- FIR filter DM24 Stage 5, SWA-D24-3D08, decimating by 5, symmetric, 501 coefficients
- FIR filter DM24 Stage 6, SWA-D24-3D06, decimating by 2, symmetric, 501 coefficients, tap for 1 sps

In August 2009, the digitizer was changed to an MK-6 A/D converter, designed and manufactured at IGF-PAS. The station name was changed to HSPB, and officially reported to the station registry of the ISC and NEIC. In the current configuration, only the 100 sps data streams are outputted. The MK-6 data acquisition unit (Wiszniowski, 2002) employs a PAC56 digitizer with Motorola DSP56 Sigma-Delta signal processors for filtration. The A/D converter applies oversampling to 12.8 kHz to achieve a resolution of 26 bit. Prior to sampling, the signal is low-pass filtered to avoid aliasing, with the analog filter described by Equation (6.5.3):

$$T_f(s) = \frac{K_f}{\prod_{j=1}^{3} (s - p_j)} , \quad (6.5.3)$$

where p_1, p_2 and p_3 are the poles and $K_f = |p_1.p_2.p_3|$. According to the response information provided by IGF-PAS, the sensitivity of the digitizer is equal to 298.02 nV/count and it employs the following filter cascade:

- Analog anti-alias filter (pac12anf)
- FIR filter (b2d6n), decimating by 2 from 12.8 kHz, symmetric, 20 coefficients
- FIR filter (b4d6n), decimating by 4, symmetric, 20 coefficients
- FIR filter (b2d8n), decimating by 2, symmetric, 10 coefficients
- FIR filter (b2d12nn), decimating by 2, symmetric, 12 coefficients
- FIR filter (pac56lin), decimating by 4, symmetric, 512 coefficients

The different configurations and corresponding Respids for the HSPBB and HSPB station are listed in Table 6.5.4.

Table 6.5.4. The different instrument configurations of the Hornsund station

Time	Installation Name	Components	Calib [nm/count]	Calper [s]
2007-2009	Initial 100 sps HSPBB (HSPHH1, HSPHH2, HSPHH3)	STS-2 CMG-DM24 digitizer LP FIR cascade, digital	0.322570*	1.00
2009-…	Current 100 sps HSPB (HSPHH4, HSPHH5, HSPHH6)	STS-2 MK-6 digitizer LP anti-alias, analog LP FIR cascade, digital	0.030014*	1.00
2007-2009	HSPBB 10 sps (HSPBB1, HSPBB2, HSPBB3)	STS-2 CMG-DM24 digitizer LP FIR cascade, digital	0.322570*	1.00
2007-2009	HSPBB 1 sps (HSPLP1, HSPLP2, HSPLP3)	STS-2 CMG-DM24 digitizer LP FIR cascade, digital	0.322570*	1.00

* Indicative value

The displacement amplitude and phase response for the configurations of the Hornsund station described in the previous paragraphs is depicted in Fig. 6.5.10. Only the vertical component case is presented, while shaded areas cover the range beyond the Nyquist frequency (50 Hz, 5 Hz and 0.5 Hz for the three different taps).

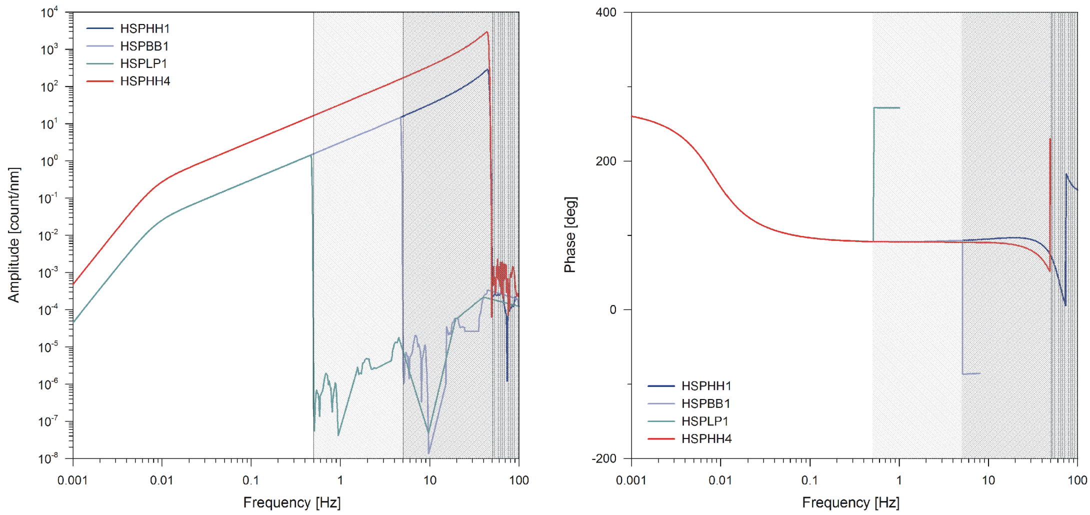

Fig. 6.5.10. Displacement amplitude and phase response curves for the different configurations of the Hornsund broadband station listed in Table 6.5.4. Shaded areas represent the range beyond the Nyquist frequency (50 Hz for the 100 sps channels, 5 Hz for the 10 sps and 0.5 Hz for the 1 sps channels).

6.5.6 Erratum: ARCES response

The response of the ARCES array was presented in Pirli and Schweitzer (2008b). The highly damped version of the new ARCES short-period channel configuration was omitted in that report. For approximately one month in 1999 (14 September – 7 October), the GS-13 seismometers operated with a damping of 1.5 instead of the typical value of 0.75 that was adopted afterwards. Thus, the highly damped version is assigned Respids ARCESSP4,5,6, while the current version is assigned Respids ARCESSP7,8,9.

Myrto Pirli

Johannes Schweitzer

References

Bergkvist, N.-O. & M. Lennartsson (2004). Upgrade of auxiliary seismic station AS101, Hagfors, Sweden. Technical Report FOI-R--1310--SE, FOI, Uppsala, Sweden, 14 pp.

Cirrus Logic (2001). Crystal Cs5376 low power multi-channel decimation filter. DSA0072869.pdf, Cirrus Logic Inc., Austin, Texas, 122 pp.

FOI, (2005). Fax with response information from M. Lennartsson(FOI) to J. Schweitzer (NORSAR).

Geotech Instruments (1999). Operation and maintenance manual portable short-period seismometer, model GS-13. 55400D0A.WFW, Geotech Instruments, Dallas, Texas, 50 pp.

GSE (1990). Sourcebook for International Seismic Data Exchange, Description of Seismic Stations, Appendix Three. Conference Room Paper /167/Rev. 2, April 1991, SWE.1-SWE.4.

GSETT3 (1995). Station Information. Chapter 2 under Sweden in Volume Three, Facilities, Conference Room Paper /243 of GSETT Documentation, 3-8.

Güralp Systems (2006). CMG-DM24 mk3 Operator's Guide. MAN-D24-0004, Güralp Systems Ltd., Aldermaston, England, 122 pp.

Güralp Systems (2009a). CMG-DM24S6DCM Digitizer and Communications Module. DAS-D24-0009, Güralp Systems Ltd., Aldermaston, England, 11 pp.

Güralp Systems (2009b). FIR filter configuration of the CMG-DM24 mk3. http://www.guralp.com/articles/20060410-technical-filter-DM24mk3/support, Güralp Systems Ltd., Aldermaston, England.

Heikkinen, P. (Ed.) (2003). Annual Report 2002. Institute of Seismology, University of Helsinki, Helsinki, Finland, 35 pp.

Korhonen, H., S. Pirhonen, F. Ringdal, S. Mykkeltveit, T. Kværna, P.W. Larsen & R. Paulsen (1987). The FINESA array and preliminary results of data analysis. Report S – 16, University of Helsinki, Institute of Seismology, Helsinki, Finland, 69 pp.

Laporte, M. (2006). System noise study. CTBTO - PS17 FINES, Lahti, Finland, Short Period Element. Document EC16003R1.mcd, Initial Release, 31 pp.

Lund, B. & M. Lennartsson (2005). Hagfors seismic array performance analysis. Technical Report FOI-R--1309--SE, FOI, Uppsala, Sweden, 48 pp.

Nanometrics (1992). NORSAR RD3 User Guide, RD3 – 1625, Revision 1.1. Nanometrics, Inc., Kanata, Ontario, Canada, 61 pp.

Pirli, M. (2010). NORSAR System Responses Manual, Version 2.0. NORSAR, Kjeller, Norway, 180 pp.

Pirli, M. & J. Schweitzer (2008a). Overview of NORSAR system response. NORSAR Sci. Rep., **1-2008**, 64-77.

Pirli, M. & J. Schweitzer (2008b). Continued overview of NORSAR system response: the NORES and ARCES arrays. NORSAR Sci. Rep., **2-2008**, 86-93.

Pirli, M. & J. Schweitzer (2009). Continued overview of system responses for seismic arrays and stations contributing to NORSAR's Data Center. NORSAR Sci. Rep., **1-2009**, 45-56.

Ringdal, R., S. Mykkeltveit, T. Kværna, R. Paulsen, H. Korhonen & S. Pirhonen (1987). Initial results from data analysis using the FINESA experimental small aperture array. NORSAR Sci. Rep., **2-86/87**, 59-83.

Schweitzer, J. & The IPY Project Consortium Members (2008). The International Polar Year 2007-2008 Project "The Dynamic Continental Margin between the Mid-Atlantic-Ridge System (Mohn's Ridge, Knipovich Ridge) and the Bear Island Region". NORSAR Sci. Rep., **1-2008**, 53-63.

Streckeisen (1986). VBB.MAN, 08-JUL-86 version, G. Streckeisen AG, Pfungen, Switzerland, 45 pp.

Streckeisen (2003). STS-2 portable very-broad-band triaxial seismometer. sts2-1.pdf, G. Streckeisen AG Messgeräte, Pfungen, Switzerland, 12 p.

Streckeisen (2006). Pole-zero representation of the STS-2 transfer function from 0.001 to 100 Hz. sts.pdf, G. Streckeisen AG, Pfungen, Switzerland, 14 p.

Tarvainen, M. (1994). The capability of three-component substation FIA1 at local and regional distances. Comparisons with FINESA and Helsinki bulletins. Annali di Geofisica, **37**, 267-285.

Teikari, P. & I. Suvilinna (1994). Seismic stations in Finland 1993. Report T – 58, University of Helsinki, Institute of Seismology, Helsinki, Finland.

Tiira, T., M. Tarvainen & A. Tuppurainen (1995). Noise characteristics of the upgraded FINESS array. Geophysica, **31**, 71-84.

Uski, M. (1990). Event detection and location performance of the FINESA array in Finland. Bull. Seismol. Soc. Am., **80**, 1818-1832.

Wielandt, E. (2002). Seismic sensors and their calibration. Chapter 5 in IASPEI New Manual of Seismological Observatory Practice, Bormann, P. (Ed.), GeoForschungsZentrum Potsdam, **Vol. 1**, 46 p.

Wiszniowski, J. (2002). Broadband Seismic System: Effect of transfer band on detection and recording of seismic waves. Publications of the Institute of Geophysics Polish Academy of Sciences, Monographic Volume **B-27 (339)**, Polish Academy of Sciences, Institute of Geophysics, Warsaw, Poland 180 pp.